PATHOPHYSIOLOGY OF BACTERIAL CARDIOMYOPATHY

A Thesis

Presented to the

University of Manitoba

In Partial Fulfillment of the Requirements

for the Degree of

Doctor of Philosophy

by

Charles W. Tomlinson

Department of Physiology

Faculty of Medicine

May, 1975

"PATHOPHYSIOLOGY OF BACTERIAL CARDIOMYOPATHY"

by
CHARLES W. TOMLINSON

A dissertation submitted to the Faculty of Graduate Studies of the University of Manitoba in partial fulfillment of the requirements of the degree of

DOCTOR OF PHILOSOPHY

TO MY FAMILY

ACKNOWLEDGEMENTS

It is with deepest sincerity that I thank Dr. Naranjan S. Dhalla for his continued support, advice, and encouragement throughout my graduate training. I am proud to consider him my friend as well as my advisor. In addition, I wish to thank Dean A. Naimark and Dr. K.R. Hughes for their active interest in my education.

The help and cooperation of my colleagues and friends in the laboratory, especially S.L. Lee, J. Harrow, A. Singh, K. Varley, D.B. McNamara, P.V. Sulakhe, J.N. Singh, A. Bernatsky, and L. Carrington, was of great value in enabling me to complete this research.

I am especially grateful to my wife, Janice, for her tolerance and help during the difficult periods associated with research. As well, I can only once again express my appreciation to my parents for the many things they have done to enable me to reach this point in my career.

I would like also to acknowledge the expert secretarial aid of Mrs. Penny Trudel for the typing of this manuscript.

This study was supported by grants to Dr. N.S. Dhalla from the Manitoba Heart Foundation and was completed while I was in receipt of a Medical Scientist Award from the Canadian Heart Foundation.

ABSTRACT

Infective endocarditis was induced in catheterized rabbits by a single intravenous injection of Streptococcus viridans and the papillary muscle from the left ventricle was examined for histological and ultrastructural changes at 3 and 6 days of infection. Papillary muscles from normal and catheterized uninfected animals were used for comparison. Although left heart hypertrophy and interstitial edema were evident in both uninfected and infected animals, the infected animals exhibited in addition, monocytic infiltration, loss of normal myocardial architecture, and muscle degeneration, as well as lung congestion and pleural fluid accumulation. The papillary muscle from catheterized uninfected animals showed some degree of mitochondrial and sarcotubular swelling as well as contracture of myofibrils; the infected myocardium exhibited dramatic changes in ultrastructure such as mitochondrial swelling and destruction, sarcotubular swelling, separation of the intercalated disc, and myofibrillar contracture and disruption. These histopathological and ultrastructural changes in papillary muscles from rabbits with bacterial endocarditis are indicative of the presence of infective cardiomyopathy.

The status of myocardial function in catheterized rabbits after infection with Streptococcus viridans was assessed at 3 and 6 days. Sham operated controls as well as uninfected catheterized animals were used for comparison. Both uninfected and infected animals had elevated levels of serum CPK, LDH, and GOT as well as electrocardiographic abnormalities such as increased amplitude of the QRS complex and flattening or inversion of the T-wave. Unlike the uninfected animals, the serum calcium, magnesium, and sodium were slightly but significantly decreased whereas serum potassium was increased in the infected rabbits. The levels of calcium and potassium were decreased whereas sodium was increased in both infected and uninfected hearts; however, magnesium levels, which did not change in uninfected hearts, were decreased at 3 days and increased at 6 days of infection. Both heart rate and pulse pressure were higher in 6 day uninfected and 3 day infected animals whereas 6 day infected animals showed a decrease in heart rate. In comparison to the sham operated controls and the uninfected animals, the infected animals exhibited depression in the rates of left ventricular pressure development

and relaxation as well as prolongation in time for half relaxation in situ. Extrapolated V_{max} from intraventricular pressure-velocity curves was decreased by 24, 52, and 76% of the control in the uninfected, 3 day infected, and 6 day infected animals respectively. The isolated perfused hearts from infected animals also generated less contractile force and showed a decrease in the rates of contraction and relaxation, but the time for half relaxation was increased. These results demonstrate myocardial dysfunction during experimental bacterial endocarditis and provide evidence that infective cardiomyopathy is associated with heart failure.

The status of membrane systems and contractile proteins in hypertrophied left ventricles from catheterized rabbits at early and late stages of cardiomyopathy and failure after 3 and 6 days of infection with Streptococcus viridans, was examined by monitoring biochemical activities and ultrastructural integrity. Control and hypertrophied hearts from sham operated and uninfected catheterized animals respectively were used for comparison. No biochemical changes in sarcolemma, microsomal, mitochondrial and myofibrillar activities were seen in hearts from 3 day uninfected catheterized animals which also showed no ultrastructural abnormalities. On the other hand, decreased sarcolemmal Mg^{++}ATPase, Na^{+}-K^{+}ATPase, adenylate cyclase and calcium binding, microsomal calcium binding and uptake, and myofibrillar Ca^{++}-stimulated ATPase as well as increased mitochondrial calcium uptake were observed in 6 day uninfected hearts. In addition, these animals had marked cardiac hypertrophy and some areas of myofibrillar contracture, mitochondrial damage, sarcotubular swelling and some degree of intercalated disc separation. Varying degrees of depression in sarcolemmal Mg^{++}ATPase, Na^{+}-K^{+}ATPase, adenylate cyclase in the absence and presence of epinephrine and NaF, and calcium binding, microsomal calcium binding, calcium uptake, and basal ATPase, and myofibrillar Ca^{++}-stimulated ATPase were seen at both early and late stages of infective cardiomyopathy and failure; however, sarcolemmal Ca^{++}ATPase, mitochondrial oxygen consumption in state 3, and myofibrillar Mg^{++}ATPase were decreased only at 6 days of infection. Mitochondrial calcium binding and uptake were increased at early stages but decreased at late stages of disease. Furthermore, mitochondrial ATPase, respiratory index, ADP:0 ratio, and phosphorylation rates were decreased, whereas oxygen consumption in state 4 was increased after 3 and

6 days of infection. Although only slight swelling of sarcotubules and occasional intercalated disc separation were observed in 3 day infected hearts, generalized severe myocardial cell damage with respect to myofibrils, mitochondria and sarcotubular system were seen at late stages of infection. The magnitude of changes in sarcolemmal, microsomal and myofibrillar activity in the infected hearts was greater than in the uninfected hypertrophied hearts whereas mitochondrial alterations were apparent mainly in the infected hearts. Although heart failure in the infected animals is superimposed upon left ventricular hypertrophy, the results demonstrate impairments in different membrane and contractile protein functions as well as ultrastructural abnormalities in bacterial cardiomyopathic hearts which are absent or of lesser magnitude in hearts with hypertrophy alone. From these observations we believe there is an association of heart failure and changes in functions of cellular components during bacterial infection.

TABLE OF CONTENTS

LIST OF FIGURES

LIST OF TABLES

INTRODUCTION AND STATEMENT OF THE PROBLEM

The changing nature of infective endocarditis has been the subject of several recent reviews especially with regard to microbiology, pathophysiology, and clinical status (1-6). Although most of the pathological studies on endocarditis have been centred around investigating the histology of the valvular tissue and vegetations (7,8), only a few reports concerning histological changes in myocardium (9-12) have appeared in the literature. Furthermore, no information concerning changes in myocardial ultrastructure is available either for patients or any experimental model. It was therefore the purpose of this study to examine the ultrastructure of myocardium during infective endocarditis produced by a single injection of Streptococcus viridans in catheterized rabbits. This experimental model has recently been developed and is regarded to simulate the clinical situation in which transient bacteremia leads to infective endocarditis (13-15).

Although a striking change in the spectrum of bacterial and viral agents responsible for endocarditis has been reported (2,3,6), Streptococcus viridans is still considered to be one of the main etiologic agents causing clinical disease. Such infection could occur following various cardiovascular diagnostic procedures or cardiac surgery (16-18), creation of arteriovenous fistulas for dialysis (19,20), narcotic injections (21,22), and different medical treatments which predispose the blood stream to bacterial invasion. In spite of the availability of effective antibiotics, the mortality of patients with infective endocarditis remains high and is mainly attributed to congestive heart failure (5,23,24). Although the role of different factors causing heart failure due to bacterial infection is not clearly defined, valvular dysfunction leading to insufficiency has been thought to account for the majority of cases. In view of the possibility of pump failure due to some defects in cardiac muscle itself, we wished to examine some of the functional changes occurring in the rabbits with infective endocarditis in order to demonstrate the presence of heart failure. The extent of myocardial damage in the experimental animals was also evaluated by monitoring the electrocardiographic changes, electrolyte shifts, and serum enzyme levels.

Involvement of biochemical mechanisms in proper heart function has been well

recognized; however, no information concerning the biochemistry of cardiac muscle particularly with respect to factors for the regulation of myocardial metabolism and function during infective endocarditis is available in the literature. It is now about 25 years since Olson discussed a hypothetical framework for the study of cardiac metabolism in relation to heart failure (25,26). It was postulated that there exist two molecular classes of heart failure: a) those in which the defect lay in energy production and b) those in which the defect lay in energy utilization. Abundant evidence has accumulated in the intervening years to justify this traditional formulation (27-29); however, some reports indicating normal energy metabolism in the failing heart have also appeared in the literature. Thus the molecular mechanisms underlying the loss of contractility in heart failure remain obscure and it is commonly held that biochemical defects are dependent on the type and degree of heart failure.

Since mitochondria and myofibrils are the major systems for energy production and utilization respectively, the respiratory and phosphorylation abilities of mitochondria and ATP hydrolyzing activity of myofibrils are usually monitored to reflect metabolic changes in heart failure (30). Changes in sarcolemma can also be conceived to be associated with abnormal myocardial function and metabolism because it is enriched with enzymes such as adenylate cyclase and Na^+-K^+ ATPase which participate in the formation of cyclic AMP and ionic movements (31,32). Furthermore, cardiac contraction and relaxation is considered to be regulated by movements of calcium across sarcoplasmic reticulum, mitochondria and sarcolemma (33-45); thus any alteration in their calcium regulating ability may result in impairment of contractile events. It was therefore decided to monitor the biochemical status of myofibrils, mitochondria, fragments of sarcoplasmic reticulum (heavy microsomes) and sarcolemma isolated from hearts at early and late stages of infective endocarditis. In addition, the ultrastructure of the infected hearts with respect to integrity of these membranes and contractile proteins was monitored to provide morphological support for the biochemical observations with these cellular components.

REVIEW OF THE LITERATURE

1. Infective Endocarditis: General Aspects

Osler in 1885 was aware of the importance of reviewing clinical features of a particular disease process (46). Referring to endocarditis he stated:

> It is of use from time to time to take stock, so to speak, of our knowledge of a particular disease, to see exactly where we stand in regard to it, to inquire to what conclusions the accumulated facts seem to point, and to ascertain in what direction we may look for fruitful investigations in the future.

This quotation is particularly applicable in the case of bacterial endocarditis, a disease which has dramatically changed in the past few decades with respect to both clinical features and pathophysiology. The changing nature of this disease has been the subject of several reviews especially concerning microbiology, pathophysiology, and clinical status (1-5). In addition, many reviewers have tended to emphasize the changing concepts of chemotherapy as well as surgical problems encountered (6,18,47). Since these topics have been adequately covered, it is the intention of this present article to highlight the important findings from these works and in addition discuss the most recent concepts of myocardial involvement in this disease.

2. The Changing Clinical Appearance of Infective Endocarditis

Although there is considerable debate as to whether the incidence of infective endocarditis has decreased (48,49), not changed (50), or increased (51,52), most studies do agree that there has been a change in age distribution since the advent of antibiotic therapy (23,51) from young adults to individuals over fifty. As well, a striking change in the spectrum of agents responsible for endocarditis has been observed (8). Although Strep. viridans and Staph. aureus still cause most clinical disease, a variety of formerly uncommon organisms such as microaerophilic strains of streptococci, enterococci, enterobacteriaceae, and several types of fungi, viruses and cell wall-deficient bacteria are appearing (3).

Clinical features of the disease have undergone tremendous changes and older classifications are now obsolete (2,3). The incidence of rheumatic and congenital heart disease, still the most common underlying disorders, is decreasing and that of arteriosclerotic valve disease or myocardial infarction has increased (49,51). Classical manifestations of infective endocarditis are now fever and a heart murmur, although the latter may be absent. Other signs and symptoms such as petechiae, subungual hemorrhages, Osler's nodes, digital clubbing and splenomegaly are less common than before. Atypical presentations are becoming increasingly more prevalent.

A number of new dimensions have been added to problems of infective endocarditis. The wide application of cardiac surgery has been followed by infective complications (16-18). Problems relating to various cardiovascular diagnostic procedures as well as infections following insertion of prosthetic valves have attracted a great deal of attention. An association with infective endocarditis has been noticed in patients with arteriovenous shunts or fistulas created for the purpose of hemodialysis (19,20,53). A widespread increase in the use of narcotics has been responsible for a rise in endocarditis in addicts (21,22,54). This group is particularly susceptible to right-sided endocarditis due to Staph. aureus. The seriousness of this problem is emphasized by the high fatality rate in these persons. A similar problem is found in the case of alcoholics who are especially prone to pneumococcal endocarditis (55). The immune aspects of endocarditis have further complicated our understanding of this disease process (56,57), and have recently been emphasized because of the prolonged survival time of patients due to improved antibiotic therapy.

3. Complications of Infective Endocarditis

In spite of the introduction of effective antibiotics, the mortality of patients with infective endocarditis remains high. The most common cause of death in such patients is now considered to be congestive heart failure caused most often by perforation of the aortic valve followed by insufficiency (5,23,24,58). It is responsible for a fatal outcome in over 60% of cases. Recently, other workers have emphasized the importance of infection toxemia as a leading cause of death (8).

Other causes of heart failure include valvular leaflet destruction, rupture of chordae tendinae, valvular stenosis, myocarditis and myocardial abscesses. Jet lesions created by aortic insufficiency may exaggerate failure by causing mitral lesions (59). Hemodynamically significant valvular stenosis may occur if vegetations are large and precipitate failure (60,61). Despite lack of knowledge concerning pathogenesis of myocarditis during infective endocarditis, it is considered to be an important complication (9-12). Myocardial abscesses and extensions through the myocardial wall may result in ventricular septal defects, cardiac tamponade and false aneurysms. Pericarditis presents as a complication in about 20% of cases of infective endocarditis (8,11,12,23).

Arterial emboli comprise the next largest group of complications and commonly involve coronary vessels, brain, spleen and kidneys (5,12). Mycotic aneurysms are often found and probably result from embolic occlusion of vasa vasorum, bacterial invasion, or injury secondary to immune complex phenomena (63-65). Neurologic or psychiatric symptoms, in addition to cerebral embolic phenomena, meningitis, or signs of toxic encephalopathy, occur in up to one third of patients (66-69). Renal lesions including glomerulonephritis and renal failure seem to be a result of the immune complex disease which may occur (70).

4. Pathology of Infective Endocarditis

A complete understanding of infective endocarditis involves knowledge of specific pathologic changes associated with it. The traditional division of this disease into acute and subacute bacterial endocarditis is gradually being discarded since differences can be related almost entirely to pathoanatomic and pathophysiologic changes induced at the primary site of infection, the heart valve, as well as the nature of the invading organism. Clinicians understand duration of illness, bacteriologists the type and virulence of the organism, and morphologists the destruction the infection has caused. The current consensus is that the subacute form of the disease is a continuum of the acute form and represents a response that differs quantitatively but not qualitatively.

Pathological changes in valve tissue during endocarditis have been thoroughly described and many studies of valvular vegetations have been done (7). Microscopy

of lesions in disease of long duration reveals slow progressive activity and early healing, but always preceded by the rate of valve destruction. Neutrophils, lymphocytes, plasma cells, and masses of bacteria are seen. In rapidly progressive disease there is conspicuous absence of healing processes. Valvular distortion including thickening with edema and fibrosis, hyalinization, cellular reaction and vegetation formation are characteristic features. The type of vegetation and degree of local destruction depend on the virulence of the organism and the resistance of the tissue to that organism. Vegetations consist of friable masses of variegated appearance varying from yellow to dark brown in colour. They consist predominantly of fibrin with clumps of platelets, enmeshed blood elements, and bacteria. Variable amounts of granulation tissue or foci of calcification are present depending on duration of the disease. As lesions progress, the character of the inflammatory infiltrate is altered in that the polymorphonuclear cells and Anitschkow myocytes are replaced by chronic inflammatory cells including palisading mononuclear cells. The site of vegetation development seems to be related to either a jet effect (71) producing vegetation in endocardium in line with the regurgitant stream, or a Venturi effect (72) which is caused by blood being driven from a high pressure source through an orifice into a low pressure sink. Such mechanical and hydraulic explanations have replaced Luschka's original concept of septic coronary embolism to vascularized heart valves (73). Electron microscopy of valvular changes as well as of vegetations support histological findings (7). Histoenzymatic studies have been done in an attempt to understand the mechanisms of vegetation formation and the enzymatic alterations in infective endocarditis (7,74). Evaluation of enzyme activity reveals diminished DPNH diaphorase activity at the base of the vegetations during active disease. Studies on adenosine nucleotidases reveal decreased ATPase and ADPase but increased AMPase activity. A decrease in alkaline phosphatase was also observed. When healing processes supervened, DPNH diaphorase, ATPase, ADPase and alkaline phosphatase reactions became evident while AMPase was weak or negligible. Thus it is apparent that the activity of these enzymes varies with the stage of the disease. However, it is difficult to evaluate the significance of such changes since histochemical methods recognize only gross changes in enzyme activity. The presence of bacteria and inflammatory cells also affect the interpretation of such

results. Clearly more work must be done before definitive conclusions can be made.

Although some early workers such as Blumer (75) considered myocardial involvement slight and infrequent in infective endocarditis, others such as Libman (76) and Clawson (77) were cognizant of its frequent occurrence. Saphir (78) described myocardial changes in human tissue consisting of cloudy swelling, fatty degeneration, petechial hemorrhages, acute myocarditis, foci of necrosis and perivascular inflammation. Myocardial lesions today are considered to be found in almost all cases of infective endocarditis (8,9-12). The most commonly accepted description of histologic myocardial changes is that of Saphir (79) and Perry (9). The inflammatory infiltration other than that localized to perivascular areas was usually focal but occasionally diffuse. Most often, it is interstitial with predominance of acute inflammatory cells in early disease with addition of mononuclear cells such as macrophages and lymphocytes in later stages of the disease. Areas of muscle necrosis containing colonies of bacteria are seen as well as areas with minute infarcts in different stages of organization. Perivascular cellular infiltration, cytologically similar to the interstitial myocarditis, is common. Papillary muscle necrosis is often observed in patients with endocarditis and is thought to be the result of poor arterial perfusion associated with heart failure (8) since papillary muscles are the last to be supplied by arterial blood (80). The role of myocardial lesions in the causation of congestive heart failure is unclear at the present time.

5. Experimental Infective Endocarditis

(a) Description of models used for the study of infective endocarditis

Numerous methods have been employed in attempts to produce endocarditis in experimental animals. The diverse experimental procedures adopted attest to difficulties encountered in finding a reliable model which can reproduce the human disease. The earliest experimental production of endocarditis (81) is usually attributed to Ribbert (1886) who injected staphylococci intravenously into rabbits, Wyssokowitsch (1886) who utilized a technique designed to damage the heart valves prior to the systemic introduction of a bacterial pathogen such as streptococci into rabbits, and Dreschfeld (1888) who produced endocarditis by injection of pathogen

isolated from a patient with endocarditis. The experimental methods employed by these early investigators, namely (1) the injection of foreign substances, (2) preliminary trauma of valves and (3) simple injection of a clinical bacterial pathogen, set a trend for later experimental models.

Two general systems have evolved. In the first, normal animals are used; in the second, the animals are subjected to some procedure intended to render their heart valves more susceptible to bacterial attack. Bacteria used most frequently have been those isolated from man. Experimental procedures include single or repeated inoculation to normal animals or those subjected to preliminary procedures intended to render heart valves more susceptible to bacterial attack: a) mechanical injury to valves b) sensitization of valves by colloidal dyes, caseine or pitressin and c) stressing the cardiovascular system by arteriovenous fistulae, high altitude or impaired cardiac lymph flow. Rarely endocarditis has been studied in animals where it occurs naturally.

Dog models for experimental endocarditis date back to 1923 when Kinsella and Sherburne produced streptococcal endocarditis in dogs after aortic valve injury (82). Vegetative lesions as well as peculiar vascular lesions in myocardium were noted (83). Repeated intravenous injections of streptococci in dogs with arteriovenous shunts caused endocarditis without the need for valve injury (84,85). However, this model depends upon the severe hemodynamic changes which occur upon creation of a fistula between the aorta and the inferior vena cava. Hamburger (80,87) reported a 55% incidence of Staphylococcal endocarditis in dogs with valve injury produced by open thoracotomy followed by mechanical valve damage and postoperative bacterial injection. Highman et al. (88) describe a model for producing endocarditis in dogs with aortic insufficiency but could not produce disease in dogs with intact aortic valves. Recently, Keys (89) has studied enterococcal endocarditis in dogs with aortic valve damage due to needle puncture via the carotid artery. Although operative mortality was 25%, upon injection of streptococcus over 75% of survivors developed vegetative endocarditis. Over 60% had evidence of myocardial involvement in addition to other thromboembolic complications.

Several experimental models have been developed using bacteria isolated from cases of spontaneous endocarditis in pigs (90,91). Without any preliminary

stressing factors, Jones injected hemolytic streptococcus in sows and produced streptococcus endocarditis in 60% of animals, primarily in the left side of the heart. A progressive increase in vegetations corresponding to duration of survival (91), and signs of myocardial infarction were found. The myocardium showed muscle degeneration accompanied by interstitial infiltration with macrophages, but few neutrophils. There was focal myocarditis in addition to multiple renal infarcts and arthritic joint lesions.

A new model similar to Jones' utilizes the spontaneous occurrence of endocarditis in captive opossums (92,93). A modification by single intravenous injection of Streptococcus viridans or Staphylococcus aureus increases the incidence of disease to over 60%. Usually the left side of the heart is affected. Valve and myocardial lesions are identical to those occurring in man and some other experimental models.

A more complicated procedure for producing endocarditis in a very high proportion of animals has been described using x-irradiated rats (94,95). The combined effects of x-irradiation and catecholamine injections to produce myocardial necrotic lesions, resulted in the production of a nidus on which subsequently injected Streptococcus mitis would attack. The myocardial microcirculation was found to be a critical factor in susceptibility of the rats to infection (94). Since propranolol but not phenoxybenzamine minimized the resulting lesions and infection, it is thought that the enhanced susceptibility induced by catecholamines is related to β-adrenergic receptor stimulation.

Most of the above models have proved unsatisfactory. Reliable preparations in larger animals require elaborate surgical procedures whereas simpler methods in small animals do not produce infection consistently. Recently a new model of inducing endocarditis in rabbits has been developed (13,96) and has precipitated a series of experiments to unravel the mysteries of infective endocarditis. A polyethylene catheter placed in either the right or left heart entrance produces a sterile endocarditis consistently and staphylococcal contamination produces bacterial vegetations. This technique was modified by Durack et al. (14,15,97),who after a sterile catheter was in place, gave the rabbit an intravenous injection of streptococcus thereby simulating the clinical situation in which transient bacteremia leads to infective endocarditis. Extending the study of this model to commonly recommended antibiotic

prophylactic regimens (98), these scientists discovered the possible practical significance in deciding which regimens would be effective in a particular clinical situation. This is important because of the popular use of cardiac prostheses, pacemakers and intravenous catheters.

The most common mechanism of experimental production of bacterial endocarditis thus requires the seeding of organisms on previously existing non-bacterial thrombotic endocarditis produced by the various surgical or stress situations described above. These initial lesions may well represent an underlying metabolic disturbance of collagen in which endocrine and nutritional factors may play a part (80,99). Lillehei (84) noted marked adrenal hypertrophy in his dogs with A-V fistulas. Non-specific stress is known to affect the endocrine system and stressed rats have been shown to develop endocarditis (100). Simulation of physical cold and high altitude with and without hemodynamic stress (101,102) and bacteremia, in addition to alteration of heart lymphatic drainage (103) have also provided useful models of either non-bacterial or bacterial endocarditis. Hormones from ovary, testicle, thyroid, pituitary and adrenal glands have been used experimentally to produce valvulitis and vegetations (104). All the above models emphasize the possible importance of endocrine balance in determining patient susceptibility to this disease.

(b) Pathophysiology of experimental infective endocarditis

Utilization of the various experimental models of infective endocarditis has centred around description of valve pathology and studies of vegetations. Scattered reports have touched on microbiological and therapeutic aspects of the disease. Most workers agree that the experimentally produced lesions are similar to those seen in humans.

Vegetations have been described as massive mulberry-like agglomerations of bacteria and fibrin usually yellow in colour. They are usually progressive depending on the period of infection. Valvular lesions vary in severity from intact, but thickened and edematous, valve leaflets infiltrated with lymphocytes and neutrophils, to a destructive valvulitis with large, poorly organized masses of inflammatory cells, bacteria, and fibrin. The localization of bacteria is dependent on site of valvular

damage as well as the particular organisms involved. Most models involve gross and/or microscopic lesions in other organs including kidney, lung, spleen, and brain. Renal infarction with neutrophilic infiltration and fibrinopurulent synovitis occur in some models (90). Right-sided lesions are often associated with hepatic congestion, pulmonary infarction and splenomegaly (15).

Several animal models reveal myocardial involvement similar to that described in humans (90,96). Early workers such as Bracht and Wachter (105) described areas of myocardial necrosis surrounded by lymphocytes and fibroblasts in rabbits after streptococcal injection. These lesions, later termed "Bracht-Wachter bodies" were also seen by Thalhimer and Rothschild (106). These myocardial changes are especially prevalent in left-sided infections. A summary of the occurrence of myocardial pathology in different experimental models is shown in Table I. Lesions can be identified in 100% of infected animals in some studies. Gross changes in myocardial size, colouring and consistency produce a mottled appearance. Histologically, changes consist of muscle degeneration and interstitial infiltration with predominance of mononuclear cells. Hearts also had signs of focal or diffuse myocarditis with bacteria infiltrating the myocardium (15). More subtle myocardial lesions have been demonstrated even in hearts with no histologically observed changes by the use of scanning electron microscopy (107). Histoenzymatic studies similar to those described above for human disease have been done in these experimental models and demonstrate comparable results (7,74).

The above experimental studies have thus laid the groundwork for further studies in morphology as well as biochemical and functional aspects of infective endocarditis about which little information is available at the present time.

6. Approach to the Present Problem

From the foregoing discussion, it is clear that catheterized rabbits injected with bacteria form a good experimental model for investigating mechanisms involved in the pathogenesis of infective endocarditis. Furthermore, very little is known concerning involvement of myocardium in this disease. It was therefore the purpose of this study to characterize this new model in which streptococcal endocarditis was induced in the left ventricle. The first series of experiments was undertaken to establish

TABLE I - Myocardial Lesions in Different Experimental Models of Infective Endocarditis

Experimental Model	Incidence of Endocarditis	Myocardial Involvement (% of Infected)	Myocardial Lesions
Single injection in pigs (90,91): -β-hemolytic streptococcus	60% entirely left-sided	100%	Myocardial degeneration with interstitial infiltration with macrophages and a few neutrophils. (Also renal enlargement, multiple infarcts, neutrophilic infiltrate, joint lesions, fibrino purulent synovitis.)
Single injection in opossums (92,93): -Streptococcus viridans	58% entirely left-sided	95%	Myocarditis with focal or diffuse aggregates of acute and chronic inflammatory cells. (Brain abscesses 40%.)
-Staphylococcus aureus	91% primarily left but some right-sided lesions		Diffuse myocarditis. (Brain abscesses 70%, Renal abscesses 90%.)
Single injection in dogs after open chest surgery to produce aortic insufficiency (86,87): -Staphylococcus aureus	90% entirely left-sided	70%	Interstitial myocarditis with focal infiltration with neutrophils. (Also lung infarction, renal lesions.)
Single injection in dogs with aortic valve damage (89): -Streptococcus fecalis	83% entirely left-sided	60%	Focal myocardial infarcts with polymorphonuclear response. (Hemorrhagic lesions in kidney, spleen and lungs.)
Single injection in catheterized rabbits (15, Present Study): -Streptococcus viridans	100% entirely left-sided	100%	Myocardial necrosis with interstitial infiltration with mononuclear cells. (Renal infarcts also present.)
Double injection in x-irradiated rats after catecholamines (94,95): -Streptococcus mitis	67% primarily left-sided	100%	Myocardial necrosis with mural vegetations.

the involvement of myocardium by histological and electron microscopic examination of papillary muscle. In a second set of experiments, some hemodynamic parameters of these animals were investigated to provide information concerning the status of cardiac function and in addition, the intensity of myocardial cell damage was monitored. The last phase of this study was concerned with investigation of biochemical and ultrastructural examination of myocardial cell components. In all these studies, animals at early and late stages of disease were employed. Sham operated controls and uninfected catheterized rabbits were used for comparison purposes. It is hoped that this study will extend our present knowledge of endocarditis and provide information to form the biochemical basis of heart failure in this disease.

METHODS

1. Experimental Preparation

Healthy, normal New Zealand White male rabbits (1 to 2 kg each) were employed in this study. In some cases Dutch rabbits were used for comparison. All animals were anaesthetized by intraperitoneal injection of sodium pentobarbital (45 mg/kg). A neck incision was made slightly to the right of the midline and the right carotid artery was exposed. In one-third of these animals, the carotid artery was ligated, the wound was closed, and these animals served as sham operated controls. The carotid arteries of the remaining two-thirds of the animals were catheterized with a polyethylene tube (external diameter 0.9 mm, internal diameter 0.6 mm) filled with sterile saline. The tip of the catheter was positioned in the left ventricle with the aid of a Stratham pressure transducer (P23Db) which indicated a sudden drop in diastolic pressure. The catheter was tied in place, heat-sealed, and buried when the wound was closed. After the rabbits had recovered for 24 hours, bacterial endocarditis was induced in half of the catheterized animals by a single injection of different doses of Streptococcus viridans into the marginal ear vein. The strain of streptococcus used was originally isolated from the blood of a patient with bacterial endocarditis and identified as Streptococcus Sanguis, Type I (American Type Culture Collection, Rockville, Md.). The bacteria were cultured on Todd-Hewitt-agar slants and then incubated overnight in Todd-Hewitt broth at 37°C before injection. The number of bacterial organisms in 1 ml suspension was adjusted by dilution of the Todd-Hewitt broth culture with saline (usually 1:100 dilution) and spectrophotometric comparison at 650 mμ against a standard curve constructed for this organism by use of a Petroff-Hauser counting chamber. The purity of this bacterial suspension was assessed by Gram stain examination. The dose employed in our experiments has been found to produce 100% incidence of infective endocarditis with valvular vegetations and characteristic lesions. The other half of the catheterized animals were injected with an equivalent volume (1 ml) of Todd-Hewitt broth diluted with saline. These uninfected catheterized rabbits were used for establishing the contribution of hypertrophic changes occurring due to catheterization. The sham

operated animals described above also received 1 ml of Todd-Hewitt broth-saline suspension. The values for sham operated animals were overlapping with those obtained from the normal healthy rabbits and therefore these animals were designated as controls. All the animals were kept in environmentally controlled infection rooms and maintained on a standard rabbit died fed ad libitum. Rectal temperature and body weight were monitored in all animals. Operative mortality within the first 24 hours was less than 5%. No spontaneous deaths occured in saline-injected catheterized rabbits whereas the survival time for the infected animals varied between 6 to 8 days.

2. Pathological Studies

(a) Gross and histological examination

Three and six days after injection the rabbits were sacrificed by cervical dislocation, the hearts quickly removed, and weighed. In one set of experiments, small portions of the left heart papillary muscles and left and right ventricles (about 2 mm thickness) were dissected out and fixed in 10% buffered formalin, pH 7.0, for one week. These tissues were dehydrated in a graded series of ethanol and xylol, embedded in paraffin, sectioned (5-10 μ thickness) and stained with hematoxylin-eosin for histological examination. In another set of experiments, left ventricle was carefully dissected and the dry weight was determined by keeping the fresh tissue in an oven at 100°C for 3 days.

(b) Electron microscopic examination

Portions of papillary muscle and biopsies of the left ventricle tissue employed for biochemical studies were fixed in 1% glutaraldehyde for electron microscopic investigation. The tissue specimens were washed overnight in 0.1 M phosphate buffer, fixed for 1 hour with 1% osmium tetroxide, dehydrated in a graded ethanol series, and embedded in Epon 812 according to the method of Luft (108). The sections obtained with the use of a Blum MT-II ultramicrotome and glass knives, were stained with uranyl acetate and lead citrate and examined with a Zeiss electron microscope (EM9S).

3. Functional Studies

(a) Serum electrolytes and enzymes

About 20 ml samples of blood were obtained by cardiac puncture from sham operated, uninfected catheterized, and infected rabbits and serum was prepared by allowing the blood to clot, followed by centrifugation to remove the clotted blood. For electrolyte determination, the serum was boiled for 30 minutes after the addition of 2 N HCl, centrifuged at 5000 x g, and the supernatant employed for analysis. The calcium, magnesium, potassium and sodium concentrations were measured by atomic absorption with a Zeiss atomic absorption spectrophotometer. Lanthanum chloride (1%) and strontium chloride (.25%) were used in the determination of calcium and magnesium respectively to prevent interference by other ions. Similarly, cesium chloride (0.1%) was added to the supernatant samples when potassium and sodium were determined.

Serum creatine phosphokinase (CPK) was determined by the method of Rosalki (109) with a Gilford 3400 automatic enzyme analyzer. Serum lactate dehydrogenase (LDH), glutamic oxaloacetic transaminase (GOT) and alkaline phosphatase were determined by routine clinical methods using a Technicon SMA Flex automatic analyzer (110-112).

(b) Myocardial electrolytes

Animals used for the study of myocardial electrolytes were sacrificed by cervical dislocation, the hearts were removed and quickly perfused with 20 ml of ice-cold, Dowex treated sucrose-histidine buffer (113) (0.32 M sucrose, 5 mM histidine, pH 7.4) via an aortic cannula. This method was found to satisfactorily eliminate all the extracellular fluid since no red blood cells were detectable upon histological examination. Portions of left ventricle from sham operated and uninfected and infected catheterized rabbits were homogenized, ions were extracted in 2 N HCl according to the method of Reynafarje and Lehninger (114). Total ion contents in the clear supernatant after centrifugation at 5000 x g were determined by atomic absorption as described above.

(c) Electrocardiographic and pressure recordings

Rabbits used for this purpose were anaesthetized with sodium pentobarbital

(45 mg/kg intraperitoneal injection) and 30 minutes later an electrocardiogram using standard limb leads was performed. A Grass Polygraph (7WC8PA) with an EKG pre-amplifier (7P6A) and pin electrode attachments to shaved areas on rabbit front and hind limbs were used for this purpose. After the EKG was recorded, the right carotid artery was exposed, the original catheter was carefully removed and a second catheter with attachment to the Polygraph was put in its place. In infected rabbits it was sometimes necessary to cannulate the artery at a point closer to the heart than initially. The catheter was moved until it was judged to be close to the carotid-aortic junction. Pressure was monitored with a Stratham P23Db pressure transducer connected to the new catheter and recordings were made on a Grass Polygraph recorder. For intraventricular recordings, the catheter was positioned in the left ventricle. The rate of change of ventricular pressure was monitored with the use of a differential amplifier.

(d) Isolated heart preparation

Rabbits used for this purpose were sacrificed by cervical dislocation, the hearts quickly removed, and chilled in ice-cold perfusion medium. After trimming of fatty material and connective tissue, the hearts were arranged for coronary perfusion by the Langendorff technique as described previously (113). Hearts were equilibrated for 15 minutes with Krebs-Henseleit solution of the following composition (mM): NaCl, 120; $NaHCO_3$, 25; KCl, 4.8; KH_2PO_4, 1.25; $MgSO_4$, 1.25; $CaCl_2$, 1.25; glucose, 8.6. The perfusion medium, pH 7.4, was oxygenated with a gas mixture of 95% O_2 and 5% CO_2 and maintained at a temperature of 37°C. Flow was kept constant at a rate of about 60 ml/min. The apex of the heart was wired to a force displacement transducer (FTO3C) by a pulley and contractile force and rate of change of force were monitored at varying degrees of resting tension.

4. Biochemical Studies

Rabbits used for this purpose were sacrificed by cervical dislocation, the hearts were quickly removed and the left ventricle dissected out and employed for isolation of various cellular components. The left ventricular tissue from the sham operated (control), uninfected catheterized, and infected rabbits were processed

simultaneously under identical conditions. The activities of all cellular fractions employed in this study were determined within 1 hour after isolation.

(a) Isolation of the sarcolemmal fraction

The sarcolemmal fraction was prepared essentially according to a method described earlier (31). The ventricular tissue was thoroughly washed and homogenized in 10 volumes of 10 mM Tris-HCl, pH 7.4, containing 1 mM ethylenediamine-tetraacetate sodium (EDTA) and 1 mM dithiothreitol (DTT). The homogenate was filtered through gauze and centrifuged at 1000 x g for 10 minutes. The sediment was repeatedly suspended (four times) in 10 mM Tris-HCl, pH 7.4 to 8.0, containing 1 mM DTT (Tris-DTT buffer) and centrifuged at 1000 x g. The residue thus obtained was extracted with Tris-DTT buffer, pH 7.4 containing 0.4 M LiBr for 45 minutes and centrifuged at 1000 x g for 10 minutes. This sediment after washing with the above Tris DTT buffer, pH 7.4, was extracted with 0.6 M KCl in Tris-DTT buffer for 30 minutes, centrifuged and thoroughly washed with Tris-DTT buffer, pH 7.4. This pellet was suspended in 1 mM Tris-HCl, pH 7.4 and employed for biochemical studies.

(b) Isolation of mitochondrial and heavy microsomal fractions

For this purpose the tissue was homogenized in 10 volumes of 0.25 M sucrose containing 1 mM EDTA, pH 7.0, and the mitochondrial (1,000 - 10,000 x g) and heavy microsomal (10,000 - 40,000 x g) fractions were separated by differential centrifugation (115). The crude mitochondrial fraction was resuspended in 0.18 M KCl containing 10 mM EDTA and 0.5% albumin (fatty acid free), pH 7.0 and centrifuged at 1000 x g. The sediment at 10,000 x g was washed twice, suspended in 50 mM KCl, 20 MM Tris-HCl, pH 6.8, and employed for calcium transport studies. The crude microsomal fraction was suspended in 0.6 M KCl, 20 mM Tris-HCl, pH 7.0, centrifuged at 40,000 x g for 45 minutes and the sediment was washed and resuspended in 0.25 M sucrose, 10 mM Tris HCl, pH 7.0.

For studying oxidative phosphorylation, mitochondria were isolated according to the method of Sordahl and Schwartz (116). This fraction was found to yield essentially similar results for calcium transport as obtained by the method outlined above. The microsomal fraction was also obtained by homogenizing the tissue by

the sodium bicarbonate method (34) and the results were similar to those obtained with the heavy microsomal fraction as described above.

(c) Isolation of the myofibrillar fraction

The myofibrillar fraction was obtained by the method of Muir et al. (117) by homogenization of the tissue in 0.1 M KCl, 5 mM histidine, pH 7.0 and centrifugation at 5000 x g. This sediment was washed and suspended in 40% sucrose solution containing 5 mM histidine, pH 7.0 and centrifuged at 15,000 x g. The residue after repeated washing and centrifugation at 5000 x g was resuspended in 0.1 M KCl histidine buffer and used for biochemical studies.

(d) Determination of calcium transport activities

Calcium accumulation by mitochondrial, microsomal and sarcolemmal fractions was determined by employing the millipore filtration technique (115). For mitochondrial and microsomal calcium binding, these particles were incubated in medium containing 100 mM KCl, 10 mM $MgCl_2$, 20 mM Tris-HCl, pH 6.8, 4 mM ATP and 0.1 mM $Ca^{45}Cl_2$ in a total volume of 1 ml. The reaction was started by the addition of $Ca^{45}Cl_2$ and stopped by millipore filtration at various times of incubation at 25°C. The radioactivity in the protein-free filtrate was estimated in a Packard Liquid Scintillation Spectrometer. The calcium uptake by the microsomal fraction was carried out at 37°C in the above medium in the presence of 5 mM potassium oxalate whereas that by the mitochondrial fraction was carried out in the presence of 5 mM inorganic phosphate and 5 mM sodium succinate. The calcium accumulation by the sarcolemmal fraction was carried out in 100 mM KCl, 20 mM Tris-HCl, pH 6.8 and 0.1 mM $Ca^{45}Cl_2$ in the absence or presence of 4 mM MgATP.

(e) Determination of ATP hydrolyzing abilities

For this purpose, the mitochondrial fraction was incubated at 37°C in medium containing 100 mM KCl, 20 mM Tris-HCl, pH 6.8, 10 mM $MgCl_2$ and 4 mM ATP. The microsomal fraction on the other hand was incubated at 37°C in medium containing 100 mM KCl, 10 mM $MgCl_2$, 20 mM Tris-HCl, pH 6.8, 4 mM ATP, 5 mM potassium oxalate and either 0.1 mM $CaCl_2$ or 1 mM EGTA (ethylenebis (oxyethylenenitrilo) tetraacetic acid). The value in the presence of EGTA is taken as basal activity whereas the difference between the basal and total (in the presence

of 0.1 mM $CaCl_2$) activities was considered due to Ca^{++}-stimulated ATPase.

The myofibrillar ATPase activity was determined in the presence and absence of 5 mM sodium azide by incubating this fraction in medium containing 60 mM KCl, 10 mM histidine, pH 7.0, 4 mM EGTA, 2 mM $MgCl_2$, and 2 mM ATP at 37°C. The calcium stimulated ATPase activity of the myofibrillar fraction was determined in the above medium without EGTA but in the presence of 5 mM sodium azide and varying concentrations of $CaCl_2$. The free calcium concentration in the presence of 0.5 mM EGTA buffer was calculated by the method described by Imai and Takeda (118). On the other hand, the sarcolemmal Mg^{++} and Ca^{++} ATPase activities were determined by incubating this fraction in medium containing 50 mM Tris-HCl, pH 7.4, and 4 mM ATP in the absence and presence of 4 mM $MgCl_2$ or 4 mM $CaCl_2$ at 37°C. The sarcolemmal ATP hydrolysis in the absence of $CaCl_2$ or $MgCl_2$ was taken as due to nonspecific ATPase. The sarcolemmal Na^+-K^+ATPase activity was estimated by finding the difference between ATP hydrolysis in the absence or presence of 2 mM ouabain in a medium containing 50 mM Tris HCl, pH 7.4, 4 mM $MgCl_2$, 100 mM NaCl and 10 mM KCl, and 4 mM ATP at 37°C.

All the reactions for ATP hydrolysis were started by the addition of ATP and stopped by the addition of 12% cold trichloroacetic acid and centrifugation. The inorganic phosphate released in the clear supernatant was measured by the method of Taussky and Shorr (119). The protein concentrations were determined by the method of Lowry et al. (120).

(f) Determination of sarcolemmal adenylate cyclase activity

The adenylate cyclase activity was assayed by employing descending chromatography according to the method by Drummond and Duncan (121). The incubation medium at 37°C contained 50 mM Tris-HCl, pH 8.5, 8 mM caffeine, 5 mM KCl, 20 mM phosphoenolpyruvate, 15 mM $MgCl_2$, 130 µg/ml pyruvate kinase, and 0.4 mM ATP ^{14}C. The adenylate cyclase activity was studied in the absence (basal) and presence of 100 µM epinephrine or 4 mM NaF.

(g) Determination of mitochondrial respiration and oxidative phosphorylation

The mitochondrial oxygen consumption and oxidative phosphorylation (ADP:O ratio) were measured polarographically at 28°C using a Gilson oxygraph and

Clarke electrode in a medium containing 0.25 M sucrose, 10 mM Tris-HCl, pH 7.4, 10 mM K_2HPO_4, 1.5 mM pyruvate and 0.3 mM malate. This method has been described by Sordahl and Schwartz (116). State 3 respiration was initiated by the addition of 200 nmoles ADP whereas state 4 respiration ensued when all the ADP was phosphorylated. The respiratory control index (RCI) was calculated as the ratio of oxygen uptake rates in states 3 and 4 whereas the phosphorylation rate was calculated by multiplying the oxygen uptake rate in state 3 ($QO_2(3)$) by the ADP:O ratio.

5. Statistical Analysis

The student's t test was used to analyze statistical significance of differences in paired and unpaired data. Data for infected animals was statistically compared with data from both sham operated control and uninfected catheterized animals at the same time period after injection.

RESULTS

1. Pathological Changes in a New Model of Bacterial Endocarditis Indicating Infective Cardiomyopathy

(a) General observations

In the first series of experiments, different doses of bacteria were injected in New Zealand White and Dutch rabbits in order to determine the number of organisms necessary to produce endocarditis without any incidence of mortality due to early toxemia. The results shown in Table II indicate that all the New Zealand White and Dutch rabbits died within 24 hours from toxemia due to overwhelming bacterial invasion after receiving 10^9 and 10^7 bacterial organisms/kg respectively. The most effective doses for producing endocarditis in all injected animals without toxic complications were 10^7 organisms/kg for New Zealand White and 5×10^5 organisms/kg for Dutch rabbits. These results suggest that not only were Dutch rabbits more sensitive to the bacteria but also the margin of safety in these animals was smaller than in the New Zealand White strain. It was also noted that the New Zealand White and Dutch rabbits with gross evidence of endocarditis died within 6-8 days and 4-6 days of infection respectively. None of the normal or saline injected catheterized animals showed any evidence of infection. All further experiments were carried out with New Zealand White rabbits and 10^7 bacterial organisms/kg were used for producing endocarditis.

Since hyperthermia and weight loss are common manifestations of the presence of infection, rectal temperature and body weight were monitored in normal and experimental animals. As indicated in Figure 1 the infected animals became hyperthermic within 2 days and demonstrated progressive weight loss whereas the normal and catheterized uninfected rabbits maintained a constant temperature and exhibited the normal rise in body weight characteristic of rabbits of this age. Furthermore, lethargy, patchy hair loss, and demonstrable pain upon handling were general characteristics of infected rabbits. In contrast to control and catheterized uninfected animals, the infected rabbits had greenish pleural and often pericardial effusions. The lungs in infected animals appeared congested; however no gross abnormalities were seen in liver, spleen or kidney.

TABLE II

Incidence of Streptococcal Endocarditis in Operated Rabbits Injected with Different Doses of Streptococcus Viridans

DOSE (No. of organisms/kg)	NEW ZEALAND WHITE RABBITS			DUTCH RABBITS		
	Toxemia and death within 24 hr.	Evidence of Endocarditis	Survival Time	Toxemia and death within 24 hr.	Evidence of Endocarditis	Survival Time
10^9	3/3*	- -	- -			
10^8	2/4	2/4	- -			
$5x10^7$	1/8	7/8	6-8 days			
10^7	0/12	12/12	6-8 days	4/4	- -	- -
10^6	0/4	3/4	- -	3/4	1/4	- -
$5x10^5$	0/4	2/4	- -	1/8	7/8	4-6 days
10^5	- -	- -	- -	0/3	2/3	4-6 days
10^4	- -	- -	- -	0/3	0/3	- -
Saline	0/10	0/10	- -	0/8	0/8	- -

* The denominator represents the number of animals employed in each experiment whereas the numerator indicates the incidence of early toxemia or endocarditis.

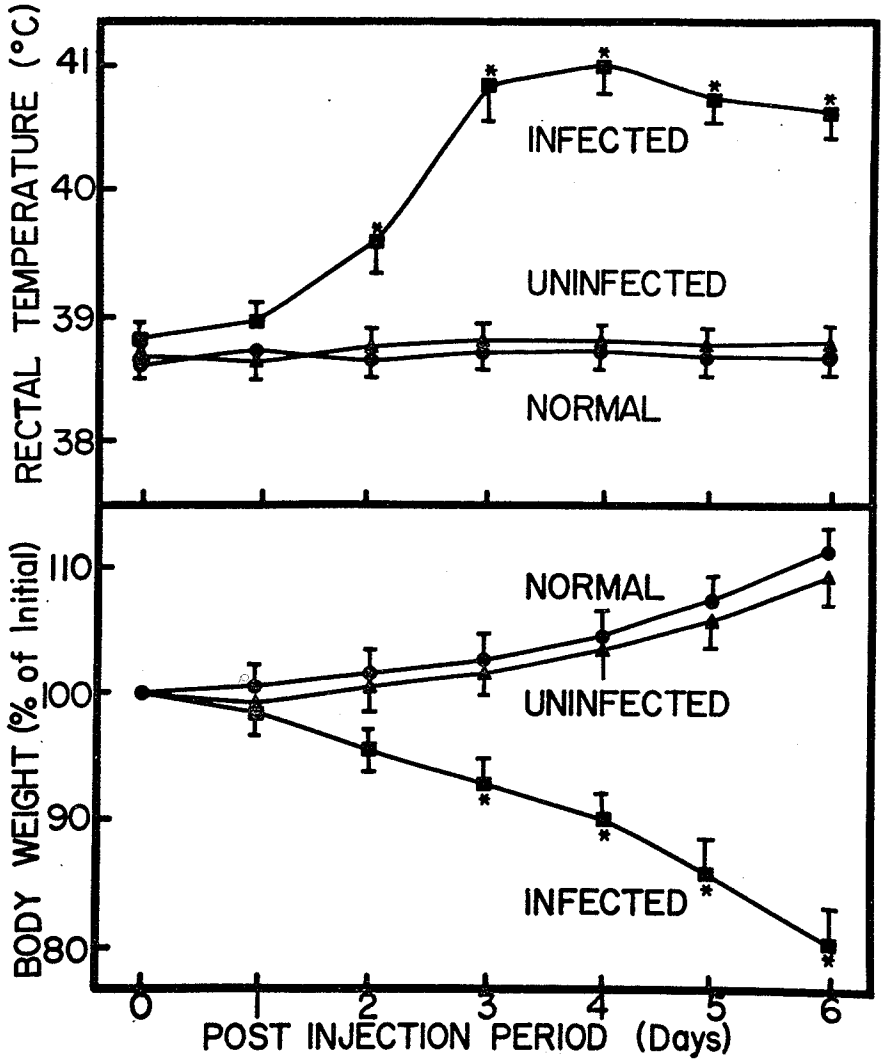

FIGURE 1 Alterations in body weight and rectal temperature following injection of saline or Strep. viridans in catheterized rabbits.
* - significantly different from control and uninfected rabbits ($P<0.05$)

(b) Gross and histological changes in heart and valve

Progressive changes in heart size and valvular vegetation were observed at 1, 3 and 6 days after infection. At 3 and 6 days after infection the hearts were obviously enlarged with marked thickening of the left ventricular wall (Fig. 2). Although operated uninfected rabbit hearts were also enlarged, the ventricular wall did not appear as thickened. At the most severe stages of disease, the infected hearts seemed more flabby and myocardium of the left ventricle appeared pale and mottled; gross examination of the aorta revealed a firm polypous mass filling most of the lumen. The results shown in Table III reveal that not only are heart and left ventricular weight increased ($P<0.01$) but also there is a significant increase ($P<0.01$) in wet weight/dry weight ratio in uninfected and infected catheterized animals in comparison to sham operated controls. The infected rabbits at 6 days after bacterial injection had significantly larger hearts ($P<0.01$) than either control or uninfected catheterized rabbits. Left ventricle/body weight ratio was significantly increased ($P<0.01$) in both uninfected and infected rabbits, and the magnitude of the change was greater ($P<0.01$) in infected in comparison to uninfected animals; however, it must be noted that the infected animals demonstrated a 20% loss of weight at later stages of disease in contrast to uninfected and control animals.

From Figure 3 it is apparent that the aortic valve area as well as part of the ventricular wall were covered with a yellowish mass of friable vegetations of rubberlike consistency. As seen in Figure 3(b) only small whitish nodules representing non-bacterial thrombotic endocarditis are seen in the catheterized uninfected hearts. Vegetations were also associated with the mitral valve; however no gross lesions were seen in the right ventricles of any hearts.

Histologically the aortic valve area appeared swollen with an increased amount of fibrous tissue (Fig. 4). Vegetations were amorphous with occasional polymorphonuclear and red blood cells and bacterial clumps. The endocardial tissue adjacent to the valve at late stages of disease revealed focal necrosis, bacterial infestation, and mononuclear cell infiltrate; polymorphonuclear cells were common at early stages of disease and also in areas of active destruction. The salient histological changes in the papillary muscles of the catheterized uninfected animals include increased myofibre size and interstitial edema (Fig. 5(a).). Papillary muscle

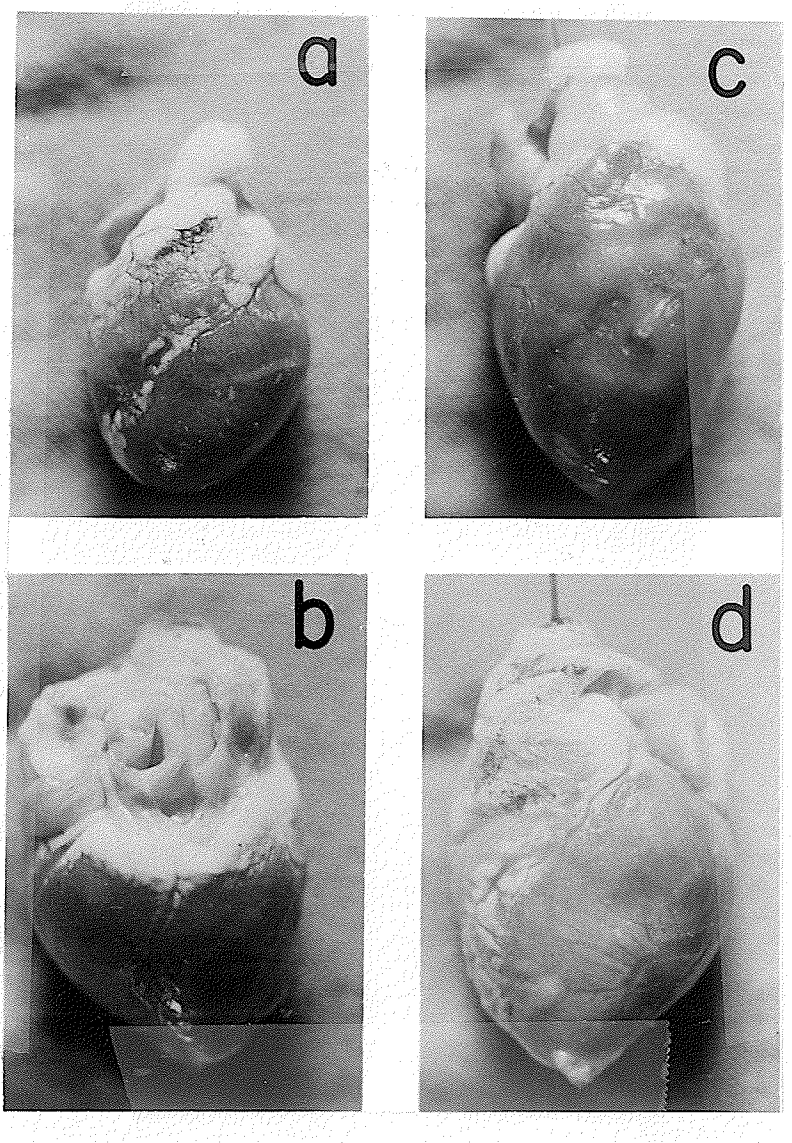

FIGURE 2 Hypertrophy in experimental bacterial endocarditis. (a) heart from sham operated control rabbit; b) heart from uninfected catheterized rabbit 6 days after saline injection; (c) heart from rabbit with bacterial endocarditis 3 days after injection of Strep. viridans; (d) heart from rabbit with bacterial endocarditis 6 days after injection of Strep. viridans. X 1.5

TABLE III

Evaluation of Cardiac Hypertrophy in Control, Uninfected and Infected Rabbits

	Heart Weight (g)	Left Ventricle (g)	Left Ventricle/ Body Weight ($\times 10^3$)	Wet Weight/ Dry Weight
Control	4.47 ± 0.16	2.91 ± 0.11	1.36 ± 0.06	4.085 ± 0.19
Uninfected (3 days)	5.01 ± 0.15	3.41 ± 0.34	1.50 ± 0.11	4.110 ± 0.26
Uninfected (6 days)	5.86 ± 0.35*	4.00 ± 0.28*	1.76 ± 0.06*	4.55 ± 0.17*
Infected (3 days)	5.98 ± 0.31*	3.95 ± 0.21*	2.10 ± 0.10**	4.49 ± 0.22*
Infected (6 days)	6.57 ± 0.30**	4.90 ± 0.16**	2.55 ± 0.09**	4.98 ± 0.15**

Each value represents the mean ± standard error of 6-10 experiments.

* - Significantly different from sham operated control hearts ($P<0.01$).
** - Significantly different from control and uninfected hearts ($P<0.01$).

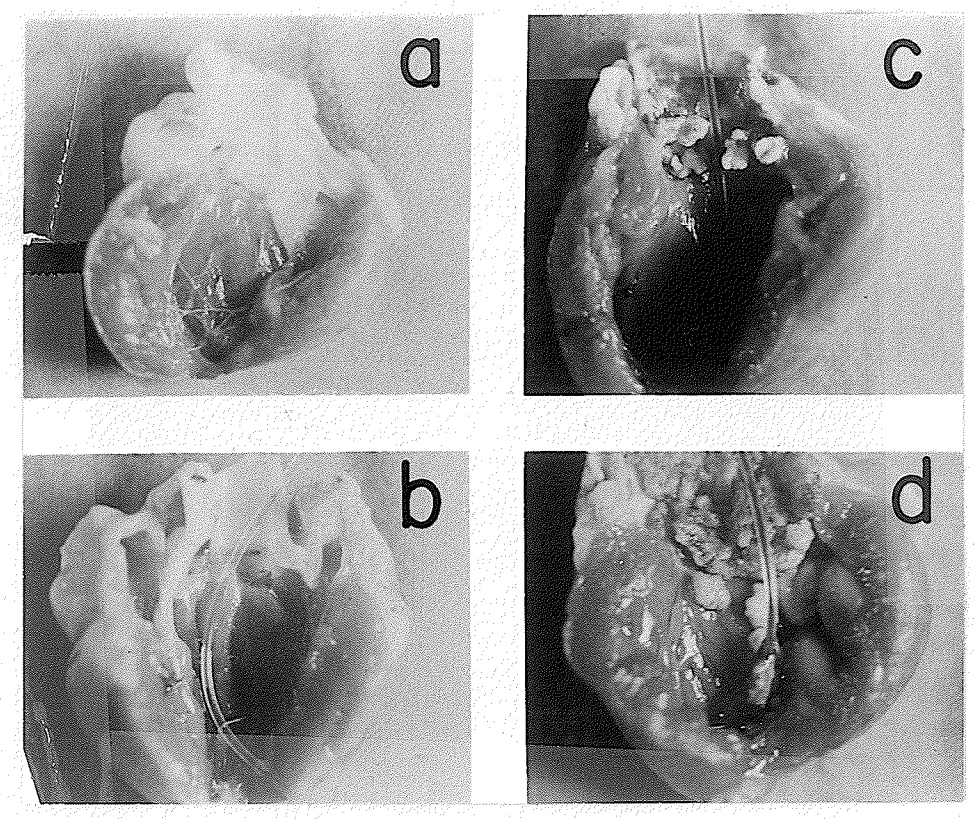

FIGURE 3 Valvular vegetations in experimental bacterial endocarditis. (a) heart from sham operated control rabbit; (b) heart from uninfected catheterized rabbit 6 days after injection with saline; (c) heart from rabbit with bacterial endocarditis 3 days after injection with Strep. viridans; (d) heart from rabbit with bacterial endocarditis 6 days after injection with Strep. viridans. X 1.5

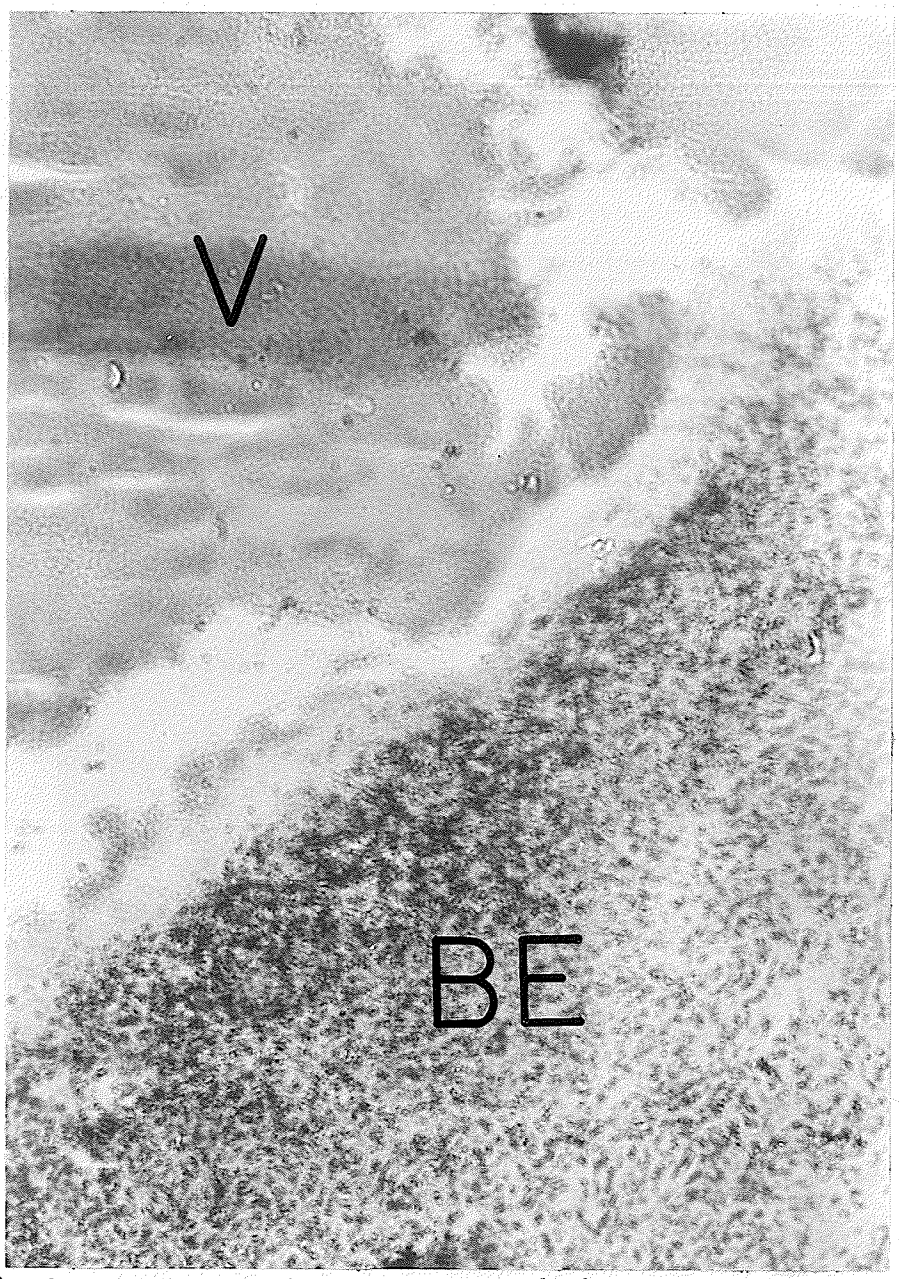

FIGURE 4 Low power magnification of para valvular area from heart of 6 day infected rabbit showing amorphous vegetations (V) and bacteria and inflammatory cell infiltration (BE). Hematoxylin and eosin. X156

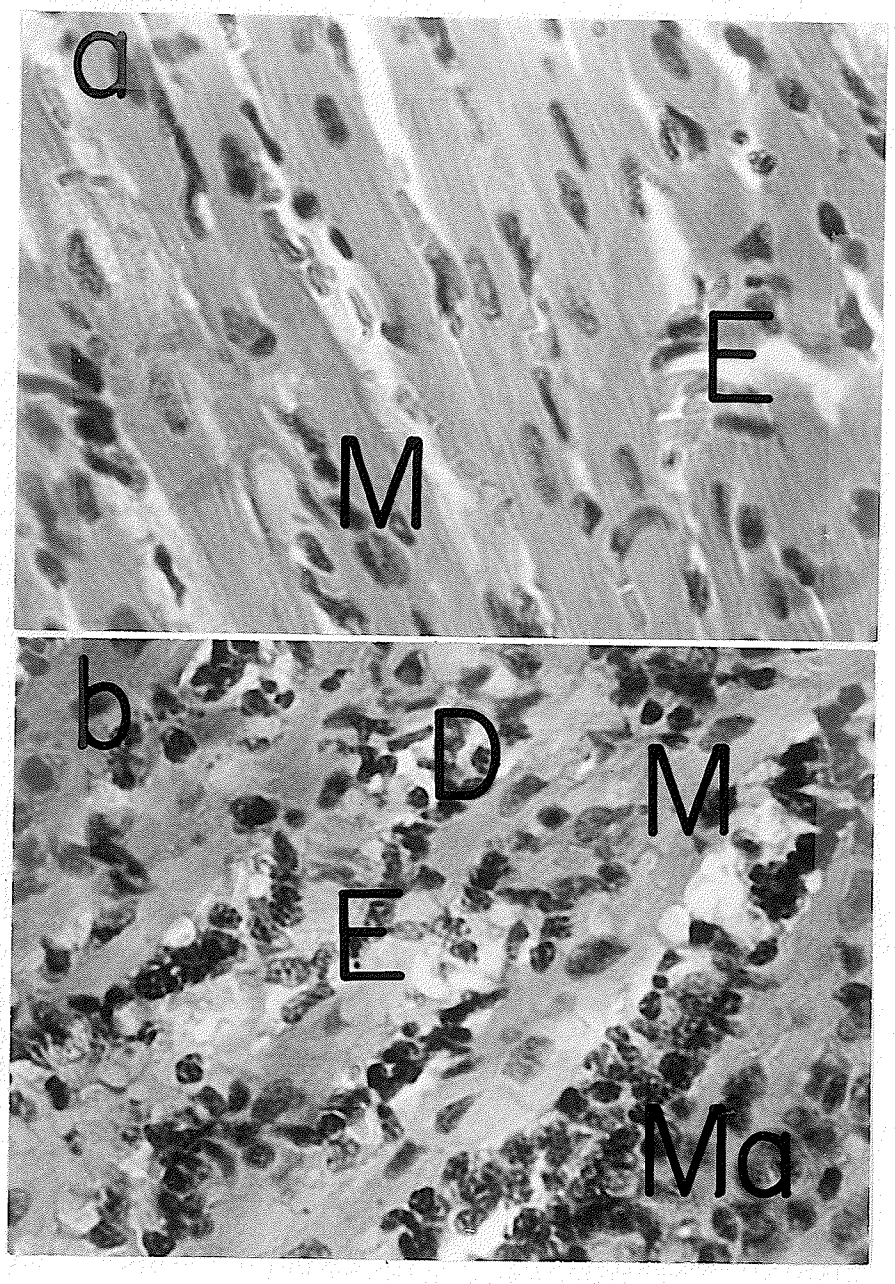

FIGURE 5 Papillary muscle histopathology in bacterial endocarditis. (a) papillary muscle from heart of uninfected catheterized rabbit 6 days after saline injection showing increased size of myofibres (M) and some edematous spaces (E); (b) papillary muscle from heart of rabbit with bacterial endocarditis 6 days after injection with Strep. viridans showing increased size of myofibres (M), monocytic infiltration (Ma), areas of muscle degeneration and fatty infiltration (D) and edematous spaces (E). Hematoxylin and eosin; X 625.

from infected hearts (Fig. 5(b)) showed signs of interstitial edema, infiltration with macrophages and other monocytic cells (traditionally called Bracht-Wachter lesions (105))(Fig. 6) and myofibre hypertrophy and destruction. Loss of the normal myocardial architecture as well as signs of fatty degeneration were seen in the papillary muscles of the infected hearts. Sections of the left ventricle tissue from sham operated, uninfected catheterized, and infected hearts were also examined microscopically. In comparison to the sham operated controls, both uninfected and infected hearts showed marked thickening of myofibres as well as interstitial edema (Fig. 7). In addition, the infected left ventricles showed monocytic infiltration with areas of muscle necrosis and fatty degeneration (Fig. 8). The monocytic infiltration and muscle necrosis was particularly severe in perivascular areas. These histological lesions, although relatively localized and less severe at 3 days of infection became consistently diffuse and more intense at 6 days of infection. No changes were seen in the right ventricular tissue of any animal.

(c) Ultrastructural alterations in myocardium

Electron microscopic examination of the papillary muscle was done at 0, 1, 3, and 6 days after infection. No changes were seen until 3 days after bacterial injection when signs of mitochondrial and sarcotubular swelling, separation of the intercalated disc and some areas of muscle contracture appeared (Fig. 9). However, at late stages of the disease (6 days after infection), the papillary muscle showed signs of immense tissue damage such as wide separation of the intercalated disc, generalized contracture, mitochondrial destruction, and disruption of myofibrillar continuity (Fig. 10). The catheterized uninfected rabbit heart papillary muscle demonstrated relatively minor changes in ultrastructure such as swelling of lateral sacs of the sarcotubular system and mitochondria, and some contracture of myofibrils (Fig. 11). Occasional signs of intermyofibrillar edema was noted in the vicinity of the intercalated disc in muscles from the catheterized uninfected animals.

2. Alterations in Myocardial Function During Bacterial Infective Cardiomyopathy

(a) Serum enzymes and electrolytes

The serum levels of some important intracellular enzymes and electrolytes were measured in sham operated, uninfected catheterized, and infected animals

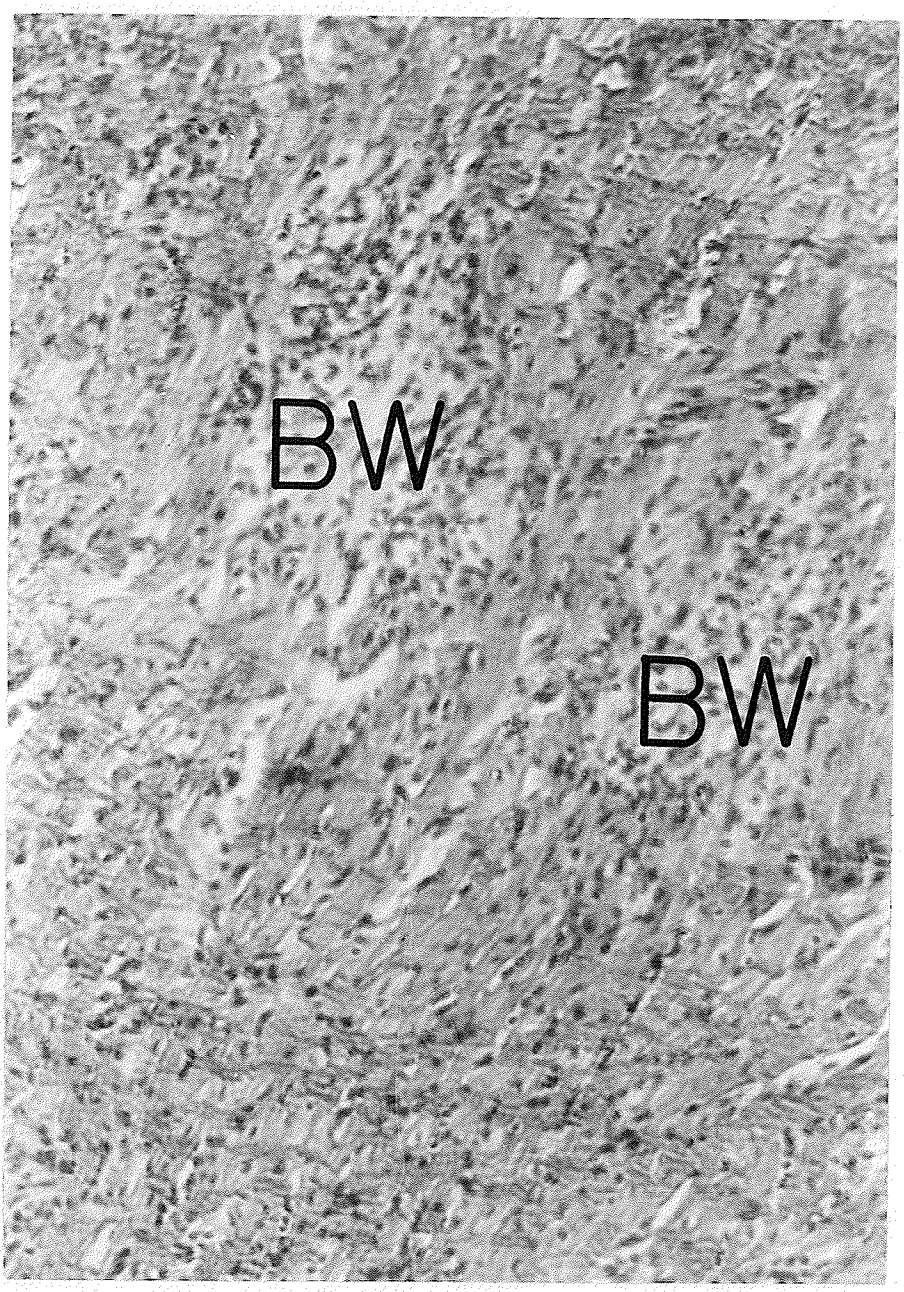

FIGURE 6 Low power magnification of papillary muscle from heart of rabbit with bacterial endocarditis showing focal areas of bacterial invasion and Bracht-Wachter lesions (BW). Hematoxylin and eosin; X 250.

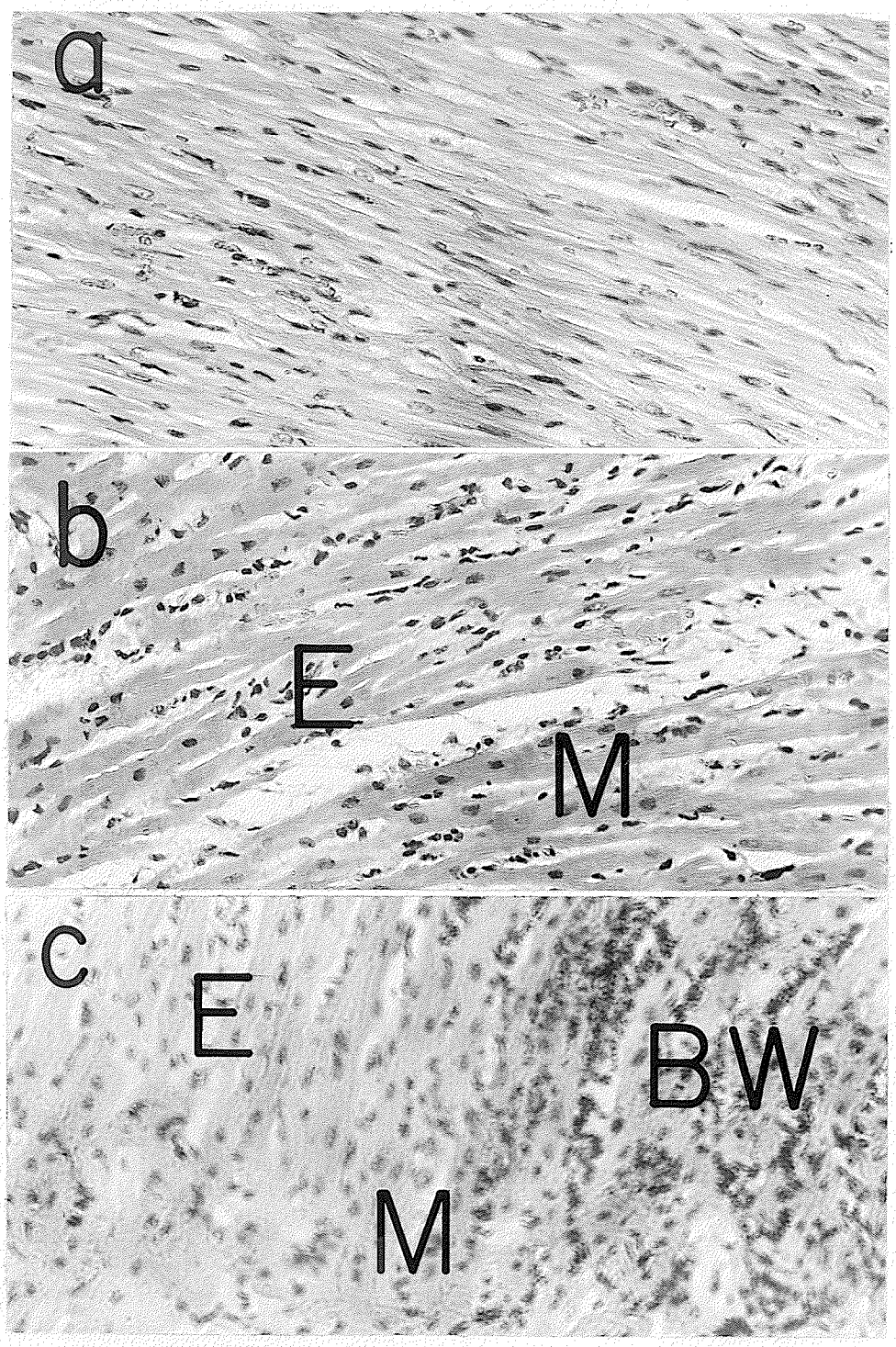

FIGURE 7 Low power photomicrograph of left ventricular myocardium from (a) sham operated control, (b) 6 day uninfected, and (c) 6 day infected rabbits, showing Bracht-Wachter lesions (BW) consisting of monocytic and bacterial infiltration and muscle degeneration, edematous spaces (E), and myofibre hypertrophy. Hematoxylin and eosin; X 250.

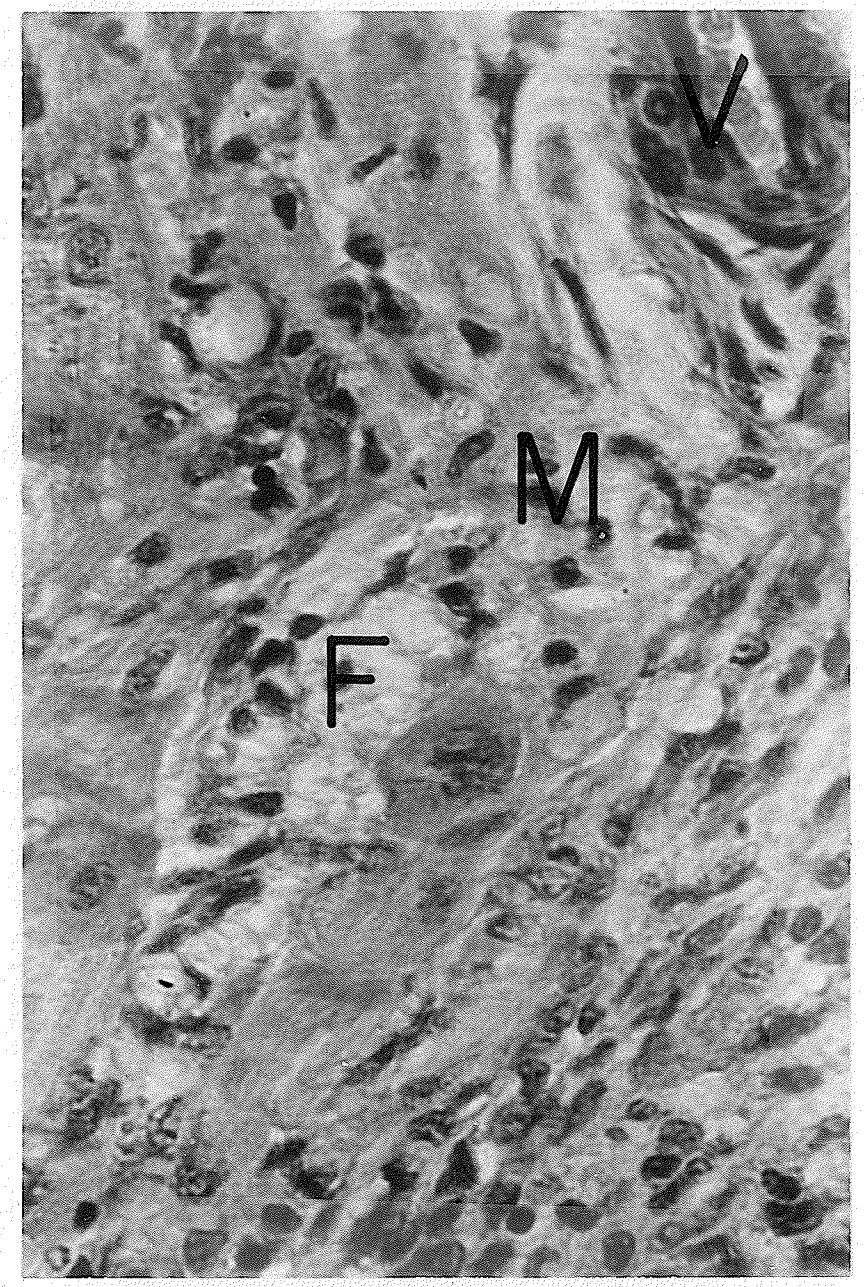

FIGURE 8 High power photomicrograph of left ventricular myocardium of rabbit with bacterial endocarditis six days after injection with Strep. viridans showing fatty degeneration (F), myofibre disruption and necrosis (M) and damage particularly severe near vessels (V). Hematoxylin and eosin; X 625.

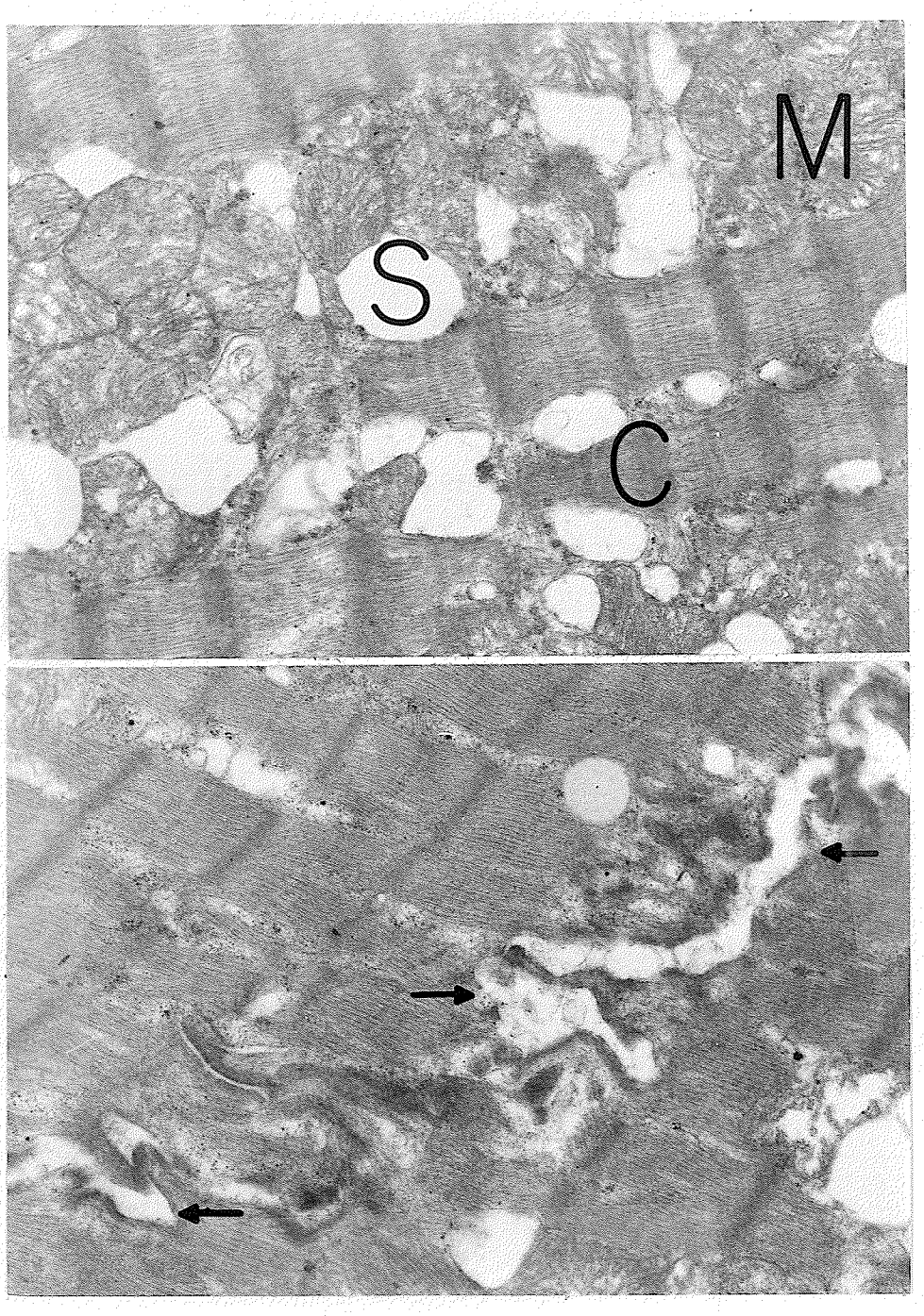

FIGURE 9 Electron photomicrograph of papillary muscle from heart of rabbit with bacterial endocarditis 3 days after injection of Strep. viridans showing mitochondria (M) and sarcotubular (S) swelling and myofibrillar contracture (C) as well as separation of the intercalated disc (arrows). Uranyl acetate-lead citrate; X 16,500.

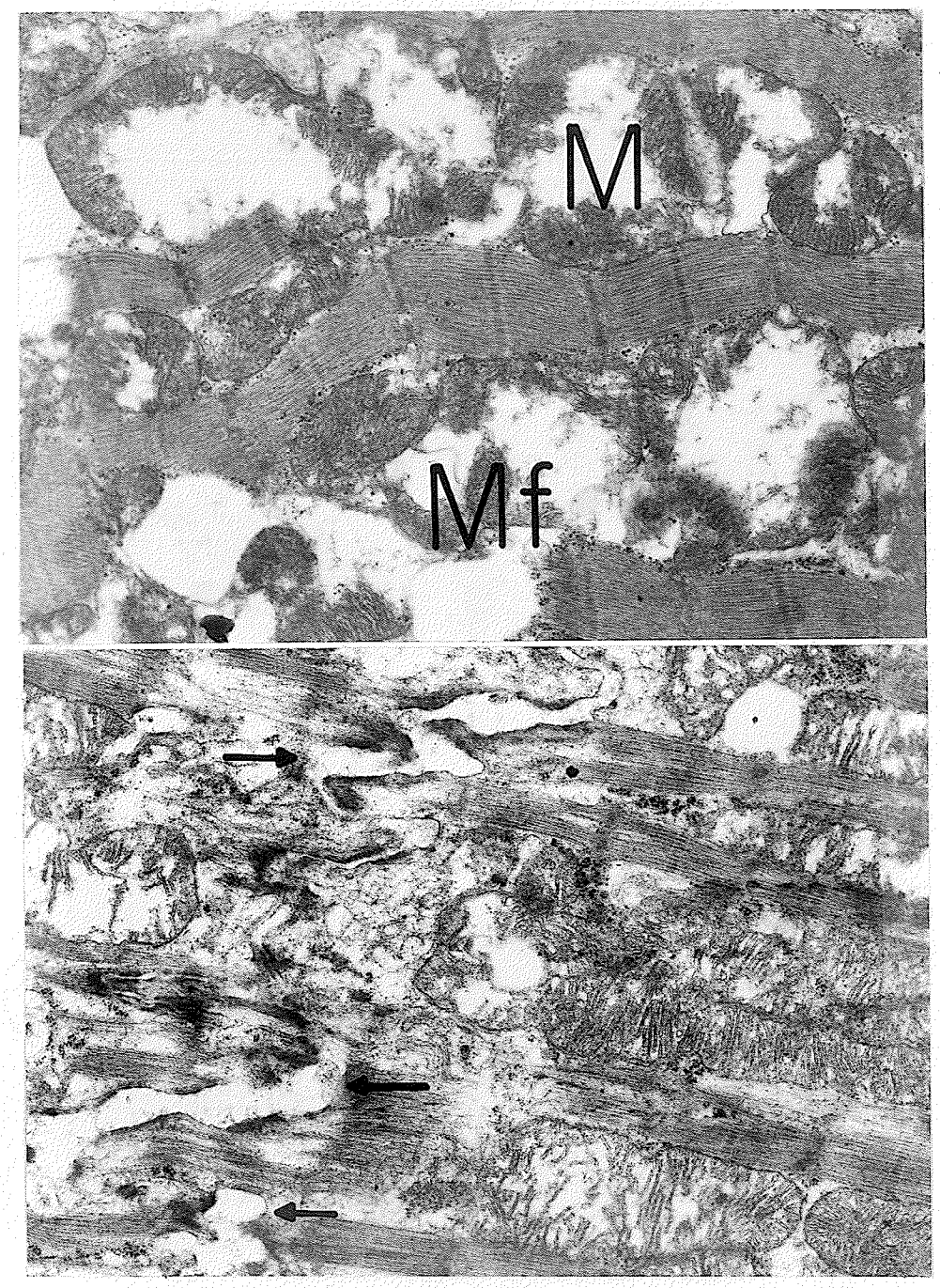

FIGURE 10 Electron photomicrograph of papillary muscle from heart of rabbit with bacterial endocarditis 6 days after injection of Strep. viridans showing drastic ultra-structural damage with swelling and destruction of mitochondria (M), myofibrillar disruption (MF) as well as wide separation of the intercalated disc (arrows). Uranyl acetate-lead citrate.

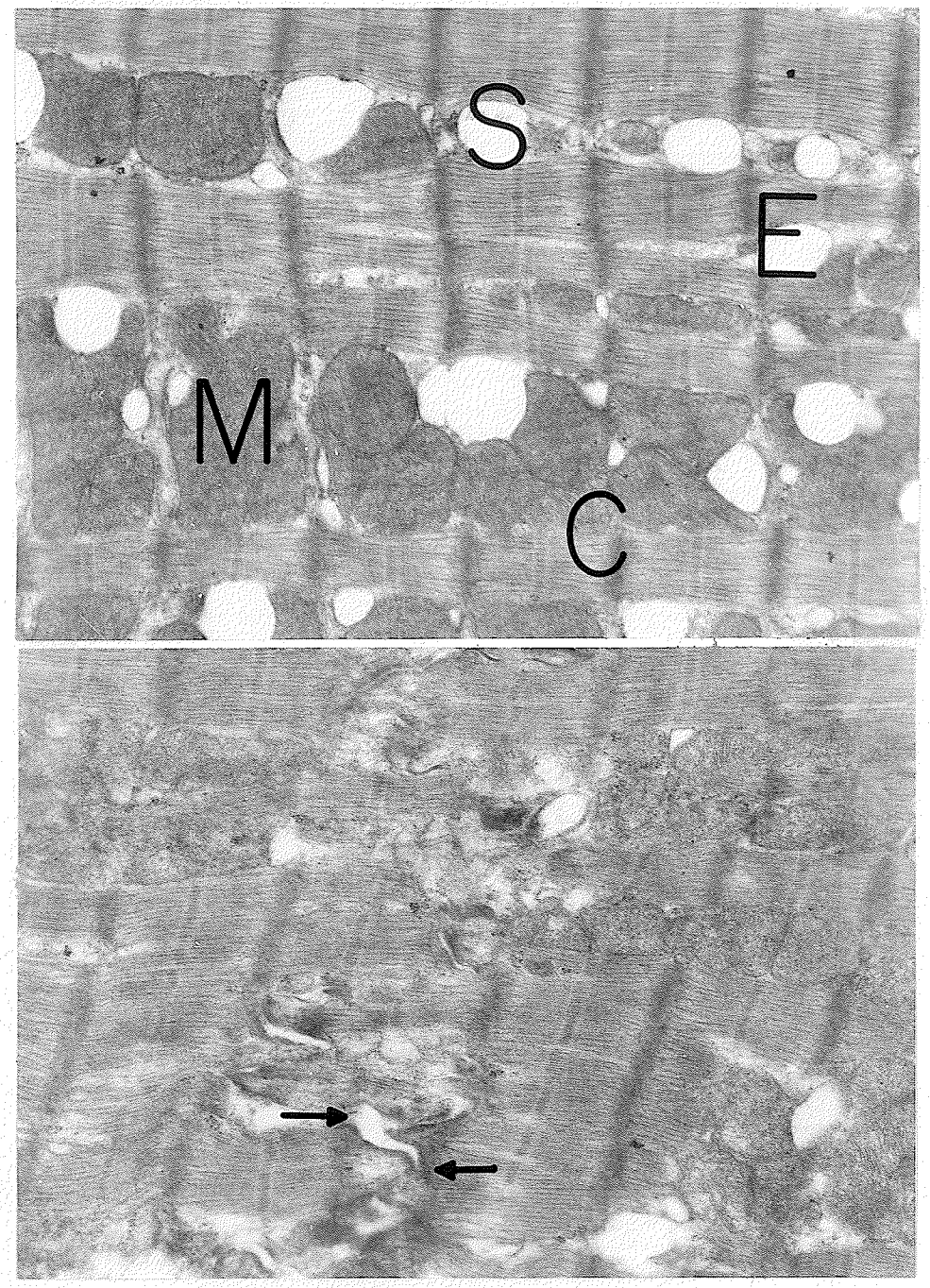

FIGURE 11 Electron photomicrograph of papillary muscle from heart of catheterized rabbit 6 days after injection of saline showing relatively minor changes in ultrastructure including myofibrillar contracture (C) edematous spaces (E) and mitochondria (M) and sarcotubular (S) swelling. Some localized widening of the intercalated disc is apparent (arrows). Uranyl acetate-lead citrate; X 16,500.

6 days after injection. Significant ($P<0.01$) elevations of CPK, LDH and GOT were observed in both uninfected catheterized and infected animals (Table IV). Although the increases in CPK and GOT in infected and uninfected animals were comparable, the elevation in LDH in uninfected catheterized animals was significantly ($P<0.01$) more than that in the infected animals. In contrast to the serum from control and uninfected animals, the serum of infected rabbits had a significant ($P<0.01$) decrease in the level of alkaline phosphatase. In comparison to both control and uninfected catheterized animals, the levels of serum calcium, magnesium and sodium were slightly but significantly ($P<0.05$) decreased whereas that of potassium was increased ($P<0.05$) in infected animals (Table V).

(b) Myocardial electrolytes

Table VI shows electrolyte contents in the left ventricular muscle from control, uninfected catheterized, and infected hearts. The levels of calcium and potassium decreased ($P<0.05$) whereas the sodium level increased ($P<0.05$) 6 days after saline injection in catheterized animals without any significant ($P>0.05$) changes in the magnesium level ($P>0.05$). Three and 6 days after bacterial injection myocardial potassium and calcium were decreased ($P<0.05$) and sodium increased ($P<0.05$) in comparison to controls. Myocardial magnesium decreased ($P<0.05$) after 3 days and increased ($P<0.05$) after 6 days of infection. On the other hand, calcium, magnesium and potassium levels in 6 day infected hearts were not significantly ($P>0.05$) different from the uninfected hearts; however, the level of sodium was significantly ($P<0.05$) higher in infected hearts.

(c) Electrocardiographic and pressure changes

Typical electrocardiographic tracings (Lead II) from sham operated, uninfected and infected rabbits are shown in Figure 12. All the infected and uninfected catheterized animals showed increased amplitude of the QRS complex and flattening or inversion of the T-wave.

Both infected rabbits at 3 days and uninfected rabbits at 6 days had an increase ($P<0.05$) in heart rate and a widening ($P<0.05$) of pulse pressure in comparison to controls (Table VII); however, no change ($P>0.05$) in pulse pressure and a decrease ($P<0.05$) in heart rate were observed in 6 day infected rabbits.

TABLE IV

Serum Enzymes in Control, Uninfected and Infected Rabbits

	Creatine Phosphokinase (CPK) (i.u.)	Lactic Dehydrogenase LDH (i.u.)	Transaminase GOT (i.u.)	Alkaline Phosphatase (i.u.)
Control	449 ± 88	281 ± 24	48 ± 6.2	125 ± 5.2
Uninfected (6 days)	1466 ± 194*	1006 ± 47*	133 ± 13.5*	122 ± 10.0
Infected (6 days)	1490 ± 120*	621 ± 81**	165 ± 2.7*	61 ± 10.1**

Each value represents the mean ± standard error of 6 experiments and is expressed in international units (i.u.).

* - Significantly different from control rabbits ($P<0.01$).
** - Significantly different from control and uninfected rabbits ($P<0.01$).

TABLE V

Serum Electrolytes in Control, Uninfected and Infected Rabbits

	Calcium (mEq/l)	Magnesium (mEq/l)	Sodium (mEq/l)	Potassium (mEq/l)
Control	6.9 ± 0.09	2.0 ± 0.09	141.8 ± 1.07	7.7 ± 0.34
Uninfected (6 days)	6.6 ± 0.10	1.9 ± 0.09	140.1 ± 0.91	7.5 ± 0.27
Infected (6 days)	6.1 ± 0.16*	1.6 ± 0.08*	137.0 ± 0.68*	8.9 ± 0.19*

Each value represents the mean ± standard error of 6 experiments.

* - Significantly different from control and uninfected rabbits ($P<0.05$).

TABLE VI

Myocardial Electrolytes in Control, Uninfected and Infected Hearts

	Myocardial Electrolytes (μmoles/g heart dry weight)			
	Calcium	Magnesium	Sodium	Potassium
Control	7.41 ± 0.28	31.75 ± 0.97	130.7 ± 9.6	342.7 ± 10.5
Uninfected (6 days)	5.69 ± 0.36*	33.66 ± 1.16	213.9 ± 14.5*	267.4 ± 14.8*
Infected (3 days)	3.87 ± 0.41*	28.45 ± 0.58*	171.3 ± 13.2*	278.5 ± 8.9*
Infected (6 days)	6.01 ± 0.29*	35.10 ± 0.72*	258.2 ± 11.9**	257.7 ± 12.3*

Each value represents the mean ± standard error of 4 experiments.

*-Significantly different from control ($P<0.05$).
**-Significantly different from control and uninfected hearts ($P<0.05$).

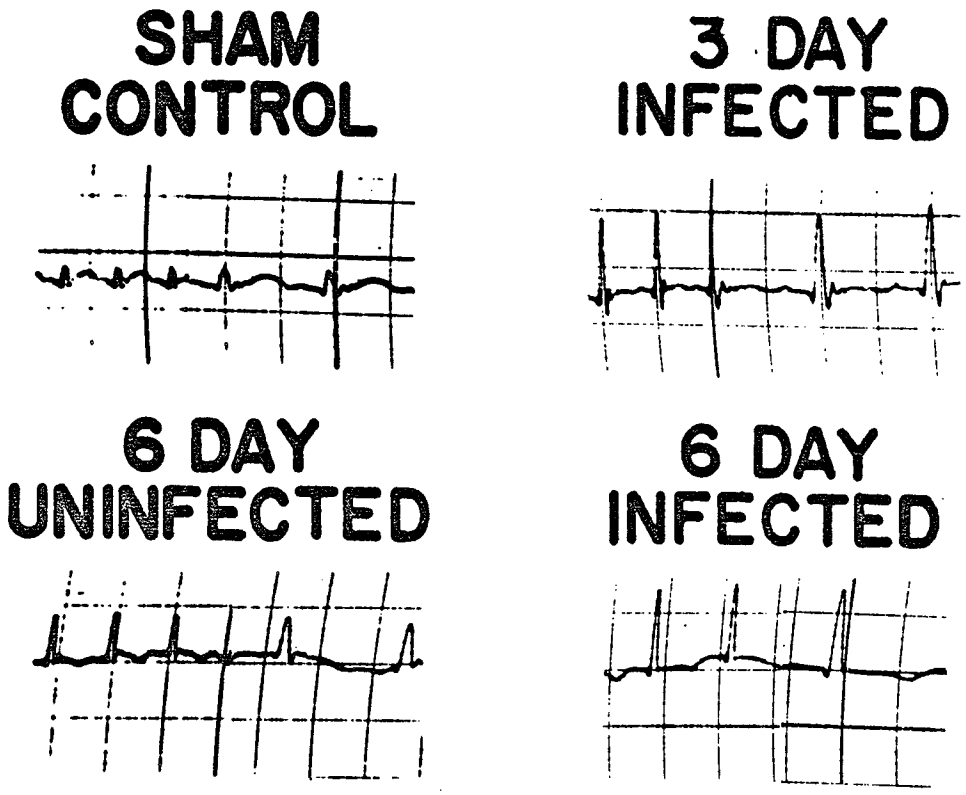

FIGURE 12 Electrocardiographic abnormalities in sham operated control, 6 day uninfected, and 3 and 6 day infected rabbits (lead II) showing increased amplitude of QRS complex and flattening or inversion of the T wave in both uninfected and infected animals.

TABLE VII

Heart Rate and Blood Pressure in Control, Uninfected and Infected Rabbits

	Heart Rate (bpm)	Blood Pressure (mmHg)		
		Diastolic	Systolic	Pulse
Control	251 ± 6.6	79.3 ± 5.4	83.4 ± 2.9	4.1 ± 0.91
Uninfected (6 days)	295 ± 6.9*	83.2 ± 3.9	92.9 ± 3.1	9.7 ± 0.87*
Infected (3 days)	280 ± 6.1*	56.4 ± 6.3**	75.9 ± 4.7	19.5 ± 1.1*
Infected (6 days)	195 ± 7.1**	63.7 ± 4.1**	69.1 ± 3.9**	5.4 ± 0.79

Each value represents mean ± standard error of 4 experiments. bpm = beats per minute.

* - Significantly different from control rabbits ($P<0.05$)
** - Significantly different from control and uninfected rabbits ($P<0.05$)

Although a decrease ($P < 0.05$) in diastolic pressure was demonstrated at both 3 and 6 days of infection, a decrease ($P<0.05$) in systolic blood pressure was only seen at 6 days of infection. The absence of widened pulse pressure at late stages of disease may be related to the extensive vegetation development seen in these animals.

Intraventricular pressure records showed a marked diminution ($P<0.05$) in the rates of pressure development and fall in infected animals at 3 and 6 days in comparison to control or uninfected animals (Table VIII). A significant ($P<0.05$) prolongation of both times to peak tension and half relaxation was also noted in the infected animals.

Recently, an indirect measurement of the velocity of shortening of the contractile element of myocardium in intact animals has been described (122,123) which involves a plot of dP/dt/P vs left ventricular isovolumic pressure. A similar graphical analysis of ventricular pressure changes is shown in Figure 13. It is apparent that extrapolated maximal velocity of shortening in animals infected for 3 and 6 days is depressed in comparison to both control and uninfected catheterized rabbits. Since no effort was made to calculate a stiffness constant value for rabbit myocardium, it must be remembered that the values given reflect only relative changes in velocity of shortening of the contractile element.

(d) Contractile force in perfused hearts

In order to rule out the effects of anaesthesia on myocardium as well as to establish the differences among contractile states of infected, uninfected, and sham operated rabbit hearts, it was decided to monitor the ability of these hearts to generate contractile force under in vitro conditions. For this purpose, hearts were perfused by the Langendorff technique and their abilities to generate contractile force were monitored at different resting tensions. The results shown in Figure 14 reveal that the ability of 6 day infected heart to generate contractile force was markedly less at each resting tension in comparison to both control and uninfected hearts. A typical experiment with sham operated and infected hearts shows that under the same resting tension (0.5 g/g heart) not only is developed contractile force decreased but also the rates of tension development and relaxation are decreased

TABLE VIII

Intraventricular Pressure in Control, Uninfected and Infected Rabbits

	Development of Left Ventricular Pressure		Left Ventricular Relaxation	
	dP/dt (mmHg/sec)	Time to Peak Tension (sec)	dR/dt (mmHg/sec)	Half Relaxation Time (sec)
Control	476 ± 26	.109 ± .007	332 ± 21	0.058 ± .002
Uninfected (6 days)	404 ± 28*	.122 ± .010	326 ± 33	0.046 ± .004
Infected (3 days)	259 ± 31*	.133 ± .007*	217 ± 22*	0.081 ± .002*
Infected (6 days)	198 ± 24**	.151 ± .009**	185 ± 27**	0.104 ± .003**

Each value represents the mean ± standard error of 3 experiments.

* - Significantly different from control ($P<0.05$)
** - Significantly different from control and uninfected rabbits ($P<0.05$)

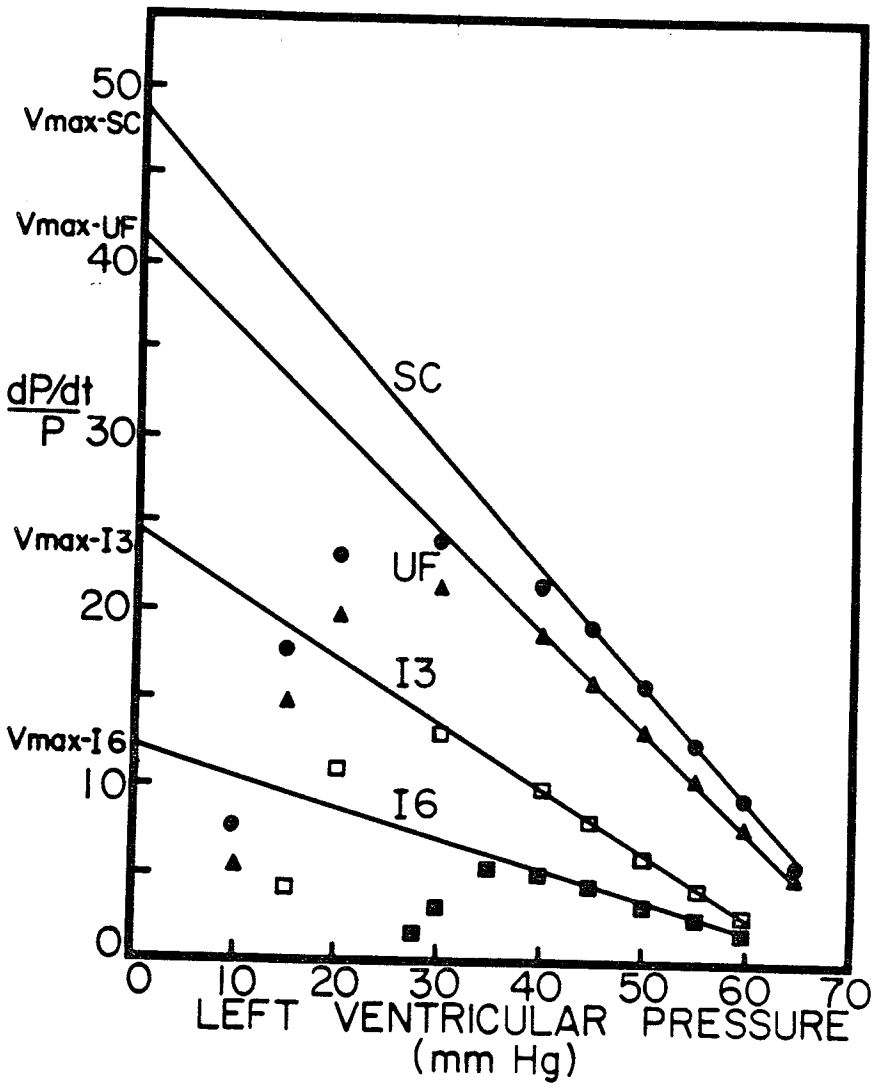

FIGURE 13 Representative comparison of the left-ventricular pressure-velocity relation during isovolumic contraction in sham operated control (SC), 6 day uninfected (UF), 3 day infected (I3), and 6 day infected (I6) hearts. V_{max}-relative extrapolated maximum contractile element velocity; dP/dt - rate of development of left ventricular pressure; P - left ventricular pressure.

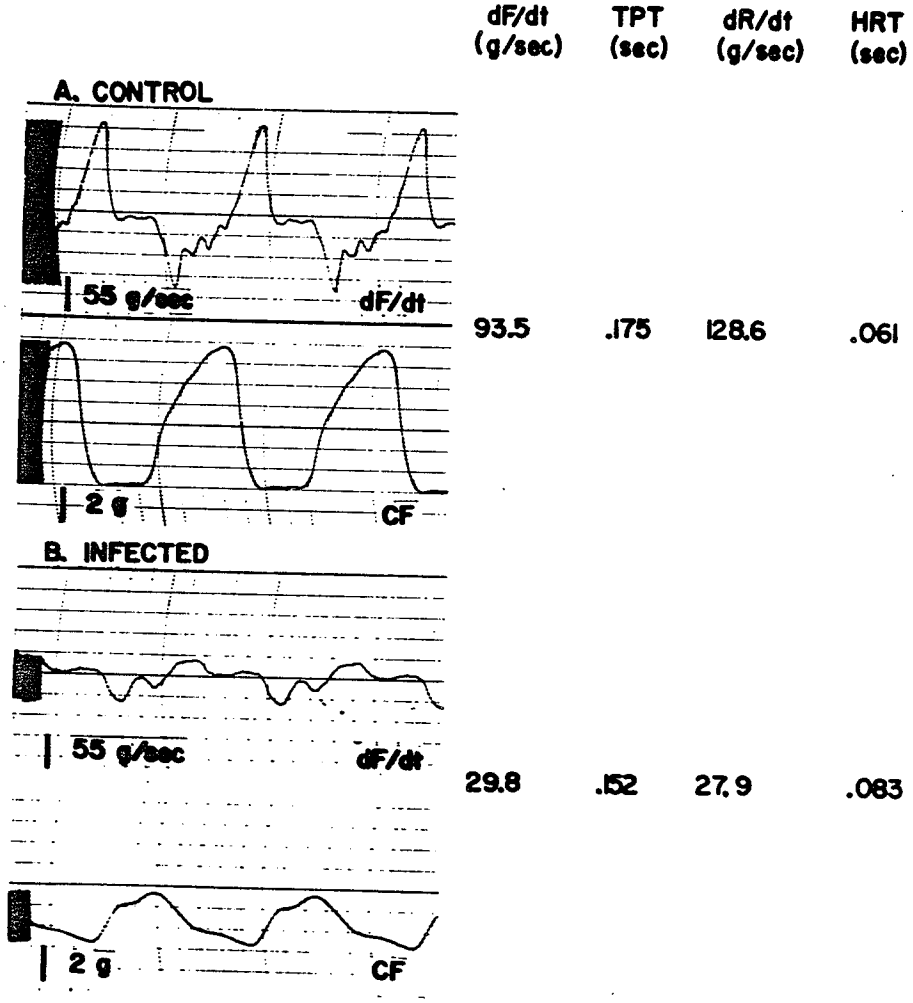

FIGURE 14 Representative tracings of force development by the isolated perfused rabbit heart. (a) sham operated control; (b) 6 day infected. CF - developed contractile force; dF/dt - rate of development of tension; dR/dt - rate of relaxation or fall in tension; HRT - time for half relaxation; TPT - time for peak tension development.

(Fig. 15). Although time for half-relaxation was prolonged, the time to peak tension was decreased.

3. Abnormalities in Heart Membranes and Myofibrils During Bacterial Infective Cardiomyopathy

(a) Sarcolemmal alterations

The ATP hydrolyzing abilities of the cardiac sarcolemmal fractions from control, uninfected and infected animals were examined and the results are reported in Table IX. The nonspecific ATPase activity was increased ($P<0.05$) whereas Mg^{++}ATPase and ouabain-sensitive Na^{+}-K^{+}ATPase activities were decreased ($P<0.05$) in comparison to control, without significant ($P>0.05$) changes in Ca^{++}ATPase activity, in sarcolemma from uninfected animals at 6 days after saline injection. On the other hand, both Mg^{++}ATPase and Na^{+}-K^{+}ATPase were decreased ($P<0.05$) in 3 and 6 day infected heart sarcolemma. The nonspecific ATPase was increased and the Ca^{++}ATPase activity was decreased significantly ($P<0.05$) in 6 day, but not in 3 day, infected hearts. The magnitude of changes in the membrane bound enzymes such as Ca^{++}ATPase, Mg^{++}ATPase, and Na^{+}-K^{+}ATPase in the 6 day infected hearts was significantly greater ($P<0.05$) than the uninfected hearts. The nonspecific ATPase activity in the absence of cations in the 6 day uninfected and infected preparations did not decrease when the assay was carried out in the presence of 1 mM EDTA or EGTA indicating that the higher levels of nonspecific ATPase activity in the operated animals were not due to cationic contamination.

In another set of experiments, the activities of sarcolemmal adenylate cyclase of control, uninfected and infected hearts were measured in the absence and presence of 100 μM epinephrine and 4 mM NaF and the results are given in Table X. The basal, epinephrine-stimulated, and NaF-stimulated adenylate cyclase activity were decreased ($P<0.05$) in 6 day uninfected as well as 3 and 6 day infected hearts in comparison to the control values. In comparison to the uninfected hearts, NaF-stimulated adenylate cyclase activities were decreased ($P<0.05$) in the 3 and 6 day infected hearts whereas basal and epinephrine-stimulated adenylate cyclase activities were decreased ($P<0.05$) only at 3 or 6 days respectively.

Calcium binding by the sarcolemmal fraction was studied in the absence

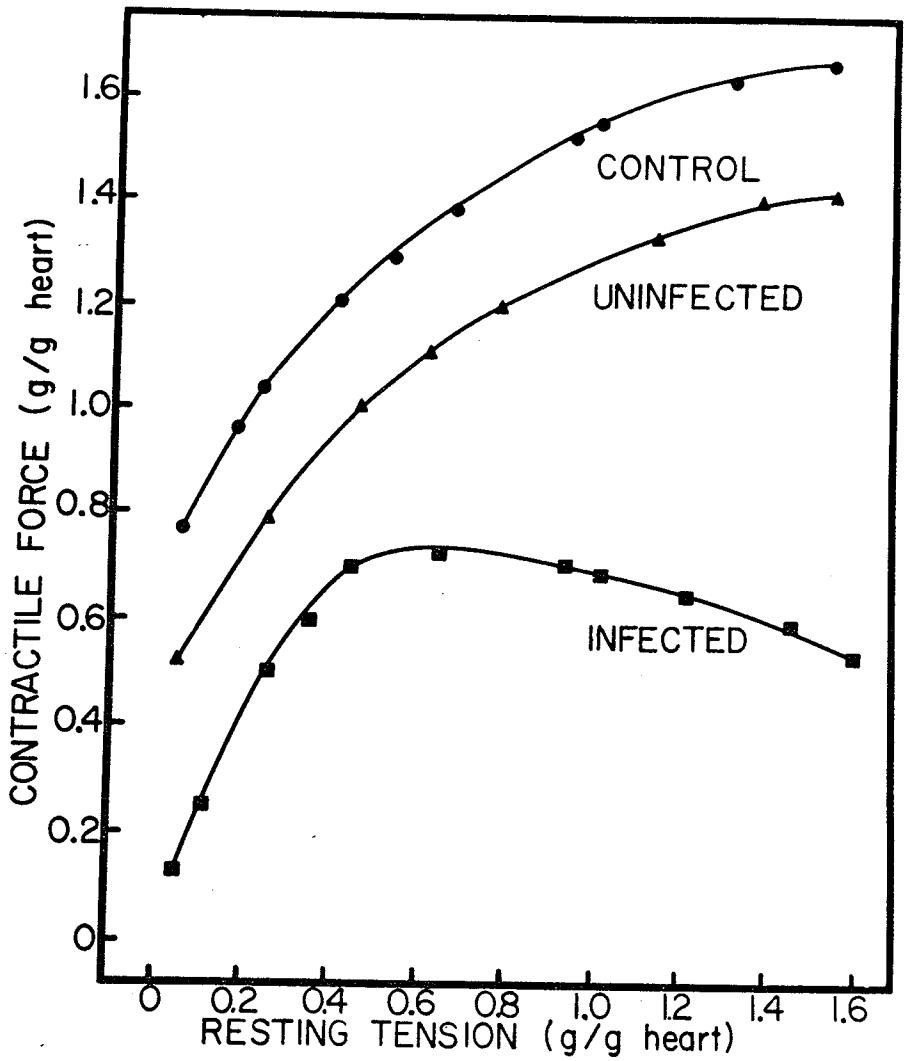

FIGURE 15 Representative comparison of the developed tension-resting tension relation in control, uninfected and infected isolated perfused hearts.

TABLE IX

ATPases of Sarcolemma from Control, Uninfected and Infected Hearts

	Non-specific ATPase (μmoles Pi/mg/hr)	Ca^{++}ATPase (μmoles Pi/mg/hr)	Mg^{++}ATPase (μmoles Pi/mg/hr)	Na^{+}-K^{+}ATPase (μmoles Pi/mg/hr)
Control	0.58 ± 0.08	18.1 ± 1.26	19.1 ± 0.98	6.2 ± 0.50
Uninfected (3 days)	0.54 ± 0.08	17.1 ± 1.03	18.3 ± 1.21	5.9 ± 0.81
Uninfected (6 days)	0.87 ± 0.05*	16.3 ± 1.29	16.4 ± 0.89*	4.6 ± 0.43*
Infected (3 days)	0.69 ± 0.06	16.7 ± 1.21	16.6 ± 1.01*	4.1 ± 0.55*
Infected (6 days)	0.98 ± 0.09*	13.3 ± 0.60**	14.0 ± 0.79**	3.1 ± 0.38**

The results are mean ± SE of 4 to 6 experiments. The sarcolemmal protein (0.05 to 0.07 mg/ml) was incubated at 37°C in medium containing 50 mM Tris-HCl, pH 7.4, and 4 mM ATP (Tris form). Ca^{++}ATPase and Mg^{++}ATPase were determined in the absence and presence of 4 mM $MgCl_2$ or 4 mM $CaCl_2$ respectively. ATP hydrolysis in the absence of added $CaCl_2$ or $MgCl_2$ was taken as non-specific ATPase. Na^{+}-K^{+}ATPase was estimated by finding the difference between ATP hydrolysis in the absence or presence of 2 mM ouabain in the above medium with 4 mM $MgCl_2$, 100 mM NaCl and 10 mM KCl.

* - Significantly different from control hearts ($P<0.05$)
** - Significantly different from control and uninfected hearts ($P<0.05$)

TABLE X

Adenylate Cyclase of Sarcolemma from Control, Uninfected and Infected Hearts

	Basal	100 μM Epinephrine Stimulated	4 mM NaF Stimulated
Control	131.9 ± 11.1	205.2 ± 6.9	637.8 ± 41.0
Uninfected (3 days)	125.4 ± 6.9	192.7 ± 7.4	594.3 ± 37.1
Uninfected (6 days)	95.9 ± 3.6*	173.3 ± 8.1*	472.9 ± 29.1*
Infected (3 days)	93.0 ± 5.1**	177.1 ± 6.2*	445.4 ± 31.3**
Infected (6 days)	81.3 ± 7.7*	132.5 ± 5.8**	396.2 ± 27.6**

The results are mean ± SE of 6 experiments. The sarcolemmal protein (0.05 to 0.07 mg/ml) was incubated at 37°C in medium containing 50 mM Tris-HCl, pH 8.5, 8 mM caffeine, 5 mM KCl, 20 mM phosphoenolpyruvate, 15 mM $MgCl_2$, 130 μg/ml pyruvate kinase and 0.4 mM ATP-^{14}C in the absence (basal) or presence of 100 μM epinephrine or 4 mM NaF.

* - Significantly different from control hearts ($P<0.05$)
** - Significantly different from control and uninfected hearts ($P<0.05$)

or presence of MgATP and the results are shown in Table XI. The calcium binding ability in the absence but not in the presence of MgATP, of sarcolemma from uninfected hearts was significantly less ($P<0.05$) than that from control; however, the values obtained in both the absence and presence of MgATP for sarcolemma from the infected hearts were decreased significantly ($P<0.05$). Furthermore, in comparison to the uninfected hearts, the infected heart sarcolemma bound less ($P<0.05$) calcium.

(b) Microsomal alterations

Calcium binding and uptake by the cardiac heavy microsomal fractions from the sham operated control, uninfected, and infected animals were studied at different intervals of incubation and the results are reported in Figures 16 and 17. The ability of the heavy microsomal fraction to bind calcium in the presence of MgATP was markedly depressed ($P<0.05$) in the 6 day uninfected, and 3 and 6 day infected hearts. On the other hand, calcium binding by the 3 day uninfected microsomal preparation was not different ($P>0.05$) from the control. In comparison to the uninfected hearts, depression in calcium binding by infected heart microsomes was significantly greater ($P<0.05$) at both 3 and 6 days (Fig. 16). The data shown in Figure 17 reveal that microsomal calcium uptake when studied in the presence of MgATP and potassium oxalate was significantly decreased in 3 and 6 day infected hearts in comparison to control whereas calcium uptake was decreased in uninfected hearts only at 6 days ($P<0.05$). In comparison to uninfected hearts, the microsomes from infected hearts accumulated a lesser amount ($P<0.05$) of calcium both at 3 and 6 days.

Basal and Ca^{++}-stimulated ATPase activities of the microsomal fraction were also examined and the results are shown in Table XII. Although no change in the Ca^{++}-stimulated ATPase was observed in microsomes from either infected or uninfected hearts, a significant depression ($P<0.05$) was observed in basal ATPase in the infected hearts in comparison to both control and uninfected hearts.

(c) Mitochondrial alterations

Mitochondrial MgATP dependent calcium binding and uptake were studied in the absence and presence respectively, of inorganic phosphate and sodium succinate

TABLE XI

Calcium Accumulation by Sarcolemma from Control, Uninfected and Infected Hearts

	Calcium Binding (nmoles Ca^{++}/mg prot/min)	
	Absence of 4 mM MgATP	Presence of 4 mM MgATP
Control	44.2 ± 2.86	19.9 ± 1.78
Uninfected (6 days)	30.7 ± 2.24*	17.7 ± 1.81
Infected (3 days)	34.1 ± 3.41*	15.2 ± 2.06*
Infected (6 days)	20.2 ± 2.89**	11.8 ± 1.95**

The results are mean ± SE of 5 experiments. The sarcolemmal protein (0.15 to 0.20 mg/ml) was incubated at 37°C in medium containing 100 mM KCl, 20 mM Tris-HCl, pH 6.8, and 0.1 mM $Ca^{45}Cl_2$ in the absence or presence of 4 mM MgATP.

* - Significantly different from control hearts ($P<0.05$)
** - Significantly different from control and uninfected hearts ($P<0.05$)

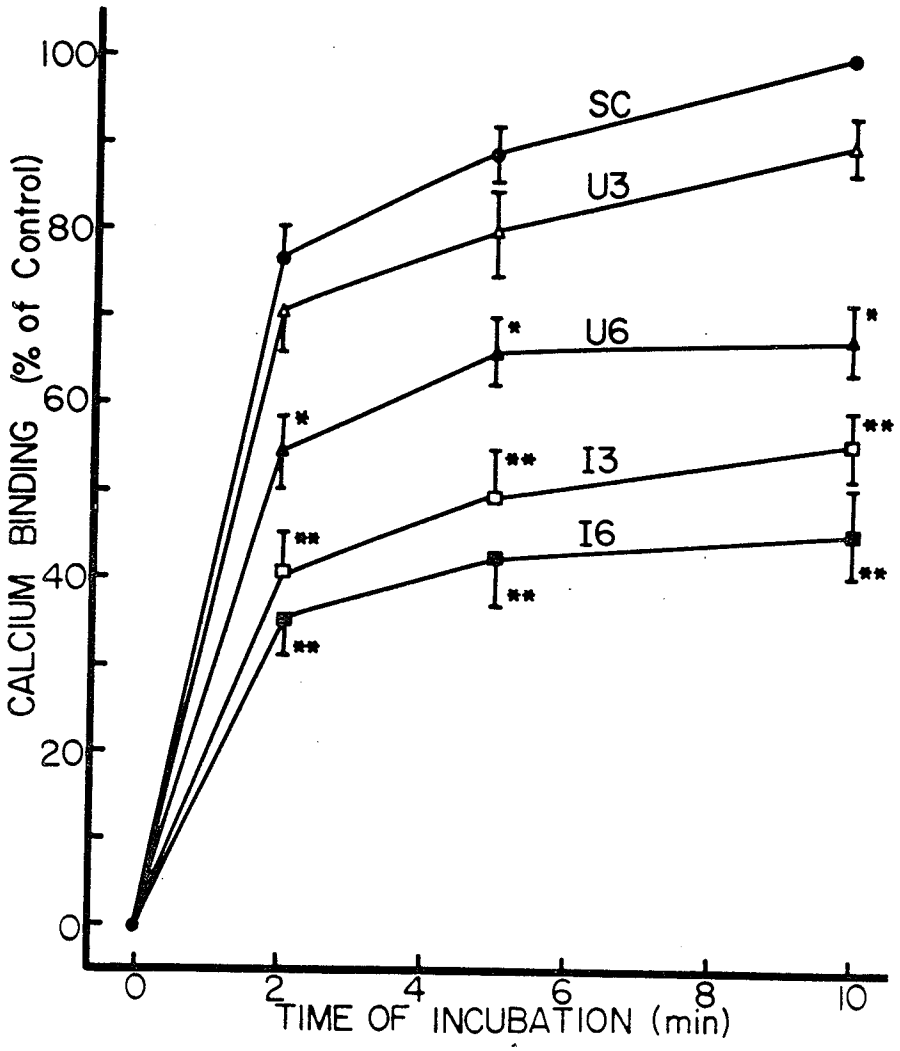

FIGURE 16 Time course for calcium binding by heavy microsomal fractions from sham operated control hearts (SC), uninfected catheterized hearts at three (U3) and six (U6) days after injection of saline, and infected hearts at three (I3) and six (I6) days after injection of Strep. viridans. The assay system was the same as in Methods and protein concentration was 0.2 to 0.3 mg/ml. Each point represents a mean ± SE of 6 experiments and is expressed as a per cent of 10 minute control binding. (Average value was 63.4 ± 4.6 nmoles Ca^{++}/mg protein.)

* - significantly different from control hearts ($P<0.05$)

** - significantly different from control and uninfected hearts ($P<0.05$)

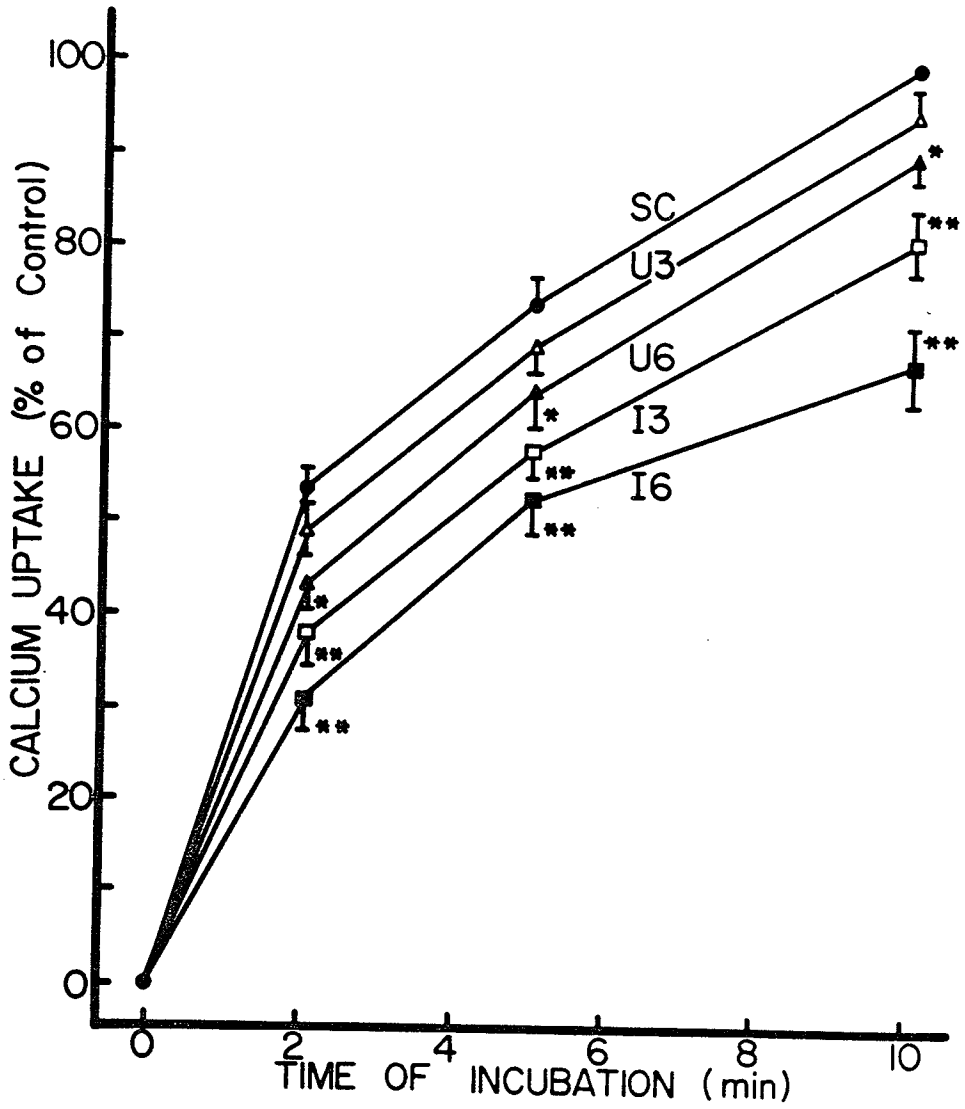

FIGURE 17 Time course of calcium uptake by heavy microsomal fractions from sham operated control hearts (SC), uninfected catheterized hearts at three (U3) and six (U6) days after injection of saline, and infected hearts at three (I3) and six (I6) days after injection of Strep. viridans. The assay system was the same as in Methods and protein concentration was 0.02 to 0.05 mg/ml. Each point represents a mean ± SE of 6 experiments and is expressed as a per cent of 10 minute control uptake.(Average value was 848.7 ± 46.7 nmoles Ca^{++}/mg protein).

* - significantly different from control hearts ($P<0.05$)

** - significantly different from control and uninfected hearts ($P<0.05$)

TABLE XII

Membrane ATPase of Subcellular Fractions from Control, Uninfected and Infected Hearts

	Heavy Microsomes (μmoles Pi/mg/min)		Mitochondria (μmoles Pi/mg/min)
	Basal	Ca^{++}-stimulated	
Control	1.182 ± 0.160	.244 ± .053	.714 ± .054
Uninfected (6 days)	1.002 ± 0.110	.237 ± .031	.683 ± .061
Infected (3 days)	0.670 ± 0.171*	.243 ± .081	.621 ± .092*
Infected (6 days)	0.560 ± 0.036**	.249 ± .073	.547 ± .047**

The results are mean ± SE of 6 to 8 experiments. The subcellular fractions (0.2 to 0.3 mg/ml) were incubated at 37°C in medium containing 100 mM KCl, 10 mM Tris-HCl, pH 6.8 and 4 mM ATP. In the case of heavy microsomes, medium also contained 5 mM potassium oxalate and either 0.1 mM $CaCl_2$ (Ca^{++}-stimulated) or 1 mM EGTA (basal).

* - Significantly different from control hearts ($P<0.05$)
** - Significantly different from control and uninfected hearts ($P<0.05$)

and the results are given in Figures 18 and 19. Mitochondrial calcium binding at different intervals of incubation by the 3 day infected hearts was significantly increased ($P<0.05$) whereas that by the 6 day infected hearts was significantly decreased ($P<0.05$) in comparison to values obtained for control or uninfected animals. On the other hand, calcium binding by the uninfected heart mitochondria was not different ($P>0.05$) from control (Fig. 18). The time course of calcium uptake by mitochondria revealed that the values for the 3 day infected and 6 day uninfected hearts were higher ($P<0.05$) whereas those for the 6 day infected hearts were lower ($P<0.05$) than control (Fig. 19). In comparison to uninfected hearts, mitochondrial calcium uptake by 3 day infected hearts was increased ($P<0.05$) but by 6 day infected hearts was markedly decreased. The mitochondria ATP hydrolyzing ability was decreased ($P<0.05$) in infected animals in comparison to control (Table XII). The mitochondrial ATPase activity of the 6 day infected hearts was less ($P< 0.05$) than that of the uninfected hearts.

The respiratory and oxidative activities of mitochondria were also monitored and the results are given in Table XIII. It was observed that the values for RCI, ADP:0 ratio and phosphorylation rate were decreased ($P<0.05$) in the 3 and 6 day infected heart mitochondria. Furthermore oxygen consumption in state 4 was increased ($P<0.05$) in 3 and 6 day infected hearts, whereas that in state 3 was decreased ($P<0.05$) only in 6 day infected hearts. In comparison to uninfected hearts, RCI, ADP:0 ratio, phosphorylation rate and oxygen consumption in state 3 were decreased whereas oxygen consumption in state 4 was increased ($P<0.05$) in 6 day infected hearts.

(d) Myofibrillar alterations

Since the myofibrillar preparation is considered to be contaminated to some extent with mitochondrial fragments, the ATP hydrolyzing activity of these proteins was determined in the absence and presence of sodium azide, a well known inhibitor of mitochondrial ATPase. The results in Table XIV show that the Mg^{++}ATPase activity in the presence of azide was lower than that in its absence. The Mg^{++}ATPase values at 2 and 5 minutes of incubation for infected hearts were significantly less ($P<0.05$) than the control only when sodium azide was used in the medium. On the other hand, total Mg^{++}-Ca^{++}ATPase values in the presence of azide for the 3 and 6

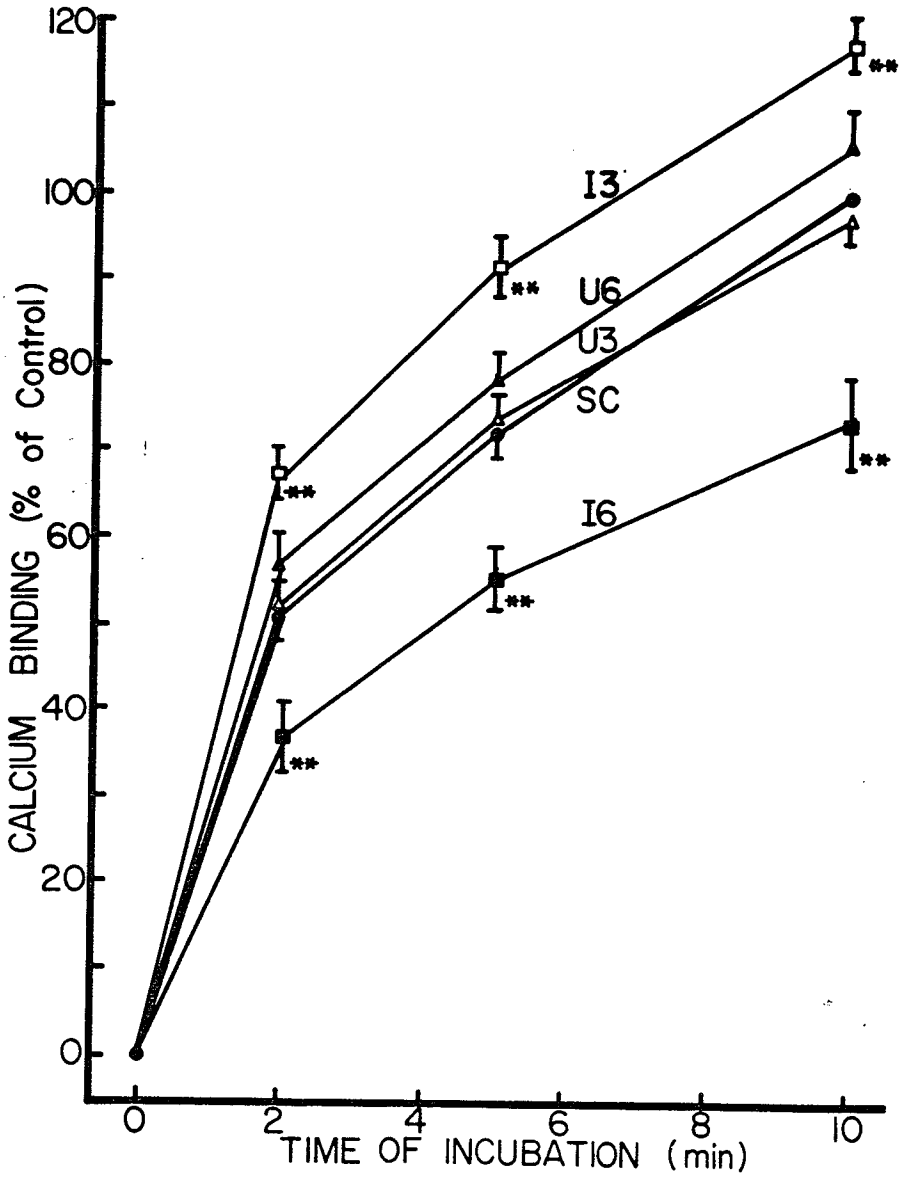

FIGURE 18 Time course of calcium binding by mitochondrial fractions from sham operated control hearts (SC), uninfected catheterized hearts at three (U3) and six (U6) days after injection of saline, and infected hearts at three (I3) and six (I6) days after injection of Strep. viridans. The assay system was the same as in Methods and protein concentration was 0.3 to 0.5 mg/ml. Each point represents a mean ± SE of 6 experiments and is expressed as a per cent of 10 minute control binding. (Average value was 87.2 ± 5.1 nmoles Ca^{++}/mg protein.)
* - significantly different from control hearts ($P<0.05$)
** - significantly different from control and uninfected hearts ($P< 0.05$)

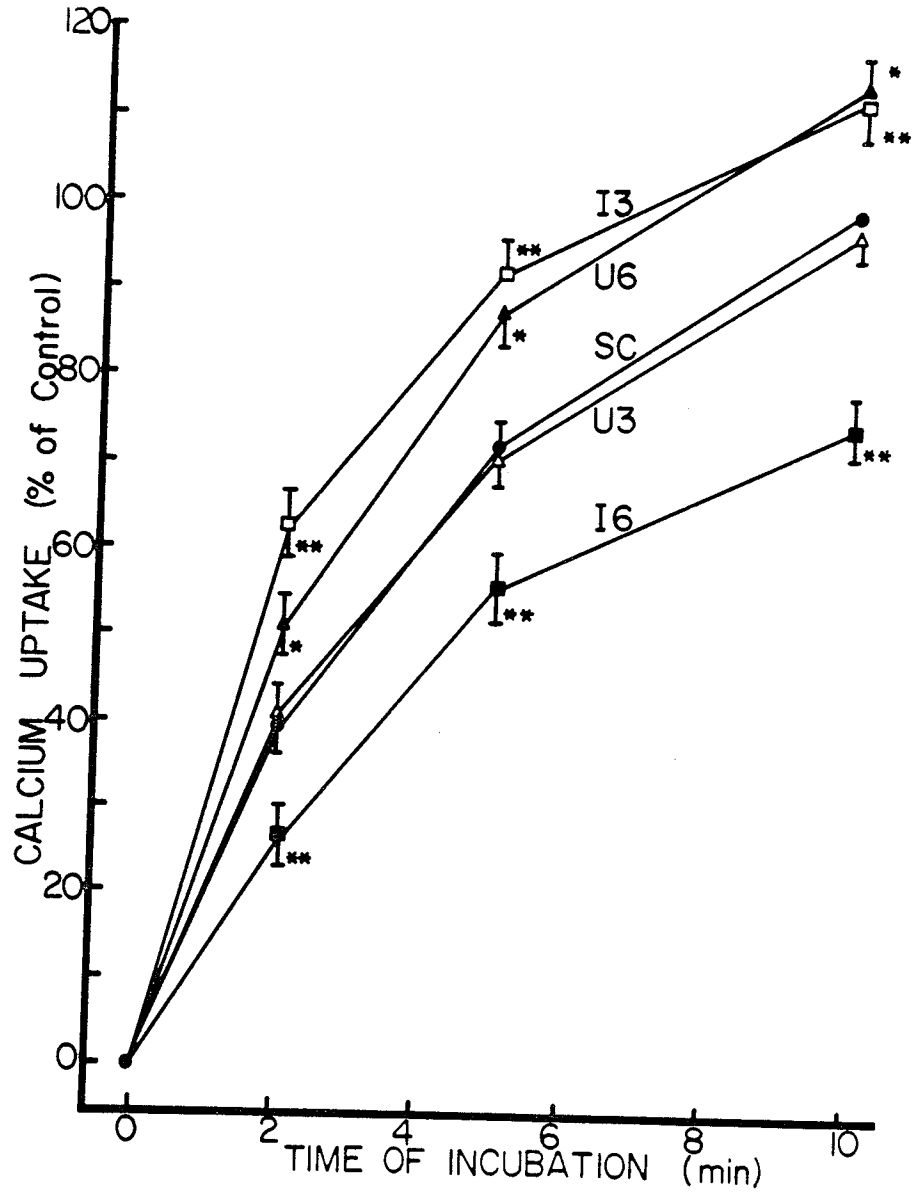

FIGURE 19 Time course of calcium uptake by mitochondrial fractions from sham operated control hearts (SC), uninfected catheterized hearts at three (U3) and six (U6) days after injection of saline, and infected hearts at three (I3) and six (I6) days after injection of Strep. viridans. The assay system was the same as in Methods and protein concentration was 0.2 to 0.3 mg/ml. Each point represents a mean ± SE of six experiments and is expressed as a per cent of 10 minute control uptake. (Average value was 203.6 ± 8.7 nmoles Ca^{++}/mg protein.)
* - significantly different from control hearts ($P<0.05$)
** - significantly different from control and uninfected hearts ($P<0.05$)

TABLE XIII

Oxidative Phosphorylation of Mitochondria from Control, Uninfected and Infected Hearts

	RCI	ADP:0	$QO_2(3)$	$QO_2(4)$	Phos. Rate
Control	6.50 + 0.41	3.23 + 0.08	38.78 + 2.92	5.98 + 0.45	116.7 + 7.6
Uninfected (6 days)	6.39 + 0.47	3.15 + 0.08	43.41 + 2.59	6.94 + 0.49	125.1 + 9.5
Infected (3 days)	4.11 + 0.36*	2.89 + 0.06*	36.84 + 2.06	7.82 + 0.61*	91.0 + 6.7*
Infected (6 days)	3.82 + 0.71**	2.72 + 0.10**	24.31 + 2.74**	8.51 + 0.40**	73.8 + 8.6**

The results are mean ± SE of 5 experiments. ADP:0 = relation of adenosine diphosphate to oxygen efficiency (phosphorylation); Phos. Rate = phosphorylation rate (ADP:0 x $QO_2(3)$); $QO_2(3)$ = oxygen consumption in state 3 (nmoles O_2/min/mg protein); $QO_2(4)$ = oxygen consumption in state 4 (nmoles O_2/min/mg protein); RCI = respiratory control index.

* - Significantly different from control hearts ($P<0.05$)
** - Significantly different from control and uninfected hearts ($P<0.05$)

TABLE XIV

ATPases of Myofibrils from Control, Uninfected and Infected Hearts

	Absence of 5 mM Na Azide		Presence of 5 mM Na Azide			
	Mg-ATPase		Mg^{++}-ATPase		Mg^{++}-Ca^{++}-ATPase	
	2'	5'	2'	5'	2'	5'
Control	.346 ± .007	.642 ± .016	.178 ± .005	.341 ± .011	.479 ± .008	.872 ± .013
Uninfected (3 days)	.344 ± .009	.651 ± .015	.181 ± .003	.353 ± .014	.467 ± .009	.883 ± .014
Uninfected (6 days)	.371 ± .012	.640 ± .016	.162 ± .004	.295 ± .009	.422 ± .010*	.820 ± .011*
Infected (3 days)	.352 ± .011	.638 ± 0.17	.191 ± .004	.331 ± .011	.416 ± .012*	.755 ± 0.16**
Infected (6 days)	.339 ± .008	.599 ± .015	.153 ± .006*	.281 ± .007*	.351 ± .008**	.701 ± .014**

The results are mean ± SE of 4 experiments. The myofibrillar protein (0.6 to 0.8 mg/ml) was incubated at 37°C in medium containing 60 mM KCl, 10 mM histidine, 4 mM EGTA, 2 mM $MgCl_2$ and 2 mM ATP in the presence and absence of 5 mM sodium azide. Mg^{++}-Ca^{++}ATPase was determined in the above medium without EGTA but in the presence of 5 mM sodium azide and 0.1 mM $CaCl_2$.

* - Significantly different from control hearts ($P<0.05$)
** - Significantly different from control and uninfected hearts ($P<0.05$)

day infected, and 6 day uninfected heart myofibrils were less ($P<0.05$) than control. In comparison to the uninfected hearts the myofibrillar total Mg^{++}-Ca^{++}ATPase activity in infected hearts was decreased ($P<0.05$). The activities of the Ca^{++}-stimulated ATPase of the 6 day uninfected, as well as 3 and 6 day infected heart myofibrils was also decreased ($P<0.05$) when monitored at different concentrations of calcium (Fig. 20). The Lineweaver-Burk (124) analysis of the above data revealed that the decrease in myofibrillar Ca^{++}-stimulated ATPase in the infected hearts was due to a depression in the maximal velocity of ATP hydrolysis (V_{max}) without any changes in the affinity (K_m) of the enzyme for calcium (Fig. 20).

(e) General characteristics of the cellular components

The data shown in Table XV indicate that the yields of sarcolemma and myofibrils from infected and uninfected hearts were not different ($P>0.05$) from sham operated controls. The yields of mitochondria and microsomes, however, were increased ($P<0.05$) in 6 day infected hearts. It is pointed out that the degree of purity of the cellular fractions employed in this study was routinely checked by different means. Sodium azide (5 mM) inhibited MgATP dependent calcium binding by mitochondria by 70 to 80% without appreciably affecting microsomes from control and experimental preparations. Furthermore, in contrast to mitochondrial and microsomal fractions, the calcium binding by the sarcolemmal fraction was inhibited by the presence of MgATP. Unlike myofibrillar, mitochondrial and microsomal fractions, the sarcolemmal fraction exhibited ouabain sensitive Na^{+}-K^{+}ATPase activity. The microsomal fraction, unlike the mitochondrial and sarcolemmal fractions, showed stimulation of energy-dependent calcium transport by oxalate. The electron microscopic examination of pellets of fractions employed in this study revealed minimal apparent cross contamination. Although we by no means claim that these fractions were pure, we believe that the degree of impurity in the experimental preparation was comparable to the control.

(f) Ultrastructural alterations of cellular components

Biopsies obtained from left ventricles employed for biochemical studies were examined under the electron microscope. In comparison to the sham operated control, the sections from the 3 day infected hearts showed only minor changes such

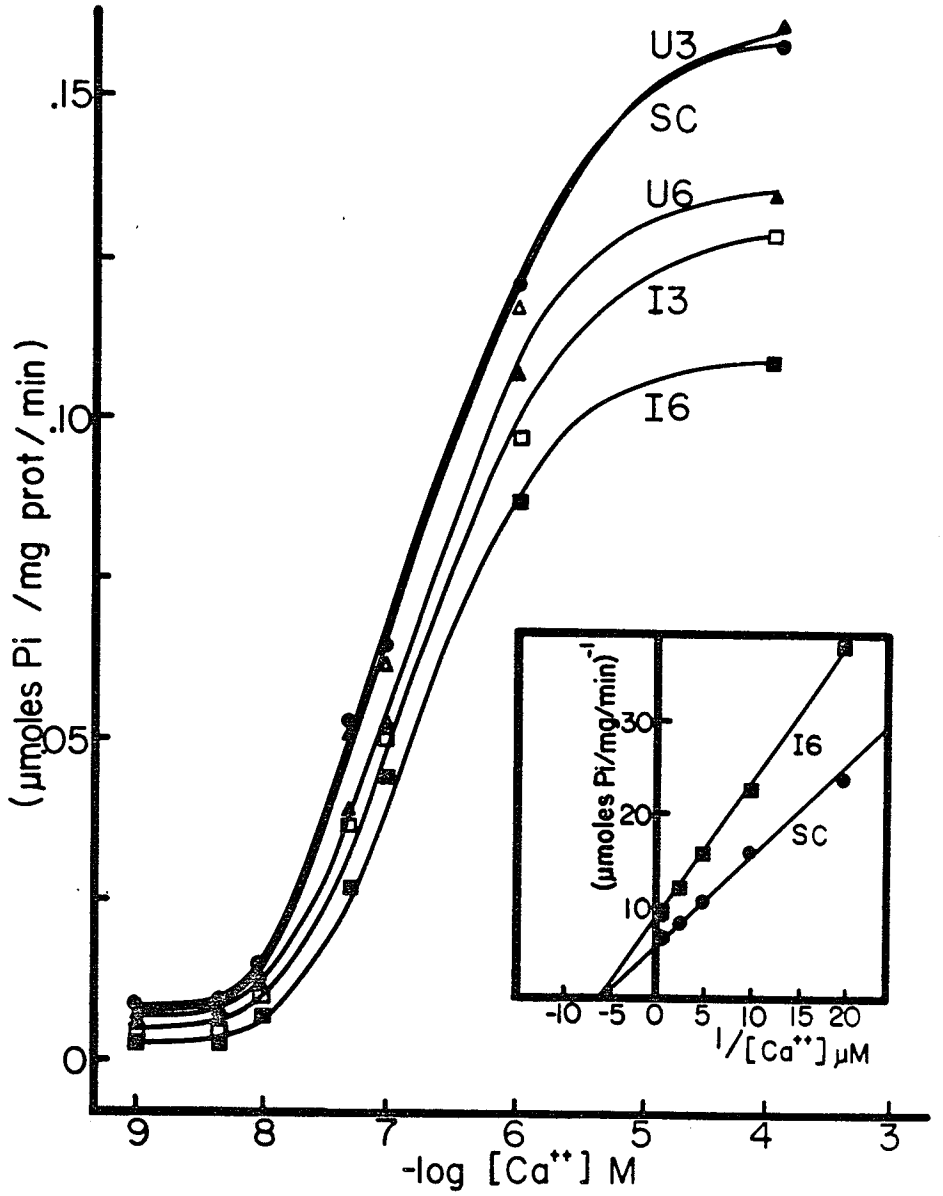

FIGURE 20 Representative comparison of myofibrillar calcium stimulated ATPase of sham operated control hearts (SC), uninfected catheterized hearts at three (U3) and six (U6) days after injection of saline, and infected hearts at three (I3) and six (I6) days after injection of Strep. viridans. The assay system was the same as in Methods except that the concentration of calcium was varied. Protein concentration was 0.6 to 0.8 mg/ml. The insert is Lineweaver-Burk analysis of the data for sham operated control and 6 day infected hearts.

TABLE XV

Yields of Membranes and Contractile Proteins Isolated from Control, Uninfected and Infected Hearts

	Sarcolemma (mg/g heart wet weight)	Myofibrils (mg/g heart wet wt)	Mitochondria (mg/g heart wet wt)	Heavy Microsomes (mg/g heart wet wt)
Control	8.75 ± 0.61	30.9 ± 2.1	4.12 ± 0.39	0.31 ± 0.04
Uninfected (6 days)	8.42 ± 0.53	28.9 ± 3.1	4.94 ± 0.52	0.29 ± 0.02
Infected (3 days)	7.97 ± 0.51	31.8 ± 1.7	5.31 ± 0.61	0.32 ± 0.06
Infected (6 days)	9.04 ± 0.62	32.1 ± 2.4	6.81 ± 0.29*	0.42 ± 0.04*

The results are mean ± SE of 4 to 6 experiments.

* - Significantly different from control and uninfected hearts ($P<0.05$)

as slight swelling of the sarcotubular system and occasional separation of the intercalated disc (Fig. 21). On the other hand, 3 day uninfected heart sections were indistinguishable from control. Examination of sections from 6 day uninfected hearts revealed areas of moderate muscle abnormality, including myofibrillar contracture, sarcotubular swelling, alteration in mitochondrial cristae, vacuolization and some degree of separation of the intercalated discs (Fig. 22). Generalized and dramatic damage to ultrastructure of the left ventricle was seen 6 days after infection. The changes included disruption of myofibrils in some areas and contracture in others, swelling and destruction of mitochondria, swelling of the sarcotubular system and marked separation of the intercalated discs (Fig. 23). Although swelling of sarcoplasmic reticulum underneath sarcolemma was noted in the 6 day infected hearts, we were unable to observe any apparent rupture of the sarcolemma in any of the experimental preparations. It should be pointed out that the myocardial cell damage in 6 day infected hearts is extremely severe in comparison to that seen in 6 day uninfected hearts.

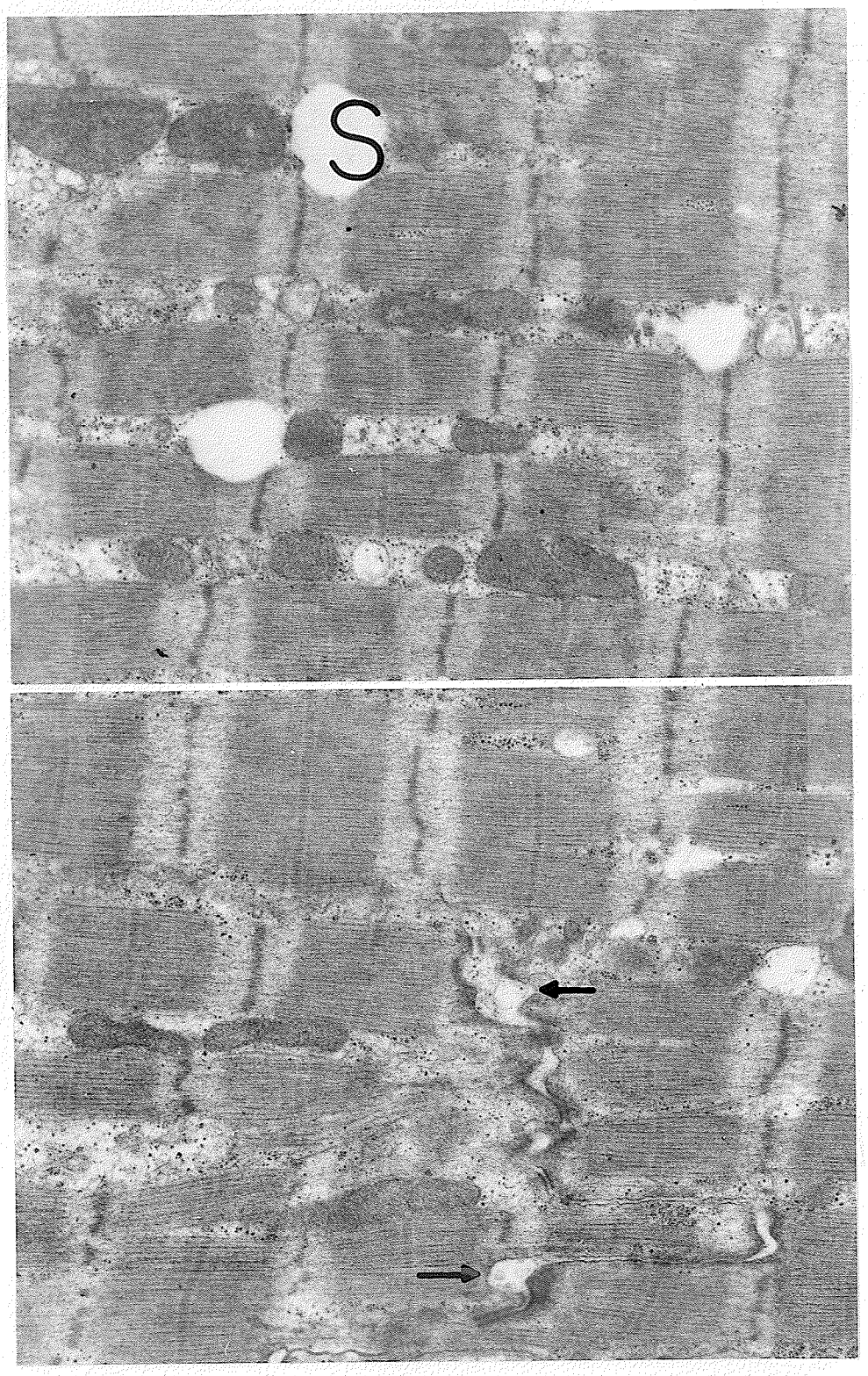

FIGURE 21 Electron photomicrograph of biopsy of left ventricle from heart of rabbit with infective cardiomyopathy 3 days after injection of Strep. viridans showing slight swelling of sarcotubules (S) and occasional intercalated disc separation (arrows). Uranyl acetate-lead citrate; X 16,500.

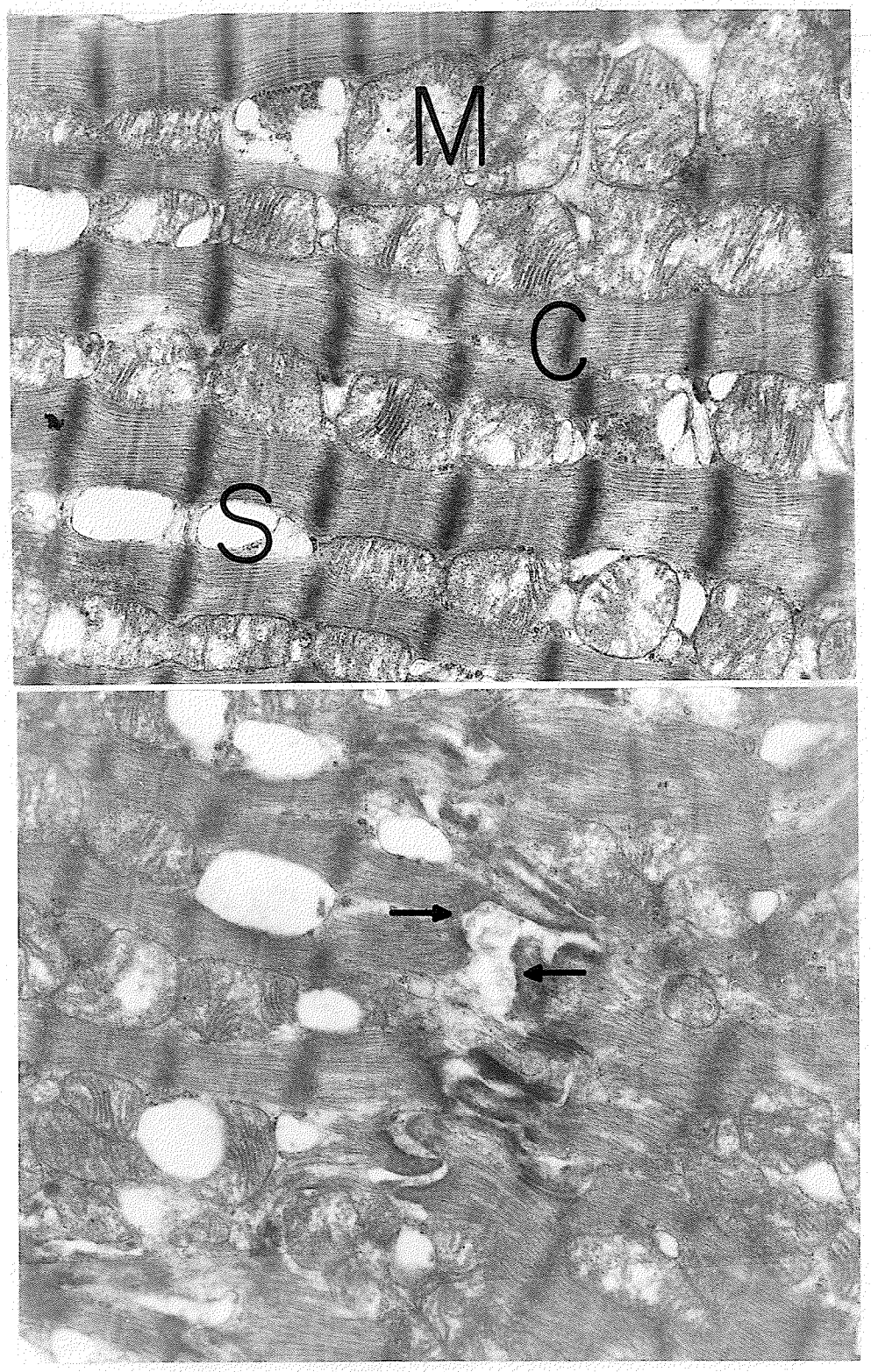

FIGURE 22 Electron photomicrograph of biopsy of left ventricle from heart of uninfected catheterized rabbit 6 days after injection of saline showing occasional areas of myofibril contracture (C), some degree of mitochondrial damage (M), sarcotubular swelling (S) and some degree of intercalated disc separation (arrows). Uranyl acetate-lead citrate; X 16,500.

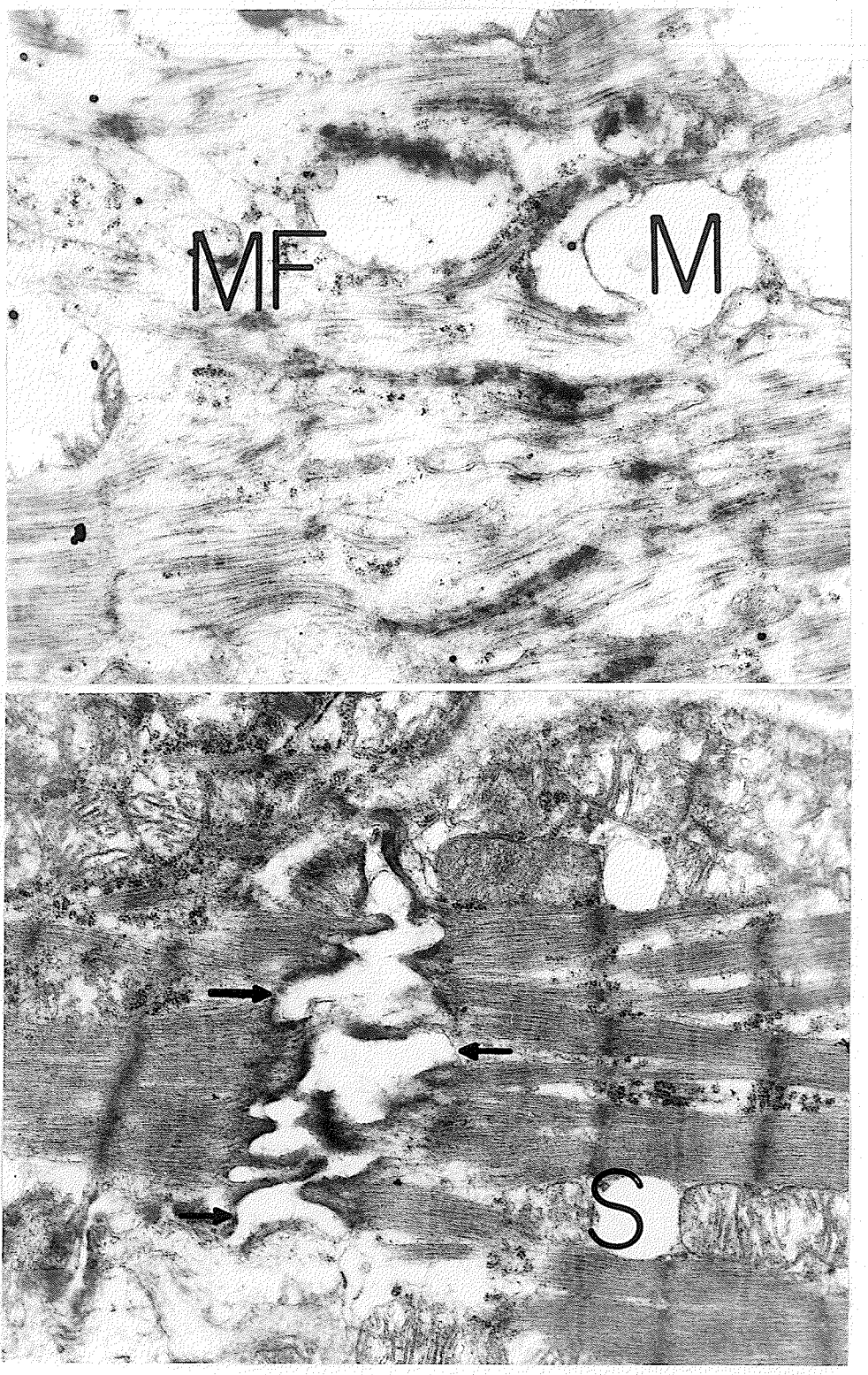

FIGURE 23 Electron photomicrograph of biopsy of left ventricle from heart of rabbit with infective cardiomyopathy 6 days after injection of Strep. viridans showing extensive damage including disruption of myofibrils (MF), swelling and destruction of mitochondria (M), sarcotubular swelling (S) and wide separation of the intercalated disc (arrows). Uranyl acetate-lead citrate; X 16,500.

DISCUSSION

1. Myocardial Cell Damage During Experimental Infective Endocarditis

Infective endocarditis in rabbits due to a single intravenous injection of Streptococcus viridans was found to be associated with hyperthermia, weight loss, development of valvular vegetations and histological features characteristic of left-sided endocarditis in human disease and several experimental models (7,8,13, 90,92). Our histopathological findings indicating involvement of myocardium support earlier studies which suggest that myocardial lesions occur in over 90% of patients with infective endocarditis (5,8-10,76,77).

It is notable that the most common cause of death in patients with infective endocarditis is congestive heart failure (5,8,24). The experimental model employed in this study was also found to exhibit clinical evidence of heart failure in all rabbits at terminal stages of disease. Defective papillary muscle and valvular lesions in infective endocarditis will produce valvular dysfunction thus leading to aortic regurgitation which will explain the observed heart failure (5,8). It should however be appreciated that the valvular vegetations may actually be obstructing the valvular orifice and thus produce a situation simulating valvular stenosis, which has been shown to occur in some patients (60,61).

In this study we have demonstrated dramatic changes in myocardial ultrastructure such as mitochondrial and sarcotubular swelling, mitochondrial damage, myofibrillar disruption and separation of the intercalated disc in infective endocarditis. These changes cannot be due entirely to hypertrophy produced by catheterization since only relatively minor changes such as swelling of sarcotubular system and mitochondria were seen in the hypertrophied catheterized uninfected hearts. The ultrastructural changes observed in infective endocarditis are similar to those reported in heart failure due to myocardial ischemia (38,125) calcium deficiency or calcium overload (126,127) myocardial necrosis (128,129) hypoxia and substrate lack (130,131) and cardiomyopathy in humans (132) and hamsters (42). Thus, it is difficult to state whether the observed ultrastructural changes in infective endocarditis are due to a direct effect of the infectious agent or is a consequence of functional ischemia due to

hypertrophy or failure due to valvular dysfunction. It is also possible that damage to myocardial ultrastructure may be due to alterations of intracellular calcium metabolism (126,127,133) and particularly intracellular calcium overload has been demonstrated to be involved in heart pathophysiology (127,134,135). In this regard it should be noted that contracture of myofibrils in infected myocardium may be a reflection of intracellular calcium overload which has also been demonstrated to produce separation of the intercalated disc (127).

Studies of the histology and ultrastructure of papillary muscle from rabbits with bacterial endocarditis provide evidence for the presence of infective cardiomyopathy. In this regard, our present experiments have indicated that myocardial cell damage in bacterial endocarditis is not only limited to papillary muscle but also extends to the ventricular muscle. Thus, this experimental model may serve as an important tool for investigating functional and biochemical changes during the development of congestive heart failure.

2. Myocardial Function During Bacterial Infective Cardiomyopathy

The experimental preparation employed for producing infective endocarditis involves catheterization of the left ventricle. Therefore, it was essential to compare the infected animals with both sham operated and uninfected catheterized animals. Although both infected and uninfected animals showed gross and histological evidence of cardiac enlargement, the degree of hypertrophy in the infected animals at 6 days was significantly greater than the uninfected animals. This difference could be due to a greater degree of valvular dysfunction caused by infective lesions in aortic valve and papillary muscle. In addition to valvular regurgitation, aortic stenosis due to the presence of massive valvular vegetations in infected animals could also be a factor in this regard. Then, aortic insufficiency and stenosis in the infected animals could lead to a combined volume and pressure overload situation causing an increase in intramyocardial tension which in turn could serve as a mechanical-biochemical transducer or coupling mechanism responsible for the increased protein synthesis and accelerated production of ventricular mass (136-138).

In contrast to the uninfected catheterized animals, the infected hearts showed muscle degeneration and monocytic infiltration. Although serum CPK,

LDH and GOT were elevated in both infected and uninfected animals, the rise in LDH in the infected animals was significantly less than that in the uninfected catheterized animals. The elevated serum levels of different intracellular enzymes are commonly considered to reflect the degree of myocardial damage (139,140); however, the magnitude of changes in serum levels of these enzymes showed no correlation with changes observed when infected and uninfected hearts were compared histologically. Similarly, an increase in QRS amplitude and flattening or inversion of the T-wave was noted in both infected and uninfected hearts. These electrocardiographic changes are indicative of myocardial hypertrophy but provide no information with respect to the extent of cardiac injury. Furthermore, in spite of a marked decrease seen in myocardial calcium levels and a slight increase in myocardial magnesium in the 3 day and 6 day infected hearts respectively, the pattern of electrolyte shifts in the infected hearts was essentially similar to that observed in the uninfected hearts. Thus some caution should be exercised in relating myocardial electrolyte shifts, electrocardiographic changes and elevated levels of intracellular enzymes with myocardial cell damage. It should, however, be noted that unlike the uninfected animals, the infected rabbits had a significant reduction in the serum levels of calcium, magnesium and sodium as well as elevation in the serum level of potassium. The significance of these changes in serum electrolytes in the infected animals is not clear at present because these observations may not be a reflection of alterations limited to the myocardium. At any rate, we have shown that bacterial infection superimposed upon myocardial hypertrophy results in histologically demonstrable lesions which may be a consequence of the infective process itself, functional hypoxia due to an excessive increase in muscle mass, and/or coronary insufficiency. It is however pointed out that no conventional electrocardiographic indications of myocardial ischemia such as ST segment elevation were noted in the infected hearts.

Increased sympathetic activity in early stages of cardiomyopathy and hypertrophy has been reported in different experimental models (141) and possibly represents a compensatory mechanism for assisting myocardial performance. It should also be recognized that late stage of heart failure has been demonstrated to be associated with depletion of cardiac norepinephrine stores (142-144). Thus it is possible that

the observed increase in heart rate in 6 day uninfected and 3 day infected rabbits may be due to an increase in the sympathetic activity whereas bradycardia in 6 day infected animals may be a consequence of depletion of the cardiac catecholamine stores. In addition to changes in circulating catecholamines, the hemodynamic changes observed in early infection and hypertrophy could be due to aortic valve incompetency, but these are further complicated in 6 day infected animals by aortic stenosis. Further detailed experiments concerning the status of catecholamine stores, cardiac output, and peripheral resistance in the infected rabbits are needed to make any definitive conclusions. The possibility that myocardial necrosis observed in the infected hearts is due to catecholamines (128,129) is also not ruled out at present.

In situations with compensated ventricular hypertrophy and heart failure, it has been shown that contractile state as measured by contractile element velocity is reduced (145-147). We have shown that dP/dt and relative V_{max} are decreased in 3 and 6 day infected and uninfected animals in comparison to the sham operated animals in situ. In addition, the abilities of the isolated perfused hearts from infected and uninfected animals to generate contractile force was also observed to be depressed. However, it should be noted that the depression in the contractile state of myocardium in the infected animals was much more severe in comparison to the uninfected animals. Therefore, we believe that the infected animals were in cardiac contractile failure. This is further evident from the clinical manifestations of left heart failure in the infected rabbits. The pattern of ventricular function curves for the isolated hearts suggests that the infected hearts may be operating on the descending limb of the Frank-Starling curve. Although it is recognized that extensive mechanical studies are needed to define the exact functional state of the infected hearts, the results at hand are indicative of impaired myocardial contractility.

According to the current concept of excitation-contraction coupling and relaxation of myocardium, the action potential is believed to release calcium from the superficial membrane sites as well as the sarcotubular system leading to an increase in the intracellular concentration of free calcium and myofibrillar activation and contraction (33,42,148). Relaxation, on the other hand, is considered to be

the result of a lowering of intracellular free calcium by energy dependent mechanisms in the sarcoplasmic reticulum, sarcolemma, and possibly mitochondria. The contractile failure seen in the infected hearts could be explained on the basis of defects in the events regulating contraction and relaxation processes. The observed decrease in the rate of development of ventricular pressure as well as contractile force may be due to a reduction in the rate of delivery of calcium whereas increased half-relaxation time probably reflects impairment in mechanisms responsible for the removal of calcium from the contractile apparatus. It was interesting to note that time to peak tension was markedly prolonged in vivo but slightly shortened in the isolated heart preparations from the infected animals. At this moment we have no explanation for this phenomenon except to mention that it may be due to differences in the environment for the in situ and in vitro preparations. It should also be pointed out that heart failure is known to occur due to defects in the processes of energy production and utilization (29).

3. Biochemistry of Heart Membranes and Myofibrils During Bacterial Infective Cardiomyopathy

Normal performance of the myocardial cell can be appreciated in terms of the functions of different cellular components. For example, myofibrils, which convert chemical into mechanical energy, are known to hydrolyze ATP whereas mitochondria, which oxidize different substrates are known to generate ATP. Sarcolemma, on the other hand, not only maintains the concentrations of various cytoplasmic constituents at a desired concentration, but also is the site of several enzymes involved in regulating several metabolic processes. In addition, the contribution of sarcoplasmic reticulum mainly, and mitochondria to some extent, in regulating the movements of cytoplasmic calcium for initiating contraction and relaxation of myocardium is widely accepted. Thus, impairment in the functions of myofibrils, mitochondria, sarcolemma and sarcoplasmic reticulum can be conceived to result in defective myocardial performance. Since techniques at hand do not permit the assessment of the status of these cellular components in the intact heart, it is necessary to separate them into different fractions and study under in vitro conditions. In spite of the numerous limitations of this approach, it is commonly

held (30,35,40,42,43) that valuable information concerning the pathogenesis of heart failure can be gained by such investigations. In particular, the results with isolated cellular fractions are considered to reflect the operations of mechanisms involved in the processes for ATP production and utilization as well as for calcium regulation in normal and diseased states.

(a) Mechanisms for ATP production

In this study we have demonstrated a progressive decrease in mitochondrial ADP:O ratio, phosphorylation rate, and respiratory control index during infective cardiomyopathy and failure. Oxygen consumption by mitochondria under state 3 conditions was also decreased at late stages whereas oxygen consumption under state 4 was increased at early and late stages of infection. These changes in mitochondrial function in the infected hearts cannot be attributed to myocardial hypertrophy since no such alterations were noted in the uninfected hypertrophied hearts. Furthermore, ultrastructural examination of the left ventricular myocardium revealed a greater degree of mitochondrial swelling and damage in infected hearts in comparison to uninfected. The biochemical and morphological changes can be interpreted to reflect a reduction in the ability of mitochondria to generate ATP in the infected myocardium. Thus, we believe that a defect in the process of energy production is one of the factors which may be associated with heart failure due to bacterial infection.

It should be noted that some investigators have claimed the involvement of changes in mitochondrial oxidative phosphorylation ability in the development of heart failure (30,37) while others have failed to obtain results which support such a contention (149,150). At any rate, a detailed study requiring measurement of high energy phosphate stores in the infected myocardium is necessary before any definitive conclusions can be drawn concerning the contribution of the observed defect in mitochondrial function in the pathogenesis of contractile failure during infective cardiomyopathy.

(b) Mechanisms for ATP utilization

Most workers in the field of experimental cardiology are of the view that a major portion of the energy stores in the heart are utilized for mechanical work

of the myocardium. Various investigators have reported that heart failure may be associated with a defect in the process of energy utilization (151-153); however reports indicating no such abnormality are also available in the literature (154,155). In the present study we have observed a decrease in myofibrillar Mg^{++}ATPase in late, but not in early, stages of infection in comparison to the control or uninfected hearts. Furthermore, myofibrillar Ca^{++}-stimulated ATPase activity was also depressed at early and late stages of infection; these changes were of greater magnitude than those seen in uninfected hearts. Extensive myofibrillar damage was also seen in the infected hearts upon electron microscopic examination. Thus, our results can be considered to indicate some impairment in the processes involved in the utilization of ATP in infective cardiomyopathy and this may represent another mechanism associated with heart failure.

(c) Mechanisms for calcium regulation

It is now being accepted that changes in the intracellular concentration of calcium play a central role in the manifestation of myocardial contraction and relaxation processes, and various membrane systems such as sarcolemma, sarcoplasmic reticulum and mitochondria are considered to participate in its regulation. We have shown that microsomal calcium binding and uptake are decreased in early and late stages of infective cardiomyopathy. Although calcium binding and uptake by microsomal fractions of uninfected hearts were also decreased these changes were of lesser magnitude in comparison to infected hearts and were only apparent at late stages of hypertrophy. Microsomal Mg^{++}ATPase activity was decreased in infected hearts, but the activity of the Ca^{++}-stimulated ATPase, which is considered to be involved in the transport of calcium across the reticular membrane (41), is not appreciably altered. Thus, it appears that changes in calcium uptake by the fragments of sarcoplasmic reticulum from the infected hearts are due to an uncoupling of the ATPase from the transport system. Reduction in microsomal calcium uptake by myopathic hamster hearts has also been shown to occur without any changes in the Ca^{++}ATPase activity (115). At any rate the defect in calcium binding by the microsomal fraction from infected hearts does not appear to be due to contamination by mitochondria since sodium azide, a well-known inhibitor of mitochondrial calcium

transport had no effect on microsomal fractions from either control or experimental preparations. Ultrastructural examination of the infected myocardium also revealed some swelling of the sarcotubular system.

Depression in the ability of the infected heart microsomal fraction to accumulate calcium can be conceived to result in a decrease in calcium stores in the sarcoplasmic reticulum. It should also be noted that sarcolemma from infected hearts bound considerably less calcium in comparison to control and uninfected preparations. Thus a lesser amount of calcium will be available for release from sarcoplasmic reticulum or sarcolemma sites upon excitation of the infected myocardial cell. This will result in decreased ability of infected hearts to develop contractile force and subsequently pump failure. Since the ability of sarcoplasmic reticulum to accumulate calcium is linked to the ability of the myocardium to relax, the observed depression in microsomal calcium binding and uptake may explain the prolongation of the relaxation phase in the infected myocardium. The contribution of changes in mitochondrial transport for the regulation of contractile activity of infected hearts is difficult to evaluate since mitochondrial calcium binding and uptake were increased in early stages and decreased in late stages of infection. However, the observed increase in mitochondrial calcium accumulation in hearts at early stages of infection as well as in uninfected hearts, may represent a compensatory mechanism. At any rate, varying degrees of changes in the abilities of both microsomal and mitochondrial fractions have been reported in different types of failing hearts by numerous workers in this field (34-39,41,43,115).

(d) Sarcolemmal abnormalities

In addition to impaired ability of the sarcolemmal fraction from the infected heart to bind calcium, we have demonstrated that the activities of sarcolemmal Mg^{++}ATPase and Na^{+}-K^{+}ATPase were lower in early stages of infection in comparison to controls, at which time no change was noted in sarcolemma from uninfected hearts. Furthermore, the activity of Ca^{++}ATPase was also lower at late stages of infection in comparison to control and uninfected hearts, at which time the degree of depression in Mg^{++}ATPase and Na^{+}-K^{+}ATPase in infected hearts was also greater than in uninfected hearts. These results suggest sarcolemmal alterations in

the infected myocardium and may account for our previous findings concerning electrolyte shifts and leakage of intracellular enzymes during infective cardiomyopathy. Although we were unable to observe disruption of the myocardial cell membrane in infected hearts upon electron microscopic examination, the possibility of sarcolemmal defect in infective cardiomyopathy is substantiated by our observations concerning changes in the adenylate cyclase activity. In this regard, we have noted that the activities of sarcolemmal adenylate cyclase in the absence and presence of epinephrine and NaF was decreased in early and late stages of infection. The changes for epinephrine and NaF stimulated adenylate cyclase activity in the infected hearts were greater than those in the uninfected myocardium. Since adenylate cyclase is known to catalyze the formation of cyclic AMP, which is involved in the regulation of various metabolic processes, the observed alteration in sarcolemmal adenylate cyclase in the infected hearts may be associated with metabolic disturbances and impaired contractility.

(e) Significance of changes in cellular components

We have shown defects in sarcolemmal, microsomal, mitochondrial and myofibrillar activities during infective cardiomyopathy. The heart failure in this experimental model is superimposed upon left heart hypertrophy which makes the effects of bacterial infection upon cellular structures rather complex to evaluate. However, it was observed that the extent of changes in sarcolemmal, microsomal, and myofibrillar activities in most cases at both early and late stages of infection was greater than in the uninfected hypertrophied hearts. Furthermore, mitochondrial respiratory and oxidative phosphorylation activity were altered only in the infected hearts and unlike uninfected myocardium, calcium transport in mitochondria was decreased in late stages of infection. The degree of myocardial cell damage was also greater in infected myocardium in comparison to uninfected. From these observations we believe that there is an association of heart failure and changes in functions of membrane and contractile protein systems during bacterial infection. At the present time, it is premature to state with certainty whether heart failure and the observed biochemical and ultrastructural changes have any cause-effect relationship or are a consequence of the infective process. However, it is tempting to

speculate that heart failure in infective cardiomyopathy may be due to some defect in processes of energy production.

4. General Comments

Infective endocarditis in rabbits is associated with extensive valvular vegetation development, marked cardiac enlargement and ultimately, left heart failure. It is interesting to note that although some of the increase in left ventricular mass can be accounted for by edema, the left ventricular weight was still increased by 24, 23 and 40 % in 6 day uninfected and 3 and 6 day infected rabbits respectively when adjustments were made for changes in the wet/dry weight ratio. Pathological examination of the myocardium in the infected rabbits indicated the presence of an infective cardiomyopathy, but it is difficult to state with certainty whether the observed changes are due to a direct effect of the infective agent, are a consequence of functional ischemia due to hypertrophy, or simply a manifestation of failure although the latter is unlikely because of the type of lesions produced.

The myocardial functional status of the diseased animals was examined by two different approaches. The first technique involves an indirect graphical estimation of contractility derived from analysis of intraventricular pressure changes in the intact animal. The second approach is dependent on the isolated perfused heart. Each of the above techniques has inherent limitations and accordingly the results must be interpreted cautiously. In the light of recent advances in the field of myocardial mechanics and widespread acceptance of the Voigt model of cardiac muscle contraction, the validity of the first approach is particularly suspect. In spite of this it is our contention that such studies do provide an accurate reflection of relative changes in contractility in control, uninfected, and infected hearts and therefore it is our conclusion that the diseased animals are indeed in contractile failure. Although the cause of failure is not clear at the present time, it is conceivable that myocardial lesions due to the infective process, superimposed upon valvular dysfunction from defective papillary muscle and valvular destruction, would result in heart functional impairment.

The presence of heart failure in infective endocarditis can be appreciated in terms of abnormalities in the functions of different cellular components. The sarcolemma

is the site of several enzymes involved in regulating cell metabolism including adenylate cyclase which catalyzes cyclic AMP formation. A defect in the activity of these enzymes may be associated with metabolic disturbances. Abnormalities at this level may be potentiated by the observed defect in mitochondrial ATP production resulting in decreased cell levels of ATP. Since ATP is needed by both the contractile apparatus and the subcellular organelles involved in regulation of contraction it is entirely plausible that impairment in production of ATP could explain the observed failure. Conversely, even if ATP stores were intact, alterations in the processes involved in the utilization of ATP such as a defect in myofibrillar ATPase, could lead to a similar result. Since calcium ion is considered to play a crucial role in regulation of myocardial contraction and relaxation, abnormalities in the ability of the cardiac cell to regulate its intracellular concentration could eventuate in myocardial dysfunction. Decreased ability of sarcolemmal, sarcoplasmic reticular, and mitochondrial membranes to transport this ion may result in intracellular calcium overload and result in functional changes in the troponin - tropomyosin regulation of actin and myosin. As well, a lesser amount of calcium would be available for release upon excitation. Such a condition would also explain the observed changes in myocardial function.

Abnormalities in several cellular components have been shown to occur during infective endocarditis and are associated with left ventricular failure. Although such studies with isolated organelles do not necessarily reflect the status of these components in the intact cell, they provide valuable insight into the pathogenesis of failure in this disease model. Extrapolation of the data obtained in this experimental model to the human disease must be done with caution; however it is possible that the pattern of myocardial alterations in patients with heart failure due to bacterial endocarditis may be similar to those observed in this study.

CONCLUSIONS

In this study, infective endocarditis was induced in catheterized rabbits by a single intravenous injection of Streptococcus viridans, and the heart was examined for pathological changes. In addition, the status of cardiac function and biochemical integrity of myocardial membranes and contractile proteins were assessed in these rabbits in comparison to sham operated control and uninfected catheterized animals. From the data obtained in this study, the following conclusions are drawn:

1. The histopathological and ultrastructural changes in myocardium from rabbits with bacterial endocarditis are indicative of the presence of infective cardiomyopathy.

2. Hemodynamic studies in intact animals as well as in vitro studies in coronary perfused hearts demonstrate myocardial dysfunction during experimental bacterial endocarditis and provide evidence that infective cardiomyopathy is associated with heart failure.

3. Biochemical and morphological changes in mitochondria can be interpreted to reflect a reduction in the ability of mitochondria to generate ATP and it is believed that a defect in the process of energy production is one of the factors causing heart failure in infective cardiomyopathy.

4. Although heart failure is superimposed upon left ventricular hypertrophy, the results demonstrate impairments in different membrane and contractile protein functions as well as ultrastructural abnormalities in bacterial cardiomyopathic hearts which are absent or of lesser magnitude in hearts with hypertrophy alone. From these observations, it is apparent that there is an association of heart failure and changes in function of cellular components during bacterial endocarditis.

5. Although extrapolation of data to the human disease must be done cautiously, it is possible that a similar pattern of myocardial alterations is present in patients with heart failure due to bacterial endocarditis.

REFERENCES

1. Hayward G.W.: Infective endocarditis: a changing disease. Br Med J 2: 706 - 709, 764 - 766, 1973

2. Linde L M, Rao P S: A modern view of infective endocarditis. Cardiovasc Clin 5: 15 - 34, 1973

3. Weinstein L, Rubin R H: Infective endocarditis - 1973. Progr Cardiovasc Dis 16: 239 - 274, 1973

4. Lerner P I: Infective endocarditis. A review of selected topics. Med Clin N A 58: 605 - 622, 1974

5. Weinstein L, Schlesinger J.L: Pathoanatomic, pathophysiologic and clinical correlations in endocarditis. New Eng J Med 291: 832 - 837, 1122 - 1126, 1974

6. Kaye D: Changes in the spectrum, diagnosis and management of bacterial and fungal endocarditis. Med Clin N A 57: 941 - 958, 1973

7. Angrist A, Oka M, Nakao K: Vegetative endocarditis. Path Ann 2: 155 - 212, 1969

8. Buchbinder N A, Roberts W C: Left-sided valvular active infective endocarditis. A study of forty-five necropsy patients. Am J Med 53: 20 - 35, 1972

9. Perry E L, Fleming R G, Edwards, J E: Myocardial lesions in subacute bacterial endocarditis. Ann Intern Med 36: 126 - 137, 1952

10. Blankenhorn M A, Gall E A: Myocarditis and myocardiosis: Clinicopathologic appraisal. Circulation 13: 217 - 223, 1956

11. Pankey G A: Acute bacterial endocarditis at University of Minnesota Hospitals 1939 - 1959. Am Heart J 64: 583 - 591, 1962

12. Guze L B, Pearce M L: Hospital acquired bacterial endocarditis. Arch Intern Med 112: 56 - 62, 1963

13. Garrison P K and Freedman L R: Experimental endocarditis I. Staphylococcal endocarditis in rabbits resulting from placement of a polyethylene catheter in the right side of the heart. Yale J Biol Med 42: 394 - 410, 1970

14. Durack D T, Beeson P B: Experimental bacterial endocarditis I. Colonization of a sterile vegetation. Br J Exp Path 53: 44 - 49, 1972

15. Durack D T, Beeson P B, Petersdorf R G: Experimental bacterial endocarditis III. Production and progress of the disease in rabbits. Br J Exp Path 54: 142 - 151, 1973

16. Bainbridge M V: Cardiac surgery and bacterial endocarditis. In, Proceedings of the National Symposium on Bacterial Endocarditis (Beeson P, Ridley M, ed). London, Beecham Research Laboratories, 1969, p 100 - 107

17. Shafer R B, Hall W H: Bacterial endocarditis following open heart surgery. Am J Cardiol 25: 602 - 607, 1970

18. English T A H, Ross J K: Surgical aspects of bacterial endocarditis. Br Med J 4: 598 - 602, 1972

19. King L H, Bradley K P, Shires D L, Donohue J P, Glover J L: Bacterial endocarditis in chronic hemodialysis patients: A complication more common than previously suspected. Surgery 69: 554 - 556, 1971

20. Kaye D: Bacterial endocarditis in the presence of arteriovenous fistulae. Am J Med Sci 264: 189 - 190, 1972

21. Conway N: Endocarditis in heroin addicts. Br Heart J 31: 543 - 545, 1969

22. Ramsey R G, Gunnar R M, Tobin J R Jr: Endocarditis in the drug addict. Am J Cardiol 25: 608 - 618, 1970

23. Robinson M J, Ruedy J: Sequelae of bacterial endocarditis. Am J Med 32: 922 - 928, 1962

24. Mills J, Utley J, Abbott J: Heart failure in infective endocarditis. Predisposing factors, course and treatment. Chest 66: 151 - 157, 1974

25. Olson R E, Schwartz W B: Myocardial metabolism in congestive heart failure. Medicine 30: 21 - 42, 1951

26. Olson R E: Molecular events in cardiac failure. Am J Med 20: 159 - 162, 1956

27. Fleckenstein A, Doring H J, Kammermeier H: Experimental heart failure due to inhibition of utilization of high energy phosphates. In, International Symposium on the Coronary Circulation and Energetics of the Myocardium Milan, 1966 Basel, S. Karger, 1967, p. 220 - 236.

28. Opie L H: Metabolism of the heart in health and disease. Am Heart J 76: 685 - 698, 1968; 77: 100 - 122, 383 - 410, 1969

29. Olson R E, Barnhorst D A: The control of energy production and utilization in cardiac muscle. In, Recent Advances in Studies on Cardiac Structure and Metabolism, Volume 3 (Dhalla N S, ed). Baltimore, University Park Press, 1973, p. 11 - 30

30. Schwartz A, Sordahl L A, Entman M L, Allen J C, Reddy Y S, Goldstein M A, Luchi R J, Wyborny L E: Abnormal biochemistry in myocardial failure. Am J Cardiol 32: 407 - 422, 1973

31. McNamara D B, Sulakhe P V, Singh J N, Dhalla N S: Properties of heart sarcolemmal Na^+-K^+ATPase. J Biochem 75: 795 - 803, 1974

32. Tada M, Kirchberger M A, Iorio J M, Katz A M: Control of cardiac sarcolemmal adenylate cyclase and sodium, potassium-activated adenosinetriphosphatase activities. Circ Res 36: 8 - 17, 1975

33. Langer G A: Ion fluxes in cardiac excitation and contraction and their relation to myocardial contractility. Physiol Rev 48: 708 - 757, 1968

34. Harigaya S, Schwartz A: Rate of calcium binding and uptake in normal animal and failing human cardiac muscle. Circ Res 25: 781 - 794, 1969

35. Muir J R, Dhalla N S, Orteza J F, Olson R E: Energy linked calcium transport in subcellular fractions of the failing rat heart. Circ Res 26: 429 - 438, 1970

36. Suko J, Vogel JHK, Chidsey C A: Intracellular calcium and myocardial contractility. III. Reduced calcium uptake and ATPase of the sarcoplasmic reticular fraction prepared from chronically failing calf hearts. Circ Res 27: 235 - 247, 1970

37. Lindenmayer G E, Sordahl L A, Harigaya S, Schwartz A: Some biochemical studies on subcellular systems isolated from fresh recipient human cardiac tissue obtained during transplantation. Am J Cardiol 27: 277 - 283, 1971

38. Schwartz A, Wood J M, Allen J C, Bornet E P, Entman M L, Goldstein M A, Sordahl L A, Suzuki M: Biochemical and morphological correlates of cardiac ischemia. Am J Cardiol 32: 46 - 61, 1973

39. Sordahl L A, McCollum W B, Wood W G, Schwartz A: Mitochondria and sarcoplasmic reticulum function in cardiac hypertrophy and failure. Am J Physiol 224: 497 - 502, 1973

40. Bing R J, Tillmans H, Fauvel J M, SeelerK, Mao J C: Effect of prolonged alcohol administration on calcium transport in heart muscle of the dog. Circ Res 35: 33 - 38, 1974

41. Dhalla N S: Defects in calcium regulatory mechanisms in heart failure. In, Recent Advances in Studies on Cardiac Structure and Metabolism, Volume 4 (Dhalla N S, ed.). Baltimore, University Park Press, 1974, p. 521 - 534

42. Dhalla N S, Sulakhe P V, Fedelesova M, Yates J C: Molecular abnormalities in cardiomyopathy. Adv Cardiol 13: 282 - 300, 1974

43. Ito Y, Suko J, Chidsey C A: Intracellular calcium and myocardial contractility V. Calcium uptake of sarcoplasmic reticulum fractions in hypertrophied and failing rabbit hearts. J Molec Cell Cardiol 3: 237 - 247, 1974

44. Singh J N, Dhalla N S, McNamara D B, Bajusz E, Jasmin G: Membrane alteration in failing hearts of cardiomyopathic hamsters. In, Recent Advances in Studies on Cardiac Structure and Metabolism, Volume 6 (Fleckenstein A, Dhalla N S, ed.). Baltimore, University Park Press, 1975, p. 259 - 268.

45. Dhalla N S, Tomlinson C W, Singh J N, Lee S L, McNamara D B, Harrow J A C, Yates J C: Role of sarcolemmal changes in cardiac pathophysiology. In, Recent Advances in Studies on Cardiac Structure and Metabolism, Volume 9 (Roy P E, Dhalla N S, ed.). Baltimore, University Park Press, 1975, (In Press)

46. Osler, W: Gulstonian Lectures on malignant endocarditis. The Lancet 1: 415 - 418, 459 - 464, 505 - 508, 1885

47. Weinstein L, Schlesinger J L: Treatment of infective endocarditis - 1973. Progr Cardiovasc Dis 16: 275 - 302, 1973

48. Kaye D, McCormack R C, Hook E W: Bacterial endocarditis: the changing pattern since the introduction of penicillin therapy. Antimicrob Ag Chemother 3: 37 - 46, 1961

49. Finland M, Barnes M W: Changing etiology of bacterial endocarditis in the antibacterial era; experiences at Boston City Hospital 1933 - 1965. Ann Intern Med 72: 341 - 348, 1970

50. Cherubin C E, Neu H C: Infective endocarditis at the Presbyterian Hospital in New York City from 1938 - 1967. Am J Med 51: 83 - 96, 1971

51. Lerner P I, Weinstein L: Infective endocarditis in the antibiotic era. New Eng J Med 274: 199 - 206, 259 - 266, 323 - 331, 387 - 393, 1966

52. Angrist A, Oka M, Nakao K: Prevention and control of bacterial endocarditis. New York State J Med 68: 1824 - 1829, 1968

53. Goodman J S, Crews H D, Ginn H E, Koenig M G: Bacterial endocarditis as a possible complication of chronic hemodialysis. New Eng J Med 280: 876 - 877, 1969

54. Cherubin C E, Baden M, Kavaler F, Lerner S, Cline W: Infective endocarditis in narcotic addicts. Ann Intern Med 69: 1091 - 1098, 1968

55. Buchbinder N A, Roberts W C: Alcoholism, an important but unemphasized factor predisposing to infective endocarditis. Arch Int Med 132: 689 - 692, 1973

56. Cordeiro A, Costa H, Laginha F: Immunologic phase of subacute bacterial endocarditis. A new concept and general considerations. Am J Cardiol 16: 477 - 481, 1965

57. Williams R C: Subacute bacterial endocarditis as an immune disease. Hosp Prac 6(6): 111 - 122, 1971

58. Stason W B, DeSanctis R W, Weinberg A N, Austen W G: Cardiac surgery in bacterial endocarditis. Circulation 38: 514 - 523, 1968

59. Gonzalez-Lavin L, Lise M, Ross O: The importance of the jet lesion in bacterial endocarditis involving the left heart; surgical considerations. J Thorac Cardiovasc Surg 59: 185 - 192, 1970

60. Roberts W C, Ewy G A, Glancy D L, Marcus F I: Valvular stenosis produced by active infective endocarditis. Circulation 36: 449 - 451, 1967

61. Sacks P V, Lakier J B, Barlow J B: Severe aortic stenosis produced by bacterial endocarditis. Br Med J 3: 97 - 98, 1969

62. Vogler W R, Dorney E R, Bridges H A: Bacterial endocarditis: a review of 148 cases. Am J Med 32: 910 - 921, 1962

63. Blum L: Development of current concepts of mycotic aneurysm. N Y State J Med 64: 1317 - 1320, 1964

64. Alvares J F, Parsonnet V, Brief D K: Mycotic aneurysm of the superior mesenteric artery. Am J Surg 111: 237 - 240, 1966

65. Stack B H R, Rankin J T, Bentley R J: Hepatic artery aneurysm after staphylococcal endocarditis. Br Med J 3: 659 - 660, 1969

66. Antel J J, Rome H P, Geraci J E, Sayre G P: Toxic organic psychosis as a presenting feature in bacterial endocarditis. Proc Mayo Clin 30: 45 - 50, 1955

67. Jones H R, Siekert R G, Geraci J E: Neurologic manifestations of bacterial endocarditis. Ann Intern Med 71: 21 - 28, 1969

68. Ziment I: Nervous system complications in bacterial endocarditis. Am J Med 47: 593 - 607, 1969

69. Greenlaw J E, Mandell G L: Neurologic manifestations of infective endocarditis: A review. Stroke 4: 958 - 963, 1973

70. Gutman R A, Striker G E, Gilliland B C, Cutler R E: The immune complex glomerulonephritis of bacterial endocarditis. Medicine 51: 1 - 25, 1972

71. Lepeschkin E: On the relation between the site of valvular involvement in endocarditis and the blood pressure resting on the valve. Am J Med Sci 224: 318 - 319, 1952

72. Rodbard S: Blood velocity and endocarditis. Circulation 27: 18 - 28, 1963

73. Harper W F: The structure of the heart valves with special reference to their blood supply and the genesis of endocarditis. J Pathol Bacteriol 57: 229 - 238, 1945

74. Oka M, Angrist A: Comparative histochemical studies of nonbacterial and bacterial valvular vegetations. Lab Invest 14: 48 - 61, 1965

75. Blumer G: Subacute bacterial endocarditis. Medicine 2: 105 - 170, 1923

76. Libman E: A consideration of the prognosis in subacute bacterial endocarditis. Am Heart J I: 25 - 40, 1925

77. Clawson B J: Myocarditis. Am Heart J 4: 1 - 15, 1928

78. Saphir O: Myocardial lesions in subacute bacterial endocarditis. Am J Path 11: 143 - 156, 1935

79. Saphir O, Katz L N, Gore I: The myocardium in subacute bacterial endocarditis. Circulation I: 1155 - 1167, 1950

80. Estes E H, Dalton F M, Entman M L, Dixon H B, Hackel D B: The anatomy and blood supply of the papillary muscles of the left ventricle. Am Heart J 71: 356 - 362, 1966

81. Nedzel A J: Experimental endocarditis. Arch Path 24: 143 - 200, 1937

82. Kinsella R A, Sherburne C C: Eperimental production of streptococcal endocarditis with glomerular nephritis. Proc Soc Exp Biol Med 20: 252 - 253, 1923

83. Kinsella R A, Muether R O: Experimental streptococcal endocarditis. Arch Int Med 62: 247 - 270, 1938

84. Lillehei C W, Bobb J, Visscher M D: Occurrence of endocarditis and valvular deformities in dogs with A-V fistulas. Ann Surg 132: 577 - 590, 1950

85. Angrist A and Oka M: Pathogenesis of bacterial endocarditis. J Am Med Assoc 62: 249 - 252, 1963

86. Walker W F, Hamburger M: A study of experimental staphylococcal endocarditis in dogs. J Lab Clin Med 53: 931 - 941, 1959

87. Hamburger M, Garancis J C, Scott N J, Carlton J, Beasley J S: Studies in experimental staphylococcal endocarditis in dogs. V. Treatment with oxacillin. J Lab Clin Med 70: 786 - 799, 1967

88. Highman B, Rosche J, Altland P D: Production of endocarditis with Staphylococcus aureus and Streptococcus mitis in dogs with aortic insufficiency. Circ Res 4: 250 - 256, 1956

89. Keys T F, Sapico F L, Touchon R, Barenfus M, Hewitt W L: Experimental enterococcal endocarditis. I. Description of a canine model. Am J Med Sci 263: 103 - 109, 1972

90. Jones J E T: The experimental production of streptococcal endocarditis in the pig. J Path 99: 307 - 318, 1969

91. Jones J E T: Experimental bacterial endocarditis in the pig. Proc Roy Soc Med 65: 990 - 994, 1972

92. Rowlands D T, Vakilzadeh J, Sherwood B F, LeMay J C: Experimental bacterial endocarditis in the opossum (Didelphis virginiana) 1. Valvular changes following a single injection of bacteria in unmodified adult opossums. Amer J Path 48: 295 - 304, 1970

93. Sherwood B F, Rowlands D T, Vakilzadeh J, LeMay J C: Experimental bacterial endocarditis in the opossum (Didelphis virginiana) III. Comparison of spontaneously occurring endocarditis with that induced experimentally by pyogenic bacteria and fungi. Am J Path 64: 513 - 520, 1971

94. Highman B, Altland P D: Effect of exercise and training on susceptibility of epinephrine-treated rats to bacterial endocarditis. Life Sciences 11: 931 - 939, 1972

95. Highman B, Cyr W H, Streett R P: Bacterial endocarditis in x-irradiated rats: Effect of isoproterenol and adrenergic receptor blocking agents. Res Common Chem Path Pharmacol 5: 311 - 318, 1973

96. Perlman B B, Freedman L R: Experimental endocarditis II. Staphylococcal infection of the aortic valve following placement of a polyethylene catheter in the left side of the heart. Yale J Biol Med 44: 206 - 213, 1971

97. Durack D T, Beeson P B: Experimental bacterial endocarditis II. Survival of bacteria in endocardial vegetations. Br J Exp Path 53: 50 - 53, 1972

98. Durack D T, Petersdorf R G: Chemotherapy of experimental streptococcal endocarditis. J Clin Invest 52: 592 - 598, 1973

99. Oka M, Shirota A, Angrist A: Experimental endocarditis. Endocrine factors in valve lesions on A-V shunt rats. Arch Path 82: 85 - 92, 1966

100. Selye H: Stress. Montreal, Acta Inc, 1950, p 489 - 602

101. Highman B, Altland P D: Effect of altitude and cobalt polycythemia hypoxia and cortisone on susceptibility of rats to endocarditis. Circ Res 3: 351 - 356, 1955

102. Angrist A, Oka M, Nakao K, Marquiss J: Studies in experimental endocarditis I. Production of valvular lesions by mechanisms not involving infection of sensitivity factors. Amer J Path 36: 181 - 191, 1960

103. Miller A J, Pick R, Kline J K, Katz L N: The susceptibility of dogs with chronic impairment of cardiac flow to staphylococcal valvular endocarditis. Circulation 30: 417 - 424, 1964

104. Oka M, Angrist A: Experimental endocarditis. Rev Can Biol 22: 297 - 308, 1963

105. Bracht E, Wachter: Beitrag zur atiologie und pathologischen anatomie der myocarditis rheumatica. Deutsches Arch f Klin Med 96: 493 - 514, 1909

106. Thalhimer W, Rothschild M A: Experimental focalized myocardial lesions produced with Streptococcus mitis. J Exp Med 19: 429 - 443, 1914

107. Geissinger H D, Miniats OP, Ruhnke H L, Djurickovic D G: Experimental staphylococcal endocarditis in pigs. Bacteriological, histopathological and scanning electron microscopic observations. J. Comp Path 83: 323 - 335, 1973

108. Luft J H: Improvements in epoxy resin embedding methods. J Biophys Biochem Cytol 9: 409 - 414, 1961

109. Rosalki S B: An improved procedure for serum creatine phosphokinase determination. J Lab Clin Med 69: 696 - 705, 1967

110. Morgenstern S, Kessler G, Auerback J, Flor R V, Klein B: An automated p-Nitrophenylphosphate serum alkaline phosphatase procedure for the autoanalyzer. Clin Chem 11: 876 - 888, 1965

111. Levine J B, Hill J B: Automated fluorometric determinations of serum glutamic oxaloacetic transaminase and serum glutamic pyruvic transaminase. In, Automation in Analytical Chemistry (Skeggs L T, ed.). New York, Mediad Inc., 1966, p. 569 - 574

112. Morgenstern S, Flor R, Kessler G, Klein B: The automated determination of NAD-coupled enzymes II. Serum lactate dehydrogenase. Clin Chem 12: 274 - 281, 1966

113. Tomlinson C W, Dhalla N S: Myocardial contractility II. Effect of changes in cardiac function on the subcellular distribution of calcium in the isolated perfused rat heart. Can J Physiol Pharmacol 50: 853 - 859, 1972

114. Reynafarje B, Lehninger A L: High affinity and low affinity binding of calcium by rat liver mitochondria. J. Biol Chem 244: 584 - 593, 1969

115. Sulakhe P V, Dhalla N S: Excitation-contraction coupling in heart VII. Calcium accumulation in subcellular particles in congestive heart failure. J Clin Invest 50: 1019 - 1027, 1971

116. Sordahl L A, Schwartz A: Effects of dipyridamole on heart muscle mitochondria. Molec Pharmacol 3: 509 - 515, 1967

117. Muir J R, Weber A, Olson R E: Cardiac myofibrillar ATPase: A comparison with that of fast skeletal actomyosin in its native and in an altered conformation. Biochem Biophys Acta 234: 199 - 209, 1971

118. Imai S, Takeda K: Actions of calcium and certain multivalent cations on potassium contracture of guinea-pig's taenia coli. J Physiol 190: 155 - 169, 1967

119. Taussky H H, Shorr E: A microcolorimetric method for the determination of inorganic phosphorus. J Biol Chem 202: 675 - 685, 1953

120. Lowry O H, Rosebrough N J, Farr A L, Randall R J: Protein measurement with the folin phenol reagent. J Biol Chem 193: 265 - 275, 1951

121. Drummond G I, Duncan L: Adenyl cyclase in cardiac tissue. J Biol Chem 245: 976 - 983, 1970

122. Mason D T: Usefulness and limitations of the rate of rise in intraventricular pressure (dP/dt) in the evaluation of myocardial contractility in man. Amer J Cardiol 23: 516 - 527, 1969

123. Mason D T, Spann J F Jr, Zelis R: Quantification of the contractile state of the intact human heart: maximal velocity of contractile element shortening determined by the instantaneous relation between the rate of pressure rise and pressure in the left ventricle during isovolumic systole. Am J Cardiol 26: 248 - 257, 1970

124. Lineweaver M, Burk O: Determination of enzyme dissociation constants. J Amer Chem Soc 56: 658 - 666, 1934

125. Bahr G F, Jennings R B: Ultrastructure of normal and asphyxic myocardium of the dog. Lab Invest 10: 548 - 571, 1961

126. Tomlinson C W, Yates J C, Dhalla N S: Relationship among changes in intracellular calcium stores, ultrastructure and contractility of myocardium. In, Recent Advances in Studies on Cardiac Structure and Metabolism, Volume 4 (Dhalla N S, ed.). Baltimore, University Park Press, 1974, p. 331 - 345

127 Yates J C, Dhalla N S: Structural and functional changes associated with failure and recovery of hearts after perfusion with Ca^{++}-free medium. J Molec Cell Cardiol 7: 91 - 103, 1975

128. Bloom S, Cancilla P A: Myocytolysis and mitochondrial calcification in rat myocardium after isoproterenol. Am J Path 54: 373 - 392, 1969

129. Rona G, Boutet M, Huttner I, Peters H: Pathogenesis of isoproterenol induced myocardial alterations: functional and morphological correlates. In, Recent Advances in Studies on Cardiac Structure and Metabolism, Volume 3 (Dhalla N S, ed.). Baltimore, University Park Press, 1973, p. 507 - 526

130. Dhalla N S, Yates J C, Olson R E: Energy state and ultrastructure of the substrate depleted heart. In, Recent Advances in Studies on Cardiac Structure and Metabolism, Volume 1 (Bajusz E, Rona G, eds.). Baltimore, University Park Press, 1972, p. 81 - 94

131. Olson R E, Dhalla N S, Sun C N: Changes in energy stores in the hypoxic heart. Cardiology 56: 114 - 124, 1971/72

132. Ferrans V J, Massumi R A, Shugall G I, Ali N, Roberts W C: Ultrastructural studies of myocardial biopsies in 45 patients with obstructive or congestive cardiomyopathy. In, Recent Advances in Studies on Cardiac Structure and Metabolism, Volume 2 (Bajusz E, Rona G, Brink A J, Lochner A, eds.). Baltimore, University Park Press, 1973, p. 231 - 272

133. Tomlinson C W, Dhalla N S: Excitation-contraction coupling in heart IX. Changes in the intracellular stores of calcium in failing hearts due to lack of substrate and oxygen. Cardiovasc Res 7: 470 - 476, 1973

134. Bloom S, Davis D L: Calcium as mediator of isoproterenol induced myocardial necrosis. Am J Path 69: 459 - 470, 1972

135. Fleckenstein A, Janke J, Doring H J, Leder O: Myocardial fiber necrosis due to intracellular calcium overload - A new principle in cardiac pathophysiology. In, Recent Advances in Studies on Cardiac Structure and Metabolism, Volume 4 (Dhalla N S, ed.). Baltimore, University Park Press, 1974, p. 563 - 580

136. Dodge H T, Baxley W A: Left ventricular volume and mass and their significance in heart disease. Amer J Cardiol 23: 528 - 537, 1969

137. Hood W P Jr: Dynamics of hypertrophy in the left ventricular wall of man. In, Cardiac Hypertrophy (Alpert N R, ed.). New York, Academic Press, 1971, p. 445 - 452

138. Laks M M, Morady F, Garner D, Swan H J C: Relation of ventricular volume, compliance and mass in the normal and pulmonary arterial banded canine heart. Cardiovasc Res 6: 187 - 198, 1972

139. Sharma G P, Varley K G, Kim S W, Barwinsky J, Cohen M, Dhalla N S: Alterations in energy, metabolism and ultrastructure upon reperfusion of the ischemic myocardium produced by coronary occlusion. Am J Cardiol, in press, 1975

140. Sobel B E: Biochemical and morphologic changes in infarcting myocardium. In, The Myocardium: Failure and Infarction (Braunwald E, ed.). New York, H P Publishing Co, 1974, p. 247 - 260

141. Chidsey C A, Braunwald E, Morrow A G: Catecholamine excretion and cardiac stores of norepinephrine in congestive heart failure. Amer J Med 39: 442 - 451, 1965

142. Chidsey C A, Kaiser G A, Sonnenblick E H, Spann J F, Braunwald E: Cardiac norepinephrine stores in experimental heart failure in the dog. J Clin Invest 43: 2386 - 2393, 1964

143. Dhalla N S, Naidu K J R, Bhagat B, Christensen K: Biochemical basis of heart function I. Relation of catecholamine stores and contractile force in an isolated rat heart. Cardiovasc Res 5: 376 - 382, 1971

144. Rutenburg H L, Spann J F Jr: Alterations of cardiac sympathetic neurotransmitter activity in congestive heart failure. Am J Cardiol 32: 472 - 480, 1973

145. Spann J F Jr, Buccino R A, Sonnenblick E H, Braunwald E: Contractile state of cardiac muscle obtained from cats with experimentally produced ventricular hypertrophy and heart failure. Circ Res 21: 341 - 354, 1967

146. Mason D T, Spann J F Jr, Zelis R, Amsterdam E A: Alterations of hemodynamics and myocardial mechanics in patients with congestive heart failure: pathophysiologic mechanisms and assessment of cardiac function and ventricular contractility. Progr Cardiovasc Dis 12: 507 - 557, 1970

147. Mason D T: Regulation of cardiac performance in clinical heart disease. Interactions between contractile state mechanical abnormalities and ventricular compensatory mechanisms. Am J Cardiol 32: 437- 448, 1973

148. Nayler W G, Morad M, Goldman Y: Excitation-contraction coupling in heart muscle; membrane control of development of tension. Progr Biophys Molec Biol 27: 257 - 313, 1973

149. Chidsey C A, Weinbach E C, Pool P E, Morrow A G: Biochemical studies of energy production in the failing human heart. J Clin Invest 45: 40 - 50, 1966

150. Sobel B E, Spann J F, Pool P E, Sonnenblick E H, Braunwald E: Normal oxidative phosphorylation in mitochondria from the failing heart. Circ Res 21: 355 - 363, 1967

151. Alpert N R, Gordon M S: Myofibrillar adenosine triphosphatase activity in congestive heart failure. Am J Physiol 202: 940 - 946, 1962

152. Chandler B M, Sonnenblick E H, Spann J F, Pool P E: Association of depressed myofibrillar adenosine triphosphatase and reduced contractility in experimental heart failure. Circ Res 21: 717 - 725, 1967

153. Luchi R J, Kritcher E M, Thyrum P T: Reduced cardiac myosin adenosine triphosphate activity in dogs with spontaneously occurring heart failure. Circ Res 24: 513 - 519, 1969

154. Davis J O, Trapasso M, Yankopoulos N A: Studies of actomyosin from cardiac muscle of dogs with experimental congestive heart failure. Circ Res 7: 957 - 968, 1959

155. Olson R E: The contractile proteins of heart muscle. Am J Med 30: 692 - 707, 1961